Measurement of Upper Motor Neuron Abnormalities with Diffusion Tensor Imaging and Transcranial Magnetic Stimulation in Amyotrophic Lateral Sclerosis

Jennica M.C. Winhammar B.Sc.(Hons) M.Sc.

A thesis submitted in fulfilment

of the requirements for the degree of

Doctor of Philosophy

Department of Neurology **University of Sydney**

Royal North Shore Hospital

January 2008

Abstract

Amyotrophic Lateral Sclerosis (ALS) is a progressive neurodegenerative disease that produces weakness and ultimately death from respiratory failure. ALS results in the death of nearly 400 Australians per year, with a median survival of only 2-3 years from diagnosis. While respiratory failure in ALS patients is generally a direct consequence of muscle weakness during disease end stage, a proportion of patients develop early and severe respiratory difficulties during sleep termed, Nocturnal Hypoventilation (NH). Hypoventilation produces nocturnal hypoxia, increasingly recognized as a predictor of survival, independent of respiratory muscle weakness. Intervention with Non Invasive Ventilation (NIV) in ALS patients with symptomatic respiratory failure improves survival. It is therefore critical to identify patients with NH, so that NIV can be offered.

NH is increasingly recognized as a predictor of survival, independent of respiratory weakness. A mean nocturnal arterial oxygen saturation of less than 93% is predictive of a dramatically shortened mean survival time of less than 6 months. Although hypoxia is a consequence of muscle weakness, the mechanisms involved in NH - early in ALS - are largely unknown. The initial aim for this research was to develop a technique that could determine the level of Upper Motor Neuron (UMN) involvement in ALS patients who suffered from NH in comparison with ALS patients who did not. After extensive data collection had already begun, there was a lack of ALS patients suffering from NH during data collecting so the focus remained on developing a better technique for determining UMN involvement in ALS.

ALS targets the Corticospinal Tract (CST), brain stem and Lower Motor Neurons (LMNs), resulting in progressive weakness in the limb, thoracic, bulbar and

abdominal musculature. The UMNs in the motor cortex and LMNs in the brainstem and spinal cord can either be affected together or in isolation. The determination of UMN involvement is more of a challenge and no objective technique exists. The sensitivity of neurological assessment is limited due to LMN signs, such as testing reflexes in weak muscles.

A marker to monitor UMN involvement in ALS is necessary to monitor disease progression, as well as to provide more pertinent insights into the pathological conditions of the neuronal tissues. Denervation and fasciculation in LMNs is examined by electromyography studies but there is no definitive diagnostic test for central nervous system injury. Transcranial Magnetic Stimulation (TMS) is a method for neurophysiological assessment of UMN function and cortical abnormalities in ALS. Diffusion Tensor Imaging (DTI) indirectly investigates CST pathology in ALS. The technique studies the water diffusion characteristics - with a higher diffusion indicating tract abnormalities. The TMS findings in this thesis back up previous studies and show that there is an increase in excitability of corticomotoneurons and a decrease in intracortical inhibition, contributing to motor cortex excitability in ALS. The DTI studies in this thesis have identified considerable differences between ALS patients and controls in diffusivity along the CST between the internal capsule and midbrain in patients with ALS.

There is a clear difference between the ALS patients and control group in both the DTI and TMS studies. There were many correlations between the TMS and DTI parameters. The most promising TMS parameter is Short-Interval Intracortical Inhibition (SICI). When SICI was divided by any DTI parameter there was a

significant difference between the ALS and control group. This simple algorithm could potentially be used as a marker of UMN involvement in ALS.

Statement

The work described in this thesis was carried out in the Department of Neurology at Royal North Shore Hospital, University of Sydney, under the supervision of Dr. Dominic Rowe, Dr. David Joffe and A/Prof. Matthew Kiernan. Unless otherwise stated, it is the original work of the author and has neither been presented nor is it currently presented for any other degree.

Jennica Winhammar

Publications

Work from this thesis was published in the following manner:

Refereed Journal Articles:

1. Winhammar JM, Joffe D, Simmul R, Schoeffel R, Kiernan MC, Rowe DB. Nocturnal hypoxia in motor neuron disease is not predicted by standard respiratory function tests. Intern Med J 2006;36(7):419-22.
2. Winhammar JM, Rowe DB, Henderson RD, Kiernan MC. Assessment of disease progression in motor neuron disease. Lancet Neurol 2005;4(4):229-38.

Book Chapter:

3. Henderson RD, Winhammar JM, Rowe DB. Assessing disease progression. In: Kiernan MC, editor. The Motor Neuron Disease Handbook. Sydney: MJA Books; 2007. p. 144-154

Abstracts:

4. Winhammar JM, Kiernan MK, Rowe DB. Transcranial Magnetic Stimulation in Motor Neuron Disease. Clin Neurophysiol 2004;115:990-993.
5. Winhammar JM, Trevillion L, Howells JT, Rowe DB, Joffe D, Kiernan MC. Mechanisms of nocturnal hypoventilation in motor neuron disease. Clin Neurophysiol 2005; 116: e19-e24
6. Winhammar JM, Trevillion L, Howells JT, Rowe DB, Joffe D, Kiernan MC. Mechanisms of nocturnal hypoventilation in motor neuron disease. ALS and

other Motor Neuron Disorders 2005, 6 (suppl 1 - Abstracts from Theme 10): 37.

7. Winhammar JM, Joffe D, Simmul R, Schoeffel R, Kiernan MC, Rowe DB. Nocturnal hypoxia in motor neuron disease is not predicted by standard respiratory function tests. ALS and other Motor Neuron Disorders 2007; 8 (suppl 1):80-81
8. Winhammar JM, Vucic, S, Joffe, D, Kiernan, MC, Rowe D. Measurement of Upper Motor Neuron Damage in Motor Neuron Disease by Transcranial Magnetic Stimulation and Diffusion Tensor Imaging. ALS and other Motor Neuron Disorders 2007; 8 (suppl 1):134-135.

Acknowledgements

I wish to thank Dr. Dominic Rowe, for his inexhaustible guidance and inspiration. I also wish to thank my associate supervisors, A/Prof. Matthew Kiernan and Dr. David Joffe for their dedication and support. I thank Dr. Steve Vucic, Louise Trevillion and Tim Howells and the Prince of Wales Medical Research Institute, for all the time and effort they contributed to the transcranial magnetic stimulation work. I also thank Dr. Sususmu Mori at Johns Hopkins University for his generosity and input on the DTI analysis and the respiratory technicians at Royal North Shore Hospital. Finally, I would like to thank all of the patients and controls who participated in this study.

I wish to acknowledge the Australian Rotary Health Research Fund and the Rotary Clubs of Belvoir-Wodonga who provided scholarship support for this study. The Australian Motor Neuron Disease Research Institute and Nick's Foundation provided funding to perform magnetic resonance imaging studies.

Dedication

I dedicate this thesis to my father, Lars Winhammar who died from this unimaginably evil disease. He continues to be my largest inspiration to research this field, his memory will live on forever.

I also dedicate this thesis to my family in England, Sweden and Australia.

Table of Contents

Abstract 2

Statement 5

Publications 6

Acknowledgements 8

Glossary of Specialist Terms 12

1. General Introduction 17

1.1 Definition, classification and diagnosis of ALS/MND 19

1.2 Epidemiology 22

1.3 Pathology 23

1.4 Assessment of disease progression in ALS 30

1.4(i) Motor Unit Number Estimation (MUNE) 30

1.4(ii) Measurement of Axonal Excitability by Threshold Tracking 32

1.4(iii) Transcranial Magnetic Stimulation (TMS) 33

1.5 Functional Scales in the Assessment of Progression of ALS 36

1.5(i) Norris Scale 37

1.5(ii) Appel Scale 37

1.5(iii) ALS Functional Rating Scale (ALS FRS) 37

1.6 Imaging Techniques 40

1.6(i) Magnetic Resonance Imaging (MRI) 40

1.6(iii) Diffusion Tensor Imaging (DTI) 44

1.7 Respiratory Function in ALS 50

2. Respiratory Function Tests and Nocturnal Hypoventilation in ALS 52

2.1 Introduction 52

2.2 Methods 57

2.2(i) Polysomnography studies 57

2.2(ii) Stardust 59

2.2(iii) SNIF 60

2.2(iv) FOT 60

2.3 Results 61

2.3(i) Data set A 61

2.3(ii) Data set B 67

2.4 Discussion 70

3. Measurement of Upper Motor Neuron Involvement in Amyotrophic Lateral Sclerosis (ALS) using Transcranial Magnetic Stimulation (TMS) and Diffusion Tensor Imaging (DTI) 76

3.1 Introduction 76

3.1(i) TMS 78

3.1(ii) DTI 79

3.2 Methods 82

3.2(i) TMS methods 85

3.2(ii) DTI Methods 89

3.3 Results 95

3.3(i) Significant findings in TMS 96

3.3(ii) Results in DTI 100

3.3(iii) Correlations between DTI & TMS 106

3.3(iv) Algorithm to calculate UMN pathology 114

3.4 Discussion 120

4.0 General Discussion 128

Abbreviations 139

References 143

Appendix A - Analysis of Upper Motor Neuron Abnormalities with Diffusion Tensor Imaging and Transcranial Magnetic Stimulation in the Parry-Romberg Syndrome. 179

Appendix B – DTI Manual 199

Appendix C – Correlation Studies 211

Appendix D - Publications 219

Glossary of Specialist Terms

This section defines the commonly measured Respiratory Function Tests (RFTs) and parameters in Transcranial Magnetic Stimulation (TMS) and Diffusion Tensor Imaging (DTI).

Terms for Respiratory Function Tests

Respiratory Function Tests (RFTs) ALS patients undergo extensive respiratory evaluation as part of their assessment including the following measurements:

Spirometry is a measurement of ventilatory function that reflects the limits of the elastic properties of the lungs and resistance of the airways. It is a useful screening test which can detect, quantify and monitor resistance properties of the airways. The measure is non specific and can be abnormal in numerous diseases. The actual measure involves a maximal inspiration followed by a forced expiration, while recording time and volume.

Forced Vital Capacity (FVC) is the volume of air exhaled during a forced expiratory effort from the **Total Lung Capacity** (TLC) to the **Residual Volume** (RV). Numerous diseases can cause a reduction in the FVC. If the reduction is due to a decrease in the TLC it is possibly due to a neuromuscular, chest wall, pleural or interstitial disease. However, if there is reduction in the RV it is more likely to be due to airway obstruction or a loss of elastic recoil. If the chest wall is normal the FVC is sensitive to disorders of the lungs and airways rather than muscle weakness.

Whole body plethysmography is a rapid and accurate way to measure absolute lung volumes. Total compressible gas in the thorax is measured, thus is unaffected by the presence of poorly ventilated air spaces.

Carbon Monoxide Diffusing Capacity (DLCO) involves gas diffusion which is the movement of gas from a region of higher concentration (alveolar gas) to one of lower concentration (pulmonary capillary blood) across a resistance to flow, or uptake of carbon monoxide. The flow is proportional to the CO pressure gradient between the alveolus and the capillary blood.

Maximal Inspiratory Muscle Strength (MIPS) & Maximal Expiratory Muscle Strength (MEPS) is useful in the diagnosis and management of patients with neuromuscular diseases and conditions affecting the muscles involved in respiration (the diaphragm, intercostals and accessory muscles).

Sniff Nasal Inspiratory Force (SNIF): takes place through a plug occluding one nostril during a maximal sniff through the other non occluded nostril and is an easy natural effort. SNIF calculates intra-thoracic pressure during a maximal sniff enabling assessment of inspiratory muscle strength. This technique can eliminate problems with mouth leak around a mouthpiece.

Forced Oscillation Technique (FOT): measures resistance in the respiratory system. A range of frequencies is applied to the air (forcing the air to oscillate) which a subject breathes during tidal breathing. A transducer records the patient's

airflow and air pressure, which is related to the mechanical properties of the airways, lungs and chest wall. The measurements of Pressure (P) and Flow (V) calculate the Respiratory System Resistance (Rrs). Airflow at the mouth is measured in L/s and as pressure cmH_2O. Multiple measurements are recorded over time and are used to calculate mean Rrs in cmH_2O/L per second.

Transcranial Magnetic Stimulation Terms

Compound Muscle Action Potential (CMAP) is the initial response which has the largest amplitude in response to supramaximal stimulus of the nerve.

F waves may follow CMAP after supermaximal stimulation of the axon. F waves are variable in latency, amplitude and configuration and may not appear after each stimulus.

Neurophysiological Index (NPI) is derived from the CMAP amplitude, F wave frequency and the distal motor latency (CMAP amplitude/distal motor latency) x F wave frequency%.

Motor Evoked Potential (MEP) is the activation of motor units in a muscle by TMS.

Resting Motor Threshold (RMT) is the stimulus intensity required to produce and maintain a target MEP response.

Cortical Motor Threshold (CMT) is the current intensity required to stimulate the motor cortex.

Central Motor Conduction Time (CMCT) is the latency from the cortex to a selected limb muscle.

Cortical Silent Period (CSP) is the pause seen in electromyographic activity when the magnetic stimulus is applied to the motor cortex during voluntary contraction of a target muscle. This can be caused by cortical inhibitory mechanisms mediated through local circuit, intra-cortical, inter-neurons.

Peri-Stimulus Time Histograms (PSTH) provides information about the function of a chosen colony of corticomotoneurons. A series of threshold magnetic stimuli induce alterations in the firing of the motor unit. The magnetic stimulus evokes corticospinal volleys that perturb the regular firing pattern of a voluntary activated motor unit. This results in a large 'primary' peak in the PSTH. There are also sub-components that reflect the sequential arrival of indirect descending volleys, initiated by a single cortical stimulus.

Short-Interval Intracortical Inhibition (SICI) reflects inhibitory and excitatory interneuronal circuits at the cortical level that are studied using a paired-stimulation paradigm with subthreshold conditioning stimulus delivered at short intervals.

Diffusion Tensor Imaging Terms

Anisotropy value is the value for the directionality of diffusion. This is obtained by a ratio of diffusivity along the axis of the fiber bundles compared with the value across the fiber. This value is higher in an ordered structure.

Fractional Anisotropy (FA) measures coherence of diffusion. FA is a measure of directionality of diffusion within a single voxel and ranges from 0 - where there is no directional dependence, to 1 - where there is diffusion along a single direction.

Apparent Diffusion Coefficient, (Trace ADC) is a measure of the magnitude of bulk diffusion and provides no directional information on the diffusion.

Eigenvalues (Ev) reflect the magnitude of diffusion both **parallel** and **perpendicular** to the fiber tracts. Water molecules move readily in parallel to the principal direction of structured material, such as nerve fibers.

1. General Introduction

Motor Neuron Disorders (MND) is a term used to describe a number of progressive neurological conditions that selectively affect motor neurons. Forms of MND include: Amyotrophic Lateral Sclerosis (ALS), Primary Lateral Sclerosis (PLS), Progressive Muscular Atrophy (PMA), pseudobulbar palsy, progressive bulbar palsy and Spinal Muscular Atrophy (SMA). ALS is the most common adult motor neuron disease[1], first described by Charcot in 1869[2].

ALS is characterized by a progressive deterioration of the CST, brainstem and anterior horn cells (AHC) of the spinal cord. Physicians rely on clinical criteria (– upper and lower motor neuron signs –) for diagnosis, as there is no single pathognomonic test for the diagnosis of ALS.

A marker of disease progression is still unavailable and remains a challenge as the presentations, clinical phenotypes and outcomes of ALS are diverse. No single algorithm combines the findings of functional assessments and rating scales, with biological markers of disease activity and findings from imaging and neurophysiological assessments.

Each ALS case demonstrates the same pathology and ultimately a similar death from respiratory failure as a result of muscle weakness. The progression of the disease varies greatly between patients. Commonly, respiratory failure is a direct consequence of respiratory muscle weakness. In addition, some patients with ALS suffer from NH and hypoxia without showing signs of weak respiratory muscles. The aim of this general introduction is to review the literature in order to provide a general background on the clinical features, pathology and theories of ALS. This introduction serves to present the reader with the original aims of the study - the

genesis of NH in ALS. It also aims to contextualize the methods used to measure the upper motor neurons, TMS, and DTI of the CST.

Whilst the initial aim of this study was to dissect the contribution of the UMN towards NH, no patients with early significant NH were seen while this study was conducted. During this period, sophisticated methods were developed for the simultaneous measurement of UMN pathology, utilizing DTI and TMS that were applicable to all patients with ALS. Therefore, although the initial goal was to use these methods in NH, they proved applicable in all patients with UMN pathology with ALS. The development of tools to measure UMN pathology in ALS are widely applicable in the measurement and diagnosis of ALS.

1.1 Definition, classification and diagnosis of ALS/MND

The nosology of ALS/MND remains difficult given its heterogeneous nature and clinical findings. Diverse presentations of ALS/MND[3, 4] are also critical to the understanding and developing measures of disease progression[5]. The presentations include: Amyotrophic Lateral Sclerosis (ALS), presenting with a combination of UMN and LMN signs in the limbs; bulbar onset MND, presenting with speech and swallowing difficulties, (sometimes with limb and cognitive features developing later in the course of the disease); less commonly Primary Lateral Sclerosis (PLS) with pure UMN involvement; and progressive muscular atrophy, with purely LMN signs. More recent sub-classifications include the flail limb variant of MND, marked by prolonged disease duration[6].

ALS is the most common form of MND and is what the patients involved in this study had. "Amyotrophic" refers to muscle atrophy, weakness and fasciculation which signify dysfunction of the LMN. "Lateral sclerosis" refers to the hardness of the lateral columns of the spinal cord in autopsy specimens[2].

The diagnostic criteria, the El Escorial criteria (EEc)[7], revised in 1997[8] are used in the diagnosis of patients displaying combinations of UMN (spasticity, weakness and hyper-reflexia) and LMN signs (fasciculation, wasting, weakness and hypoflexia) (Table 1.1). Most clinical trials have tended to enrol patients with either probable or definite ALS according to the EEc, which are regarded as too conservative[9, 10]. The EEc may also lack sensitivity and may not pick up the early stage of ALS where patients may benefit the most from therapeutic intervention[9]. Thus, there remains a clear need for the inclusion of additional quantitative methods

of assessment to improve diagnostic accuracy when undertaking clinical trials in ALS.

The most important disorder in the differential diagnosis for ALS is multifocal motor neuropathy. This disorder is dominated exclusively by LMN signs and is characterised by multiple motor-conduction blocks on electrical testing[11]. Importantly, multifocal motor neuropathy responds to treatment with intravenous immunoglobulin[12].

The diagnosis of ALS requires the presence of each of the following
1. LMN signs (by clinical, electrophysiological, or neuropathological examination) in one or more of four regions (bulbar, cervical, thoracic and lumbosacral) 2. UMN signs (by clinical examination) in one or more of the four regions 3. Progression of signs within a region or to other regions
Definite ALS = UMN + LMN signs in three regions **Probable ALS** = UMN + LMN signs in two regions with UMN signs rostral to LMN signs **Possible ALS** = UMN + LMN signs in one region or UMN signs in two or three regions, such as monomelic ALS, progressive bulbar palsy, and primary lateral sclerosis **Suspected ALS** = LMN signs in two or three regions, such as progressive muscular atrophy, and other motor syndromes

Table 1.1. – El Escorial criteria for the diagnosis of ALS

The El Escorial criteria (EEc)[7] was revised in 1997[8] and are used in the diagnosis of patients displaying combinations of UMN and LMN signs.

1.2 Epidemiology

ALS results in the death of approximately 500 Australians per year with a median survival of only 2 to 3 years from diagnosis[10]. While there are accurate data for deaths from ALS in Australia, there is no accurate measure of incidence or prevalence. In 2004, 507 Australians died from ALS[13]. The incidence estimate is 1 in 40,000, with the prevalence estimated as approximately 1 in 15,000 people. Therefore, there are approximately 1,300 to 1,400 people living in Australia with ALS.

Approximately 10% of cases of ALS are familial, with the other cases believed to be sporadic in aetiology. Mutations in a gene encoded on chromosome 21q22.1 involving the copper/zinc superoxide (SOD-1) account for ~ 20% of cases with familial ALS[14] but the remaining 80% of cases are caused by mutations on other genes, most of which remain to be discovered[15]. The SOD1 gene codes the superoxide dismutase enzyme, which is a free radical scavenger that reduces oxidative stress in the cytosol. More than 100 SOD 1 mutations exist[16]. Mutation D90A can either be recessive[17] or dominant[18]. The mutation A4V is the most common SOD1 mutation in North America, but this mutation is uncommon in Australia. Mutations can be substitutions, deletions or insertions. Different SOD1 mutations cause distinct syndromes[19, 20], although the variance of the age and site of onset is increasingly recognised[21]. Penetrance is typically 100%, but the SOD1 activity of erythrocytes, onset age, survival and clinical manifestation depend on the mutation. In rare kindreds, mutations have been linked to other genes including those that encode alsin[22], dynactin, VAMP association protein B and C (VAPB) and angiogenin ribonuclease RNASE A family 5 (ANG)[23].

The remaining 90% of ALS cases are thought to be multifactorial with both environment and genetic components[24-26]. Environmental factors, such as toxins, chemicals, metals, previous infections and trauma, may trigger a genetic susceptibility[10].

1.3 Pathology

ALS produces abnormalities primarily in the motor system, resulting in the dysfunction and death of the UMNs and/or LMNs. UMNs arise from the primary motor cortex, and project axons down the CST to synapse with the LMNs in the brainstem nuclei and spinal cord. LMNs then project axons to innervate muscles. (Figure 1.1) Clinically, LMN abnormalities produce muscle wasting, twitching (fasciculation), weakness and reduced reflexes. Disturbances of the UMNs produce spasticity, clumsiness, weakness, brisk reflexes and extensor plantar responses. Patients with ALS usually have a variable combination of UMN and LMN features, although their clinical presentation can either be LMN or UMN predominant, leading to the clinical heterogeneity that is typical for the disease. There is no single dominant theory regarding the pathogenesis of ALS[10]. There remains no universally recognized rating scale to categorise the severity and progression of patient symptoms, despite Charcot's clear original description[2]. The pathophysiology of sporadic ALS is still controversial[27], the only known cause for MND is the inherited version[28].

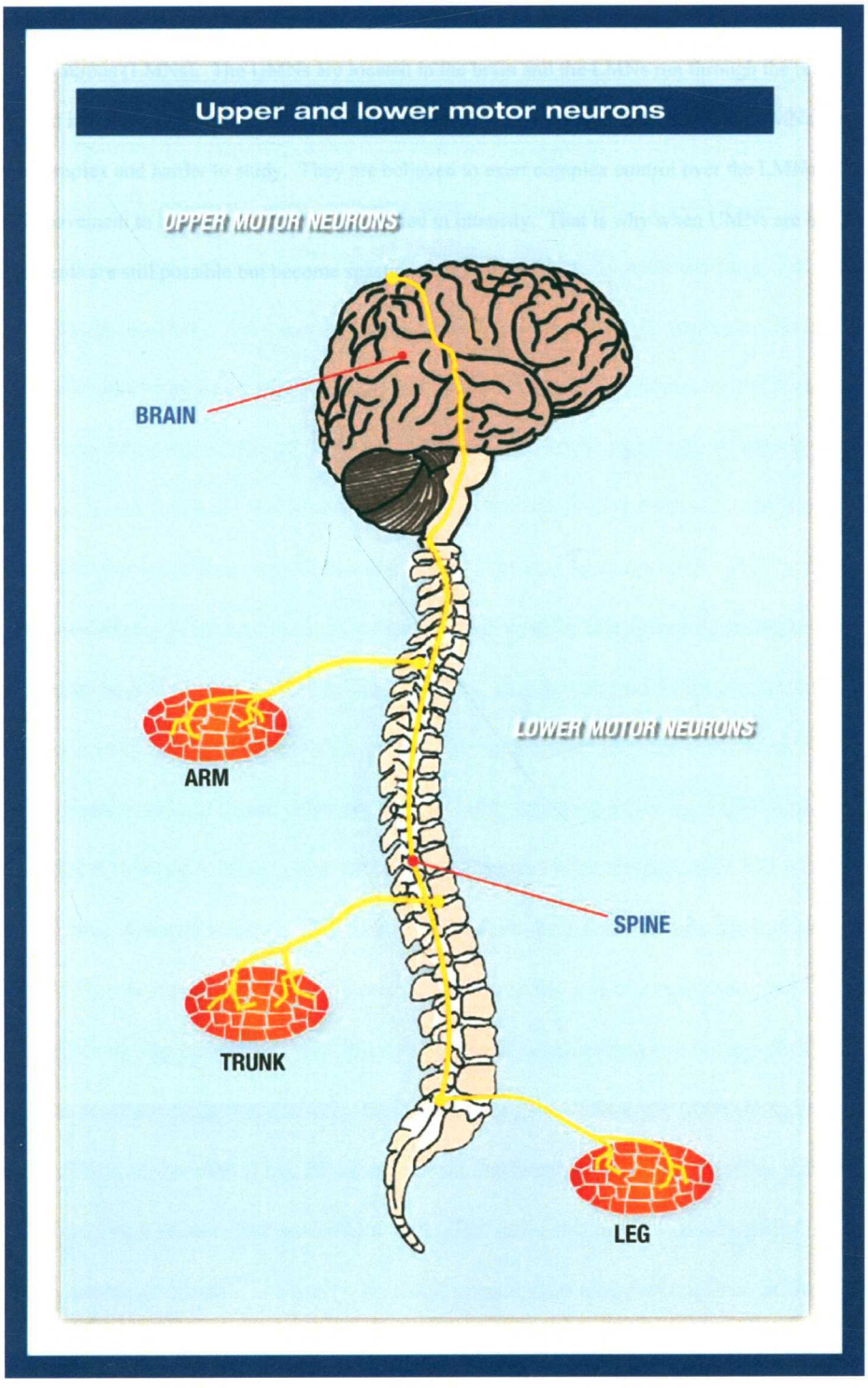
Upper and lower motor neurons
UPPER MOTOR NEURONS
BRAIN
ARM
LOWER MOTOR NEURONS
SPINE
TRUNK
LEG

Figure 1.1.

Figure 1.1. Motor neurons are divided into two types: Upper Motor Neurons (UMNs) and Lower Motor Neurons (LMNs). The UMNs are located in the brain and the LMNs run through the brain stem and into the spinal cord. LMNs send impulses to muscles to make them contract. UMNs are more complex and harder to study. They are believed to exert complex control over the LMNs. They allow movement to be smooth, directed and varied in intensity. That is why when UMNs are lost, movements are still possible but become spastic.

The mechanisms which are responsible for the selective death of motor neurons in ALS are not yet fully known. Numerous hypotheses exist, including: oxidative damage[29], toxicity from intracellular aggregates[30], cytoskeletal abnormalities[31], loss of trophic factor support[32] and glutamate-mediated excitotoxic neuronal damage[33] (Figure 1.2). All of these hypotheses may at least in some part be correct. They may all contribute to death of motor neurons. There is experimental evidence to partially support each of these hypotheses, but still the overall mechanisms which produce selective degeneration and death of motor neurones in ALS are not yet known. Recently, Caroni et al. genetically engineered SOD1 mice to have fluorescent markers in their motor neuron axons. This research uncovered three different types of muscles. Fast-twitch, fast fatigable muscles are the first to be affected in SOD1 mice; secondly, fast-twitch and fatigue resistant muscles and thirdly slow-twitch fibers that are in constant use, are unaffected[16].

Sanes and Lichtman developed time-lapse imaging in living SOD1 mice and determined two types of neurons within the same motor pathways in SOD1 mice: 'losers' and 'compensators'. The 'loser' type have their connections broken and die whereas the 'compensators' have new axonal branches and attempt to regrow[34]. This opens up the possibility that the environment surrounding the 'compensators' may not be supporting the growth. Neighbouring glial cells were once thought to have nothing to do with ALS, however recent findings suggest that healthy glial cells can protect sick motor neurons, whilst sick glial cells can induce degeneration in healthy motor neurons[16]. Finally, neurofilaments may also be involved in the ALS disease process. The number of neurofilaments is higher in larger diameter axons which are more susceptible to ALS. When high amounts of neurofilaments

accumulate in axons they block the flow of nutrients from the cell body to the synapse. One percent of all ALS cases arise from mutations in the gene coding for neurofilaments[16]. Intracellular transport may also be involved in ALS as many critical substances need to be transported within the axon. This requires molecular motors and a breakdown in any of these processes can lead to motor neuronal death[16].

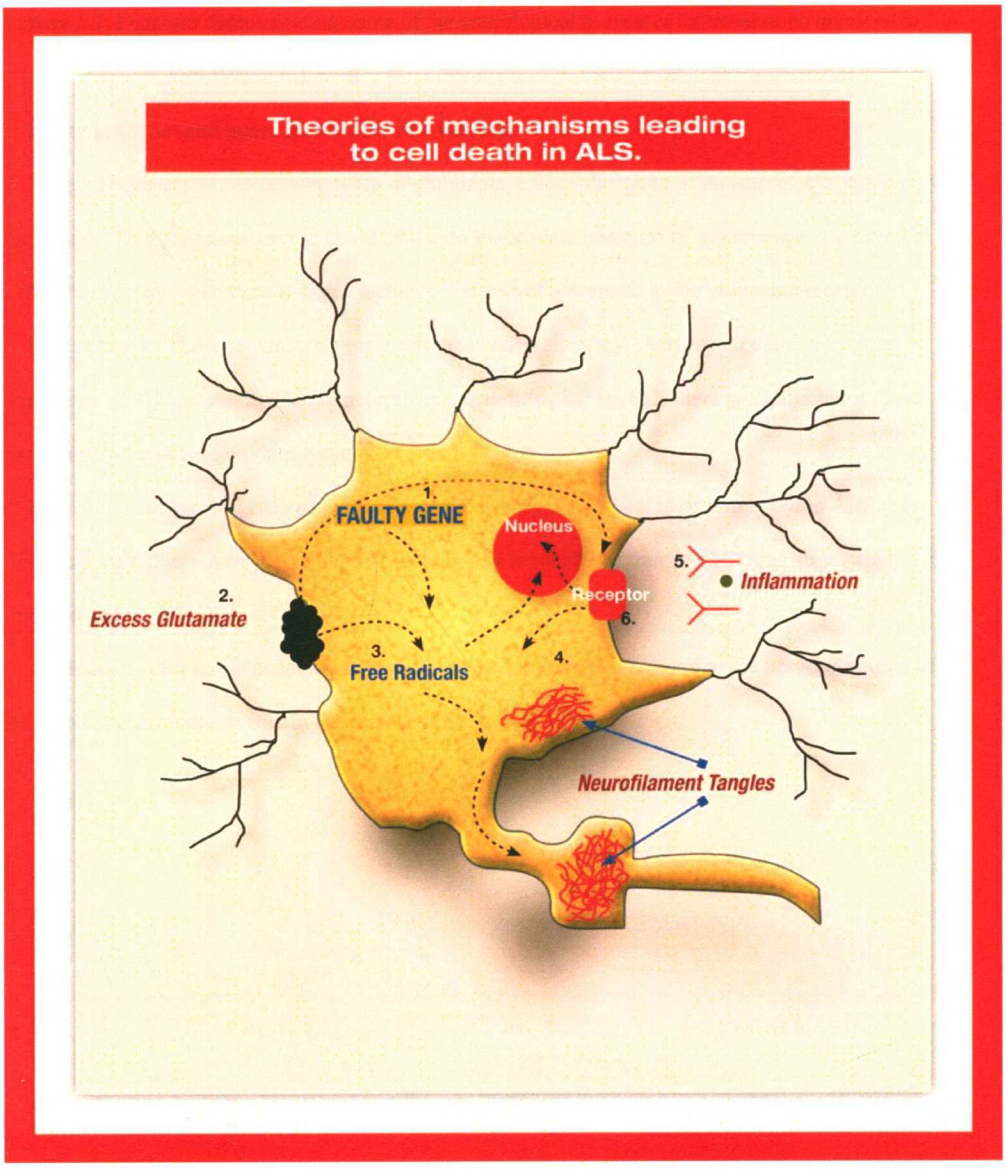
Theories of mechanisms leading to cell death in ALS.
1.
FAULTY GENE
Nucleus
2.
Excess Glutamate
3.
Free Radicals
4.
Receptor
5.
Inflammation
6.
Neurofilament Tangles

Figure 1.2.

Figure 1.2. Diagram demonstrating some of the pathological processes believed to be involved in ALS.

1. Faulty gene: Several genes are associated with ALS.

2. Excess glutamate: An excess build up of glutamate, causes the death of the nerve cells that receive the signal. This glutamate excess could be due to inadequate transport of glutamate away from the cell, or there may be an excess in production or release of glutamate in the glutamate receptors.

3. Free radicals: These are unstable molecules that carry electrical charges and damage cellular structures. Cells are usually able to neutralize free radicals but in ALS there is a build up of these molecules which cause oxidative stress.

4. Neurofilament tangles: Neurofilaments aids the nerve cells to hold their shape, but in ALS these filaments may clump near the cell body blocking any intracellular transport causing strangulation of the axon.

5. Antibodies, Immune Mechanisms and Glial cells: are sometimes found in the nervous system in ALS and appear to play a role in the disease process.

1.4 Assessment of disease progression in ALS

Clinical features in combination with neurophysiological investigation are required for the clinical diagnosis of ALS. There is no single test that enables the diagnosis of ALS. There are many conditions that can appear clinically similar, or even identical, to some forms of ALS and require careful consideration in the evaluation of the individual presenting with an ALS phenotype. The investigation of all of the alternative causes of clinical features similar to ALS is beyond the scope of this introduction and is dealt with in expert fashion elsewhere[35]. Nevertheless, potentially treatable LMN disorders confined to motor fibers such as immune-mediated demyelinating neuropathies[36-39] and multifocal motor neuropathy[40-46], must be identified by clinical evaluation Nerve Conduction Studies (NCS) and Electromyography (EMG), then supported by laboratory investigations. These neurophysiological investigations (NCS and EMG) are the cornerstone of the electrodiagnostic investigations of ALS[47, 48]. However, a motor unit has a limited repertoire of responses to different disease processes and therefore, alternative methods are required to investigate the LMN. Recent developments include methods to serially quantify the loss of motor units, in addition to techniques that may provide insight into the pathophysiology of ALS at the axonal level. These include: Motor Unit Number Estimation (MUNE), Threshold tracking methods of axonal excitability and Transcranial Magnetic Stimulation (TMS).

1.4(i) Motor Unit Number Estimation (MUNE)

The motor unit consists of the anterior horn cell in the spinal cord, its corresponding motor axon, neuromuscular junctions and muscle fibers. The associated weakness in ALS is due to the progressive loss of motor units which can

be quantified with strength testing[49]. This weakness is only apparent with a moderately severe loss of motor units by denervation, partially compensated by reinnervation of the muscle fibers caused by the sprouting of the surrounding 'normal' motor units. As nerve biopsy is impractical, a neurophysiological method to measure the loss of motor units was developed, termed MUNE[50].

The aim of MUNE is to determine the number of motor nerves supplying a muscle. For MUNE to be usefully incorporated into the evaluation of therapy in ALS clinical trials, a MUNE method needs to be widely available on EMG machines and applicable to different disease stages. There are various methods of estimating the number of motor units. The first method of MUNE was developed by McComas[51, 52] and made use of the gradual increments in the compound muscle action potential that happen with small initial increases in stimulus intensity. Unfortunately, this method was recognized as unreliable when motor-unit firing is variable (alternation or probabilistic firing)[53].

Another early method made use of the volley from an anterior horn cell after retrograde travel of the stimulus, also known as the F-wave[54]. Through calculation of the mean size of reproducible F-waves and division into the total compound muscle action potential, the number of motor units is estimated. This technique is simple but has given variable results, so is now rarely used in the evaluation of ALS.

Calculation of the mean motor-unit size and sampling of the motor units along different parts of the nerve (multiple point stimulation), or using surface EMG to show single motor units (spike-triggered averaging) are now more commonly used[55-57]. Spike-triggered averaging has the advantage of including different nerve-

muscle combinations. Multiple point stimulation is the most widely used MUNE technique and correlates with histological methods[58].

As there is variable activation of motor units after stimulation, statistical MUNE techniques were developed. The most widely used is the Poisson statistical method[59], which seems faster and more reproducible than the multiple point stimulation method[60]. The Poisson method was modified to enable calculations of a mean motor-unit size, it is reasonably reproducible in ALS patients with moderate severity[59-62] but is not as accurate in advanced ALS patients[63, 64].

MUNE has been used as a clinical assessment tool in ALS with varying success. The incremental method and multiple point stimulation methods successfully follow the loss of motor units over time[57, 65], arguably more accurately than other clinical and respiratory measures of disease progression[65, 66]. A multi-centre trial of creatine for ALS used the Poisson statistical method found a 23% decline in MUNE over a 6 month period[64]. A widely available method which is reliable and applicable to different ALS stages needs to be available in order for MUNE to be utilised in clinical trials. Bayesian statistics may be applied to MUNE in the future to establish such a method[67].

1.4(ii) Measurement of Axonal Excitability by Threshold Tracking

Threshold tracking measurements of nerve excitability are sensitive to membrane potential at the site of stimulation and complements conventional nerve conduction studies[68]. Membrane potential and the biophysical properties of peripheral axons can be produced by changes in excitability by a combination of test and conditioning currents.

The first clinical application used the method of threshold electronus[69] and found that peripheral axons in ALS had abnormal membrane properties despite having normal conduction velocities. There was an increase in excitability when the axonal membrane was depolarised ("Type 1 response"), due to a reduction in potassium channel activity. Further studies confirm that threshold electronus is commonly abnormal in ALS[70, 71] with the additional finding of high persistent sodium ion conductances[68, 72]. A decrease in potassium would decrease hyperpolarizing tendency, an increase in sodium would increase a depolarising drive. Together, this probably underlies the axonal hyperexcitability present in many ALS patients and may contribute to the development of fasciculation and cramp[73, 74].

Whether nerve excitability techniques are effective in picking up abnormalities in axonal properties remains largely unanswered, as there still remains a degree of variability when applying such techniques to investigate patients serially. This is probably due to the fact that these studies only provide information about the surviving normal and injured axons[75] and provide no information about destroyed axons. Longitudinal studies show that abnormal waveforms subsequently normalise despite the disease progression, probably due to the death of the previously abnormally responding axons[75]. One way to measure disease severity may be to study the behaviour of a single motor unit. However, this may not be a clear representation of the patient overall, thus a combination of motor unit observation and nerve excitability is probably the best representation[76-78].

1.4(iii) Transcranial Magnetic Stimulation (TMS)

TMS is the only neurophysiological method available to study UMN function and cortical abnormalities. TMS allows insight into the discharge characteristics of

single motor units or compound motor responses. Numerous studies using TMS examining cortical changes in ALS show somewhat varied findings (Table 1.2). While TMS is non-invasive and well tolerated by patients, universally accepted criteria need establishing before it can become a useful surrogate marker for UMN dysfunction or loss in ALS. As TMS ultimately requires measurement via the muscle action potential, TMS is not effective in patients who have lost their muscle action potential in their hands.

Cortical motor threshold The current needed to stimulate the motor cortex is normal or low early in the course of ALS, possibly owing to reduced inhibition, and increases with disease progression[79]
Cortical silent period The pause in electromyographic activity after motor-cortex stimulation is reduced in ALS[80-82], possibly owing to loss of GABAergic neurons and motor-cortex reorganisation.
Peristimulus time histograms TMS changes the firing of the motor unit such that there is higher resynchronisation over time, [80, 82], reflecting dysfunction of corticomotoneuron pathways[83]
Central conduction time The latency from cortex to selected limb muscle is normal or slightly prolonged in ALS owing to preferential degeneration of the fastest axons, derived from larger anterior horn cells.
Motor evoked potentials Activation of motor units by TMS suggests upper motor neuron dysfunction and seems to relate to functional deficit.

Table 1.2. TMS measurements routinely used in patients with ALS.

TMS is a non-invasive technique used to identify UMN involvement in ALS. Numerous parameters are found to be abnormal in ALS. The cortical motor threshold, cortical silent period, peristimulus time histograms, central conduction time and motor evoked potentials, are just a few of the most popular parameters studied.

Cortical motor threshold and central conduction time are the most frequently used parameters. TMS also measures cortical excitability in an attempt to elucidate the initial site of involvement of motor pathways in the development of ALS[82].

There are conflicting reports concerning the correlation between TMS abnormalities and the degree of UMN involvement in ALS, which this chapter will subsequently review. In addition, a novel method of TMS, using threshold tracking techniques to explore excitability of cortical motor neurons[84], will be discussed further in Chapter 3.

1.5 Functional Scales in the Assessment of Progression of ALS

At present, the best balance between function, impairment and disability is still unavailable in a single ALS functional scale. Ideally, functional scales should provide a measure of these different aspects of ALS, reliably and independently. Most functional scales rely on patient self report methods, often in conjunction with scales ranked by clinicians using items related to the function of different anatomical domains. Given that these clinical scales are often undertaken in a multi-disciplinary ALS clinical setting, issues related to ease of completion, method of administration, time and training required, equipment, fatigue and psychological effects are all key factors when determining which scale to use[85]. The study sample is equally critical: if small standard deviations of a clinimetric scale score are obtained, the study may not represent the broader range of ALS patients[85]. Finally, the scale selected needs to have high inter-rater reliability to ensure consistency by examiners while remaining responsive to change[85].

1.5(i) Norris Scale

The ***Norris scale*** was the first of many ongoing attempts to quantify the progressive deficit in ALS[86]. This scale appeared reliable since it integrated clinical and functional data with linear decline, and was used in numerous clinical trials[87]. Twenty-two functional parameters were used including bulbar, respiratory, trunk, arm, leg and general domains, with additional ratings for clinical signs (e.g. reflexes, fasciculations, muscle atrophy). While capable of measuring impairments and disabilities in a single patient, the key disadvantages of the Norris scale were that disparate parameters were equally weighted (for instance, breathing and the ability to empty the bladder were equal), and the scale could be insensitive to change due to a 'ceiling effect', particularly as it uses a limited rating scale of 0-3[88].

1.5(ii) Appel Scale

The ***Appel scale*** provided compound quantitative estimates of clinical status linked to ALS disease progression. Bulbar, respiratory, muscle strength, lower extremity function and upper extremity function were all assessed. The scale yielded reproducible data for each group of functions tested, leading to a 'total' ALS score[89]. One disadvantage of this scale is that it needs to be carried out by the clinician and cannot be administered via the telephone.

1.5(iii) ALS Functional Rating Scale (ALS FRS)

The ***ALS functional rating scale*** (ALS FRS) was designed with disease-related disability as the focus. Whilst generally regarded as being internally consistent and reliable, this scale requires that all parts are performed by the same assessor at each visit[85, 87]. The total score obtained from using ALS-FRS at the time

of diagnosis significantly correlated with the progression of symptoms and ALS outcome[90], prompting incorporation of this scale into numerous pharmacological trials[91]. However, there remain problems using the scale, particularly when assessing patient swallowing with the *bulbar sub-score,* measured by means of the patient's diet (e.g. chopped or ground foods, or thickened liquids), showing poor correlation when compared to videoflourography[92].

The other chief weakness of the scale, is the disproportionate weighting of limb and bulbar measurements relative to respiratory dysfunction[88]. A revised version (ALSFRS-R) incorporates additional assessments of dyspnea, orthopnea and need for ventilation[93]. This revised scale correlates with the Global Clinical Impression of Change (GCIC) scored by neurologists[94] and sickness impact profile[93]. However, direct comparison of Appel, Norris and ALSFRS scales has established different responsiveness of each over time, a major drawback in the incorporation of such scales into a clinical trials setting[85] (Table 1.3).

Time	Scale	Measure	Advantages	Disadvantages
1979	Norris	Integrated clinical and functional data	Reliable, linear decline, easy to administer[87], used in riluzole clinical trials[95, 96]	Bulbar and respiratory function only assigned 21% of total-score weighting Assesses bowel and bladder function (typically not affected) Self reported symptoms, functions and clinical signs are combined (mixes impairments and disabilities)
1989	ALSSS (Hilliel)	Pure disability, four domains (two bulbar, spinal and FVC)	Valid, sensitive, reliable, easy & quick[87]	Excludes respiratory assessment Poor prognostic information
1987	Appel	Clinical and functional data, five domains: bulbar, respiration, strength, UMN or LMN	Five ratings per domain, simple, validated, reliable, easy to administer. Used in IGF-I clinical trials[97, 98]	Reproducibility not widely accepted Difficult to use in patients who are severely affected. Unclear relation to function Mixes impairments and disabilities.
1996 1999	ALS FRS ALS FRS-R	Ten domains, including three bulbar, two UMN, two LMN and one respiratory	Easy to administer and sensitive to change. Widely used in clinical trials (BDNF[99], CTNF[100, 101], gabapentin[102, 103], Xaliproden and topiramate[104].	Reliability of statistical methods questioned. Assessment grades are arbitrarily assigned.

Table 1.3. Functional scales for the assessment of patients with ALS.

Numerous functional scales exist for ALS. The Norris scale was the first one to be developed in 1979 and the most recent one is the ALSFRS-R scale. All of the scales have their own advantages and disadvantages. A functional rating scale is vital for the ongoing assessment of ALS patients.

1.6 Imaging Techniques

Diagnosis of ALS is currently based on the clinical history of a patient with progressive weakness in a pattern typical of upper and lower motor neuron involvement, typical electrophysiological findings and the exclusion of other conditions[7, 105] . The primary role of imaging studies in ALS is to rule out an alternate cause for UMN pathology in a patient with suspected ALS. Imaging is able to exclude alternative causes of impairment of the CST as it passes from the motor cortex, through subcortical white matter, through the brainstem to the motor nuclei and down the spinal cord synapse on the LMN.

A secondary and more recent role is to evaluate possible diagnostic changes on MRI with ALS, and to assess correlations between the ALS disease progression and the MR abnormalities[106] .Many neuroimaging studies like proton magnetic resonance spectroscopy[107-109] , positron-emission tomography[110] and magnetization transfer contrast[111, 112] have tried to determine the characteristics of ALS but there is a considerable overlap between patients and controls[113] .

1.6(i) Magnetic Resonance Imaging (MRI)

Magnetic Resonance Imaging (MRI) is non-invasive using, nuclear magnetic resonance to obtain images of an object. It relies on the relaxation properties of excited hydrogen nuclei in water and fats. Studies in ALS show pathological alteration of the UMN in some ALS patients. The involvement of the CST is investigated using various MRI techniques. T2 weighted sequences[114] , proton density sequences[115, 116] and Fluid Attenuated Inversion Recovery (FLAIR) sequences[117] , sometimes show changes in the signal intensity along the internal capsule (Figure 1.3). T2-weighted images are reported to sometimes show

hypointensity in the gray matter of the motor cortex next to the central sulcus[115-120] and in the precentral gyrus.[114, 116, 118, 121] Signal changes are predominantly and more frequently identified in FLAIR sequences[116, 117]. In FLAIR studies the signal increase is most readily identified at the posterior limb of the internal capsule[116] and could reflect abnormal water content in the CST fibers[112, 122] and magnetic resonance spectroscopy show abnormal values in the primary motor cortex[123-125]. These abnormalities may represent abnormal water content, and may represent oedema, gliosis, and/or Wallerian degeneration at various stages of the disease[126].

Signal change in the CST is not specific for ALS and can also occurs in ischemic disease, vitamin B12 deficiency and Friedrich's ataxia[127, 128]. There may be high signal in the posterior limb of the internal capsule bilaterally in normal controls[129-132] which may be due to the presence of large fibers with thick myelin sheaths[126].

The sensitivity and specificity of the presence of UMN involvement that conventional imaging offers is variable, depending on the sequence parameters used and the subjective observations of the rater[114-116, 118, 133-139]. There are no commonly used MRI sequences or analyses in the diagnosis or assessment of the progression of ALS.

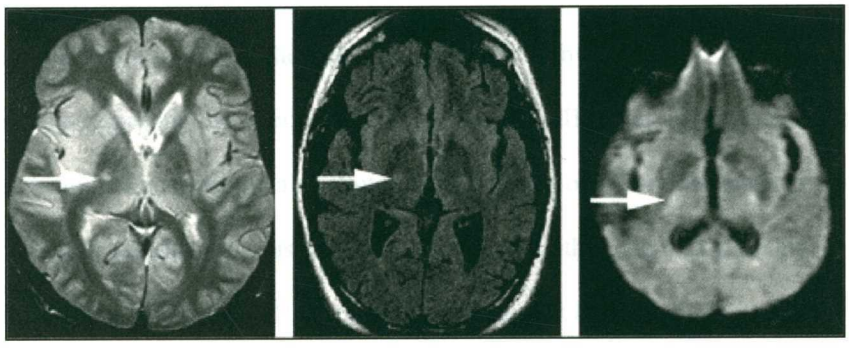

Figure 1.3. Imaging techniques for the identification of corticospinal-tract abnormalities in ALS . (refer to Appendix D for Winhammar et al. 2005). Axial proton-density-weighted image (left), fluid-attenuated inversion-recovery image (middle), and diffusion-weighted image (right), of patients with upper motor neuron features in ALS.

The arrows show areas of axonal degeneration in the corticospinal tracts.

1.6(ii) Proton MRS

Proton Magnetic Resonance Spectroscopy (Proton MRS) obtains biochemical information about tissues in the human body in a non-invasive way. MRI gives information regarding the structure of tissue whereas MRS can be tuned to detect signals from different chemicals. Protons (hydrogen atoms), are the most common signal studied but phosphorous, sodium, fluorine and other chemicals are also studied. Proton MRS (1H-MRS) studies have assessed UMN pathology in ALS[108, 123, 124, 140-142]. These studies show a reduction in the N-acetyl-aspartate (NAA) / Creatine (Cr) ratio in the motor cortex in ALS[108, 141, 143]. As NAA is only found in the nerve cell bodies, its induction is attributed to neuronal loss and dysfunction[124, 140, 141, 144]. This reduction is also found in the brain stem[144] unfortunately there is again an overlap between patients and controls[124, 145]. Progressive reduction in NAA/choline and NAA/Cr ratios exist in the motor cortex of ALS patients on follow-up visits,[108] suggesting a potential role for this technique as a disease marker. NAA/Cr ratios are also decreased in ALS in the precentral gyrus[108, 123, 125, 141, 145-148].

Although spectroscopy studies show a reduction in N-acetylaspartate (NAA) in the motor cortex of ALS patients there is a need for a standardized routine clinical evaluation[149]. This technique is criticized for not being very sensitive in the early stages of the disease[125, 145]. However, in a stereological study, the average number of neurons in the motor cortex in ALS patients was identical to that of the control group[150], suggesting neuronal dysfunction, rather than neuronal death, may produce the reduced NAA in the motor cortex of ALS patients.

1.6(iii) Diffusion Tensor Imaging (DTI)

DTI is a MR technique sensitive to the diffusion of water molecules[151] and may be able to detect neuronal and axonal abnormalities earlier than conventional imaging techniques[152, 153] as water diffusion is not the same in all directions in brain white matter. This limitation of water diffusion in the white matter of the brain is referred to as an anisotropic tissue[154] and is fully expressed by the effective symmetric diffusion tensor, **D**. Diffusion refers to Brownian motion (random translational motion of molecules) resulting from the molecules' thermal energy. DTI measures diffusion tensor **D** and further analysis is able to give detailed information about the tissue. The apparent diffusion coefficient is a quantitative measure of diffusion in one direction and can be derived by acquiring a series of images with differing amounts of diffusion weighting in a single direction.

Eigenvectors and eigenvalues (Ev1, Ev2 & Ev3) represent the main diffusion directions and associated diffusivities of water molecules[151]. The largest eigenvalue (Ev1) is the direction of the fastest diffusion corresponding to the fiber direction. The smallest (Ev3) and middle value (Ev2) are used to determine diffusion along the orthogonal directions perpendicular to fiber bundles. Fractional Anisotropy (FA) and Trace ADC (or sometimes referred to as mean diffusivity, MD) are commonly derived values and are used for quantitative maps of isotropic and anisotropic diffusion in tissues and can be represented as colour maps (Figure 1.4). Trace ADC and FA can be compared between individuals as they are orientation independent[155].

Trace ADC assesses the restriction of movement of water molecules, regardless of direction, low diffusivity implies more restriction and vice versa.

Water molecules collide with cell membranes and macromolecules in biological systems. Thus, in white matter the Trace ADC value is low[156]. Water molecules move readily in parallel to the principal direction of structured material such as nerve fibers[154, 157-159]. Tractography is a procedure to demonstrate neural tracts which are carried out by fiber tracking in DTI (Figure 1.5). This enables locating white matter tracts throughout the brain.

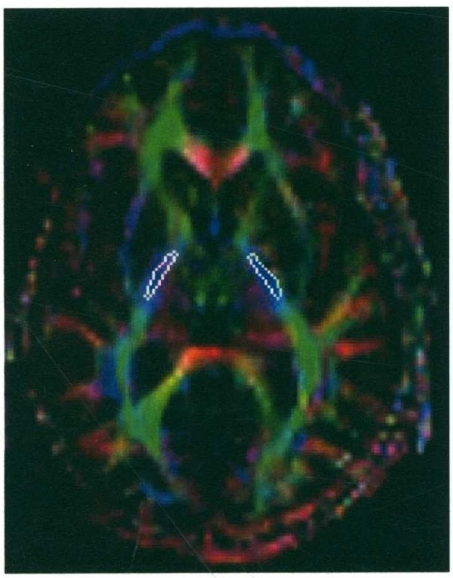

Figure 1.4. DTI Colour-coded white matter fiber maps are generated on the basis of fractional anisotropy and vector maps (red = x axis – right to left, green = y axis – posterior to anterior and blue = z axis – foot to head) . White circles demonstrate manual regions of interest.

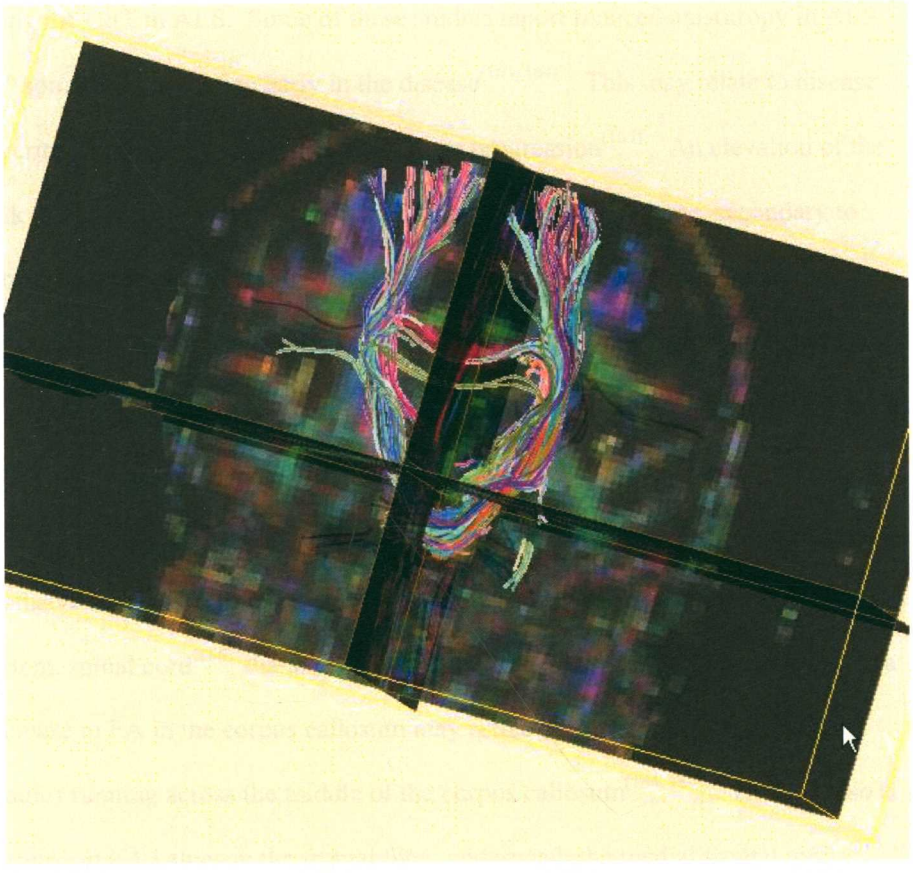

Figure 1.5. Tractography using DTIstudio

Tractography calculates the position of white matter tracts within the brain and spinal cord. It infers continuity of fibers from voxel to voxel and reconstructs a putative white matter pathway based on probability[160]. The Corticospinal Tract (CST) is easily identifiable from motor cortex, as it runs through the internal capsule to the brainstem when using tractography[160].

Numerous studies show abnormalities in FA and bulk diffusion within areas along the CST in ALS. Some of these studies report reduced anisotropy in ALS[161, 162], sometimes occurring early in the disease[163, 164]. This may relate to disease severity[161] and may correlate with disease progression[165]. An elevation of the bulk diffusion may represent an increase in extracellular volume, secondary to axonal loss. Although changes in bulk diffusion and FA are not disease specific, they may add to the pathophysiology of ALS. Whole brain diffusion tensor images in patients with ALS reveal that FA in the CST is lower in ALS from the capsules to the pyramids[162].

Previous DTI findings demonstrate that the neurodegenerative process is not exclusive to the motor pathways in ALS but also affects the basal ganglia, limbic system, spinal cord[166] thalamus and corpus callosum[164]. Findings suggesting a decrease in FA in the corpus callosum may reflect degenerated pyramidal tract bundles running across the middle of the corpus callosum[164, 167]. There is also a decrease in FA values in the frontal lobe, underneath the medial frontal gyrus[110, 142, 164] and in the thalamus[164].

There are a few limitations regarding DTI such as diffusion being highly variable[168, 169]. Diffusivity and diffusion anisotropy values are substantially affected by architectural and structural features[168-170]. For example, diffusion anisotropy is high in the cerebral peduncle and low in the pons and medulla. The reduction of diffusion anisotropy cannot be attributed to true pathological changes because there are **anatomical mismatching results**. In the pons and medulla, anisotropic values vary greatly between contiguous slices, showing histological heterogeneity. Pyramidal tracts in the medulla are very small and close to other

structures making it prone to partial volume **contamination**. However, it is believed that the cerebral peduncle shows similar diffusion anisotropy values in all slices in both patients and controls and thus are relatively homogenous and may be an ideal region to investigate for potential "pathological" changes.

It is believed that DTI can be used to detect early lesions of the CST in patients with ALS[164] and may be used for earlier diagnosis and possibly as a disease marker.

No convincing correlations exist between markers of clinical disability and indices of water diffusion but this may be due to the functional scale used not being able to monitor the clinical involvement of the UMN with sufficient sensitivity[162].

DTI was chosen as a tool to measure UMN involvement in ALS for this project due to its ability to measure the integrity of white matter tracts early in the disease process as it measures the diffusivity of water rather than an actual pathological mechanism. Tractography also aids in finding the location of the CST, using programs that locate tracts that are connected within the brain, instead of having to use a 'best guess' model. This enables the location of the CST with more accuracy than with any other imaging technique.

1.7 Respiratory Function in ALS

Death in ALS patient is usually from respiratory failure, a direct consequence of muscle weakness during the endstages of the disease[171]. Forced vital capacity (FVC) does not predict survival, but the rate of change in the FVC value gives an idea of the decline in respiratory function in the patient. Most trials of MND therapy use FVC as a survival indicator.

A proportion of patients develop early and severe respiratory difficulties during sleep, termed nocturnal hypoventilation (NH). NH is a predictor of survival, independent of respiratory muscle weakness[172]. Nocturnal hypoventilation (NH) can be measured using over night oximetry and carbon dioxide retention and is very much dependent on the measure. Velasco et al. demonstrated that a mean nocturnal arterial oxygen saturation of less than 93% is predictive of a dramatically shortened mean survival of less than six months.

There is a high incidence of NH in ALS, although the mechanisms that produce NH are not known[173]. ALS patients may have nearly normal daytime pulmonary function, but severe NH. It is suggested that ALS patients with excessive daytime sleepiness or insomnia should undergo sleep studies of breathing and Polysomnography (PSG) to diagnose nocturnal respiratory insufficiency and/or sleep disturbance[174, 175].

Sleep itself may negatively influence respiratory function. During rapid eye movement (REM) sleep there is an additional decrease in muscle tone, which can lead to complete muscular atonia (excluding the extra ocular and diaphragmatic muscles). This decrease in muscle tone can lead to a reduction in the upper airway diameter and increase in airway resistance[174], resulting in NH. The consequences

of NH are elevation of carbon dioxide and a fall in arterial blood oxygen concentration. When oxygen levels fall to a critical level, protective mechanisms induce arousals from sleep, so that the patient does not become unconscious as a result of respiratory failure. These arousals result in sleep fragmentation. Eventually, sleep fragmentation produces daytime fatigue, somnolence, impaired cognition and other physical symptoms such as headache, due to an increase in $PaCO_2$.

There is a strong correlation between NH, survival and quality of life in ALS[172, 173, 176]. NH may also have an effect on cognitive function, which may be reversed by non-invasive ventilation[177], a recent respiratory intervention that uses bi-level intermittent positive pressure ventilation (Bipap). This method of ventilation reduces the work of breathing, improves gas exchange, exercise tolerance and sleep quality by improving nocturnal respiratory insufficiency[178]. Another study of Bipap in ALS demonstrated that if it was used for >4 hours a day, patients had a slower decline in vital capacity and prolonged survival[179].Thus NH is a potent factor in cognitive function, quality of life and survival in ALS. However, little is known of the mechanisms that produce NH in ALS and this is the main focus in Chapter 2.

The initial hypothesis for this study was that NH in early ALS was a manifestation of UMN involvement. From the literature, NH was not predicted by routine respiratory function tests, and therefore better instruments to measure early change in the UMN and its projection, the CST, were required. It was sought to determine whether NH was indeed predicted in early ALS by routine respiratory tests, and to measure cortical abnormalities via TMS and the CST via DTI.

2. Respiratory Function Tests and Nocturnal Hypoventilation in ALS

Aim

This chapter is written in two parts. The first study was designed retrospectively, to see whether standard respiratory function test, that are routinely used in the ALS clinic, can identify ALS patients with NH from those without NH, and also if there is any difference in the respiratory function in ALS patients when compared to controls. This initial study was published in the internal medicine journal, (refer to Appendix D for Winhammar et al. 2006). In a subsequent study routine RFTs were repeated in addition to newer measurements of respiratory function (SNIF and FOT).

2.1 Introduction

Amyotrophic Lateral Sclerosis (ALS) produces weakness and ultimately death occurs very often from respiratory failure. Muscles of respiration are invariably affected in ALS and most people die from respiratory complications. While a small percentage of patients with ALS initially present with severe respiratory muscle involvement [180, 181] there is no reliable method to predict when respiratory muscle weakness will occur. All patients will eventually develop respiratory muscle impairment, which makes respiratory management extremely important[182] which can improve both the quality of life and survival of the patient[183].

Respiratory function can be assessed in numerous ways and each method has its own advantages and disadvantages. Respiratory function tests can be categorized into those which test inspiratory muscle strength, expiratory muscle strength, diaphragmatic strength and overall respiratory function tests. The diaphragm largely

controls inspiration but is also assisted in inspiration by accessory muscles. During a forced expiration such as a cough, abdominal muscles contract, as otherwise this part of respiration is passive. Inspiratory strength is most commonly measured by maximal inspiratory pressure (MIP) but is effort dependent and thus difficult for some people to perform[184].

The gold standard for measuring inspiratory pressure is to insert a balloon catheter into the stomach and mid-esophageus and then measure the pressure difference across the diaphragm. This technique is invasive and not well tolerated by many patients. A more recent test to measure inspiration is Sniff Nasal Inspiratory Force (SNIF) which involves inserting a pressure transducer into one nostril[185]. Common tests for measuring expiratory strength are Maximal Expiratory Pressure (MEP) and cough peak flow. Spirometry measures pulmonary function and Forced Vital Capacity (FVC). This is usually reduced in ALS and reflects changes in the airways, muscles, chest wall and lung parenchyma[182]. Standard respiratory function tests such as volumes, MIPs, MEPs and plethysmography are routinely carried out in ALS patients to assess the need for intervention and management.

There are a battery of respiratory function tests that are used to measure respiratory decline in ALS. These include: spirometry, plethysmography, maximal inspiratory/expiratory pressure, diffusion of gases, sniff nasal inspiratory pressure.

Spirometry is a measure of ventilatory function that reflects the limits of the elastic properties of the lungs and resistance of the airways. It is a useful screening test and can detect, quantify and monitor resistance properties of the airways. The measure is non specifically affected in ALS and can be abnormal in numerous other diseases. The actual measure involves a maximal inspiration and then a forced

expiration, while recording the time and volume. Measures of spirometry include: Total Lung Capacity (TLC), Residual Volume (RV), Forced Vital Capacity (FVC), Peak Expiratory Flow (PEF) and Forced Expiratory Volume in one second (FEV1).

Whole body plethysmography is a rapid and accurate way to measure absolute lung volumes. The total compressible gas in the thorax is measured and this is unaffected by the presence of any poorly ventilated air spaces. It can also use a pressure plethysmograph to determine changes in the alveolar volume.

Another common respiratory function test is the carbon monoxide diffusing capacity (DLCO). This is obtained by measuring the rate of transfer of carbon monoxide (CO) across the alveolar-capacity membrane into the pulmonary capillary blood from an inspired gas. The test gas consists of air containing 0.3% of carbon monoxide and is diluted with an inert gas.

Maximal respiratory pressures measure both the Maximum Inspiratory Pressure (MIP) and Maximum Expiratory Pressure (MEP). This measures all of the muscles involved in respiration (the diaphragm, intercostal and accessory muscles). The diaphragm is the major inspiratory muscle, when it contracts it elevates and expands the lower rib cage. The accessory muscles, which elevate the upper rib cage and the intercostal muscles, are also involved in inspiration. The muscles in the abdominal wall, the intercostal and pectoral muscles are all involved in expiration.

While respiratory failure in ALS patients is a direct consequence of muscle weakness during disease end-stage[171], a proportion of patients develop early and severe respiratory difficulties during sleep, resulting in NH. There is an imprecise relationship between clinical weakness, its distribution or the site of first onset, and the onset of respiratory muscle involvement in the early stages of the disease, as

some patients develop NH without manifesting respiratory muscle weakness. NH is increasingly recognized as a predictor of survival, independent of respiratory muscle weakness. Velasco and colleagues (2002) demonstrated that a mean nocturnal arterial oxygen saturation of less than 93% is predictive of a dramatically shortened mean survival time of less than six months[172].

The mechanisms involved in NH in early ALS are largely unexplained. It is observed that Rapid Eye Movement (REM)-related desaturation often precedes the development of daytime symptoms of respiratory failure. This suggests that simple measures of lung physiology, even when considered along with daytime symptoms, are poor predictors of respiratory failure in sleep and therefore survival in ALS.

Consequently, the initial aim of this study was to explore the relationship between commonly utilised respiratory function tests and nocturnal oxygen saturation levels in patients with limb onset ALS.

In the second part of this chapter additional subjects were recruited and underwent further tests using Sniff Nasal Inspiratory Force (SNIF) and Forced Oscillatory Technique (FOT). Sniff pressures are measured by plugging one nostril during a maximal sniff through the other non occluded nostril and is an easy natural effort. SNIF calculates intra-thoracic pressure during a maximal sniff enabling assessment of inspiratory muscle strength. This technique can eliminate problems with mouth leak around a mouthpiece.

In FOT, a range of frequencies are applied to the air (forcing the air to oscillate) that a subject breathes during tidal breathing. A transducer records the patient's airflow and air pressure, which is related to the mechanical properties of the airways, lungs and chest wall. As energy is required to move air into the lungs, the

viscosity of the air and the calibre of the airways determine the amount of energy that is required. The amount of energy required to move one litre of air into the lungs in one second is recorded as the resistance. The resistance increases as the friction increases due to a decrease in the airway diameter e.g. bronchial - constriction. This technique uses the principle that when a known flow is applied through a single tube and the resulting pressure change is recorded then resistance can be calculated. Thus, resistance is inversely proportional to the cross sectional area of the tube squared. As the diameter of the tube decreases the resistance increases. The lungs are more complicated than a single tube. There is varying flow due to the differences in the size and shape of individual airways. Elastic properties of the respiratory system also contribute to making the calculation of airflow resistance more complex. However, a known oscillating flow applied to the air at the mouth results in an oscillating pressure signal and subsequently resistance can be calculated. As there may be considerable variability over time the measurement needs to be applied for a sufficient amount of time to obtain an appropriate estimate of the mean resistance. No previous studies of FOT in ALS exist in the literature.

FOT is a novel technique that measures the resistance and reactance in the respiratory system. It requires minimal patient cooperation and is ideal for the determination of the respiratory function in patients with ALS. SNIF has been shown to be a predictive measure of survival, with sensitivity and specificity greater than conventional lung function tests[186]. These techniques will be described in more detail later in this chapter.

2.2 Methods

Data set A

Data was collected during the course of standard ALS assessments from sixteen consecutive, limb-onset ALS patients with no symptoms of diurnal respiratory failure or nocturnal hypoxia. All patients were diagnosed with ALS by El Escorial criteria[105], referred to the Multidisciplinary ALS Clinic at Royal North Shore Hospital. In addition, nine healthy controls underwent similar assessment. The study approved by the Human Ethics Committee at Royal North Shore Hospital.

Data set B

Data was then collected from a further ten consecutive early ALS patients without respiratory symptoms. All patients were diagnosed with definite ALS by El Escorial criteria[105] and were referred to the Multidisciplinary ALS Clinic at Royal North Shore Hospital (Table 3.1). In addition, ten healthy controls underwent similar assessment with the study approved by the Human Ethics Committee at Royal North Shore Hospital.

All subjects underwent one night of continuous nocturnal oximetry (Invivo 4500 Oklahoma, USA & Stardust, Respironics, Pennsylvania, USA). All ALS patients were taking riluzole as part of their therapy.

2.2(i) Polysomnography studies

Polysomnography (PSG) was performed for 6-8 hours of nocturnal sleep in patients with ALS, using a standard 21 channel computerised polysomnography apparatus (Compumedics E-Series Multi-channel, Melbourne). All of the control

subjects underwent portable sleep monitoring (Stardust, Respironics, Pennsylvania, USA), and underwent full polysomnography if indicated by the portable data.

Collected data included: electroencephalogram (EEG) (Multi-channel C3, C4, A1 & A2), submental electromyography (EMG), electrooculography (EOG), thoracic and abdominal movement by inductive plethysmography, airflow by pressure transducer, airflow by thermistor, finger oximetry, tibialis EMG and diaphragmatic surface EMG.

Apnoeas and hypopneas were defined according to standard criteria as a greater than 10 second obstructive apnoea (complete cessation of airflow) or obstructive hypopnoea (50% or greater reduction in tidal volume)[187]. All respiratory events required a >/= 4% desaturation with a 10 second duration to be included in the analysis. The total apnoeas and hypopneas for REM and NREM sleep were derived separately. An average across the night score was calculated to derive the total respiratory disturbance index (RDI). All the PSG studies were independently scored by the same experienced senior sleep physiologist. All the sleep studies were then reviewed and reported by an experienced respiratory physician.

Sleep stages were scored according to the standard criteria, defined as:

I: Low voltage mixed frequency with or without slow rolling eye movements.

II: Presence of spindles or K-complexes.

III: Presence of $\geq$ 20% and >50% delta waves per epoch.

IV: Presence of $\geq$ 50% delta waves per epoch.

REM: Low voltage mixed frequency, together with reduction in chin EMG signal was required and fast eye movements on the EOG needed to be present.

Arousal from sleep was scored when an abrupt shift in EEG frequency, which may involve theta, alpha and/or frequency > 16Hz (but not spindles) of 3 seconds or greater in duration was recorded. Arousals were scored in REM sleep only when accompanied by concurrent increases in submental EMG amplitude.

2.2(ii) Stardust

All control subjects were studied using a Stardust (Respironics. Pennsylvania USA) portable unit to limit costs. This portable device an airflow sensor for breath rate, pulse rate and oxygen saturation via oximetry, and chest or abdominal effort via an effort sensor with fully adjustable strap for body position monitor inside the recorder to measure supine or non-supine sleep positioning. The data from the device was downloaded onto a computer and a standard report generated via proprietary Stardust host software (Respironics, Pennsylvania, USA).

Nocturnal hypoxia was defined as desaturation to a level of 90% or less for a period of more than 2 minutes. The pattern of desaturation was deemed consistent with hypoventilation on the basis of poor re-saturation with a fall from the baseline saturation of ≥4%. The absence of obesity or demonstrable underlying cardio-respiratory disease was therefore, by exclusion, consistent with respiratory failure of an alternative cause. There was an absence of repetitive episodes of desaturations and resaturations with an absence of airflow, indicating hypoventilation as oppose to obstructive sleep apnoea. There was also a concomitant reduction in chest wall

movement in NH. Furthermore, in those in whom a Stardust study was available, analysis of the respitrace signal was consistent with hypoventilation, as opposed to obstruction.

2.2(iii) SNIF

At the time of study, a commercial nasal inspiratory pressure meter was not available, so the device for maximal inspiratory pressure was modified for SNIF measurements. A plug of wax was placed around the outside tip of a polyethylene catheter which was inserted into the nostril that was going to be measured. The catheter, 30cm in length with an internal diameter of 2mm, was attached to the pressure transducer. The subjects were then instructed to breathe out, close their mouth and take a deep sniff while the contralateral nostril was occluded. Recordings were taken from both nostrils and the highest of six recorded values was used.

2.2(iv) FOT

All subjects followed a breathing maneuver modified from the method of Johns et al. 2000[188]. Sixty seconds of stable tidal breathing was followed by two maximum inspiratory capacity breaths.

FOT was measured in the seated and supine positions to determine whether position might influence measurements. Respiratory system resistance (Rrs) was measured at 6 Hz[189]. A sinusoidal pressure wave was induced at the mouth during normal breathing via a three-way flow splitter, using an in-house device developed in the Respiratory Investigation Unit at Royal North Shore[190]. Both flow and pressure were measured and six measurements per second of Rrs were calculated as the real part of impedance. The volume was determined by the integration of flow. Extreme

Rrs values (>5 Standard deviations above the mean, <5 standard deviations below the mean, or any negative resistance values) were excluded from further processing. All other Rrs values were ignored, representing combined effects of flow and variations in lung volume[191]. The reciprocal of Rrs, reactance (Grs), was used because of its linear relationship to lung volume[192]. Predicted values of Pasker et al (1996) were used as normative data[190].

All subjects from data set A and B underwent standard respiratory function tests, including the measurement of spirometry (forced expiratory volume in one second & vital capacity), lung volumes by whole body plethysmography and diffusion for carbon monoxide, as well as measurement of Maximal Expiratory Pressure (MEP) and Maximal Inspiratory Pressure (MIP). The subjects in data set B additionally underwent SNIF and FOT (seated and supine). The same experienced respiratory scientists performed all of the tests in the Respiratory Investigation Unit at Royal North Shore Hospital.

2.3 Results

2.3(i) Data set A

The demographic details of the subjects, at the time of entry into the study are given in Table 2.1. Sixteen patients with ALS and nine control subjects were studied. NH was detected in eight of sixteen of the ALS patients and in none of the controls. For analytical purposes the ALS patients were split up into two groups: those who demonstrated NH (ALSNH+) and those who did not (ALSNH-).

Typical NH is illustrated in an ALS patient in Figure 2.1, which demonstrates ongoing diminished effort of the chest wall (measured by chest wall expansion)

followed by a lack of return to the baseline for saturation. Since there is still air flow, this hypoxic event is caused by hypoventilation rather than an obstruction.

Statistical analyses were performed using paired t-tests where appropriate. Otherwise analysis of variance (ANOVA) methods were employed with Scheffe's F test for measures of lung function[193]. Significance was determined at a level of $p<0.05$. All statistics were performed using Statview V5 ™, SAS Institute, NC USA.

	ALSNH+	ALSNH-	Controls
Subjects	8	8	9
Sex, M/F	7m 1f	4m 4f	6m 3f
Age (years) ±SD	58.9±15.1	58.8±11.8	55.2±10.2
Body Mass Index, kg/m2 ±SD	24.8±5.4	25.4±5.1	27.4±7.8

Table 2.1. Demographic data for the three groups, ALS patients who also suffer from nocturnal hypoventilation (ALSNH+), ALS patients who do not suffer from nocturnal hypoventilation (ALSNH-) and Controls in data set A.

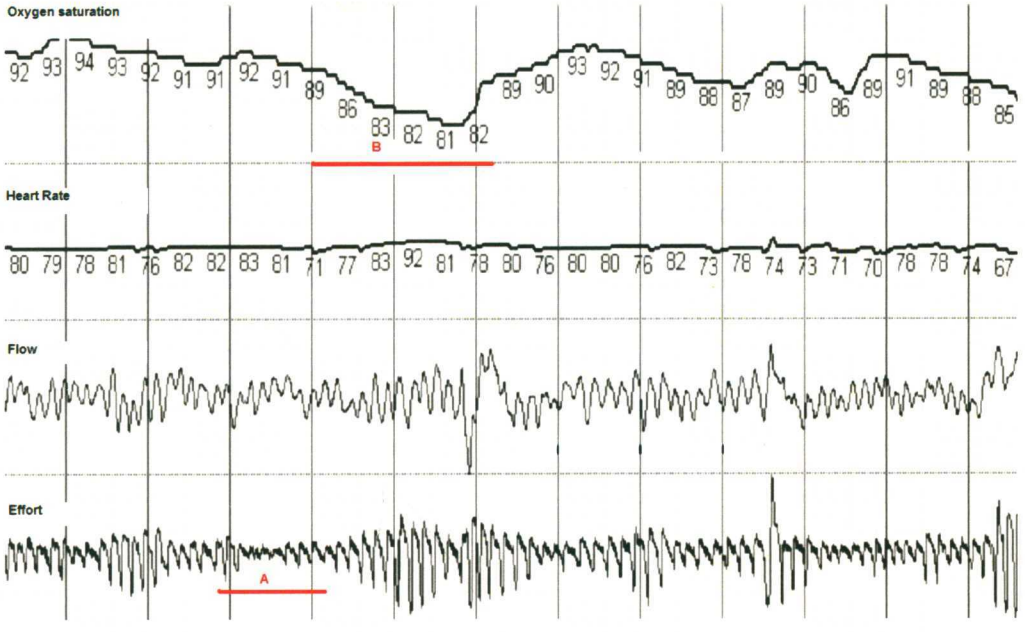

Figure 2.1. This is a sleep study recording of an ALS patient demonstrating a low resting baseline in the absence of underlying lung disease and a low-normal body mass index with a concomitant period of hypoventilation with additional hypoxia associated with diminished effort. The trace represents hypoventilation at (A) in the setting of diminished effort and reduced air flow, without evidence of airflow limitation (snoring). This is followed by a slow return to the diminished baseline (B) which is consistent with poor re-saturation. There is still flow, therefore the hypoxia is not caused by an obstruction.

Results of the respiratory function tests for data set A are demonstrated in Figure 2.2. The results show seven parameters for the three groups, ALSNH+, ALSNH- and the control group. The parameters included Forced Expiratory Volume in one second (FEV1), Forced Vital Capacity (FVC), Peak Expiratory Flow (PEF), Vital Capacity (VC), Residual Volume (RV), Maximal Inspiratory Pressure (MIP) and Maximal Expiratory Pressure (MEP).

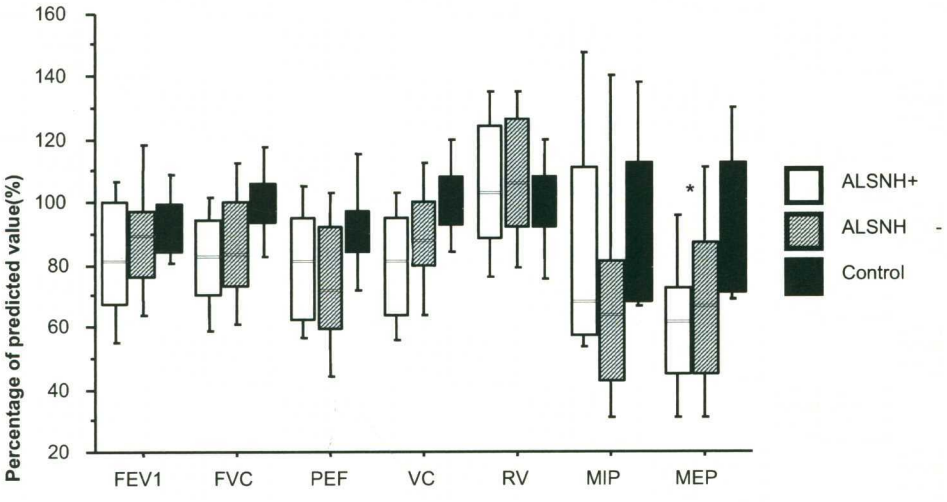

Figure 2.2. Cell charts of respiratory function test results in ALSNH+, ALSNH- and the control group. Forced Expiratory Volume in one second (FEV1) Forced Vital Capacity (FVC), Peak Expiratory Flow (PEF), Vital Capacity (VC), Residual Volume (RV), Maximal Inspiratory Pressure (MIP) & Maximal Expiratory Pressure (MEP). A borderline significant difference between the ALSNH+ and control groups was only found for MEP ($p=0.049$).

There were no statistically significant differences for commonly measured respiratory function tests between the ALSNH+ and ALSNH- groups or between the ALSNH- and control group, with the exception of MEP.

There was borderline significant difference ($p=0.049$) between the ALSNH+ and the control group only in the MEP measurement, with a mean MEP value in the ALSNH+ group of 61% ± 24% of the predicted value and 96% ± 26% of the predicted value in the control group. It is important to note that in threshold analysis, no arbitrary MEP value was able to discriminate between ALSNH+ and ALSNH-.

2.3(ii) Data set B

The demographic details of the subjects at the time of entry are given in Table 2.2. Ten patients with ALS and ten control subjects were studied. Concordant with the study described above, MEP was lower in ALS patients compared with normal controls ($p<0.01$). Interestingly, no patient with ALS had nocturnal hypoxia, as measured by overnight oximetry. SNIF as measured as percent predicted of normative data was significantly lower in the ALS group compared with controls ($p=0.003$) (Figure 2.3). There were no significant differences in FOT resistance or FOT reactance between the ALS and control group in FOT when measured in the seated ($p=0.13$ & 0.73), or supine ($p=0.28$ & 0.58), position (Figure 2.3).

Patient Number	Sex	Age	Disease duration (months)	Total Appel Score	Onset
1	F	33	2	44	Limb
2	M	44	7	66	Limb
3	M	79	4	78	Limb
4	M	54	3	41	Limb
5	M	55	6	70	Bulbar
6	F	54	4	68	Limb
7	F	71	6	53	Bulbar
8	M	53	7	46	Limb
9	M	73	3	43	Limb
10	M	71	5	40	Limb
Mean	**3 F, 7 M**	**58.7**	**4.7**	**54.9**	**2 B, 8 L**
Control Mean	**4 F, 6 M**	**55.7**			

Table 2.2. Demographic data of the subjects in data set B.

The disease onset was classified as either limb or bulbar. Disease duration refers to the period of diagnosis to the date of testing. The subjects were clinically graded using the Appel scale.

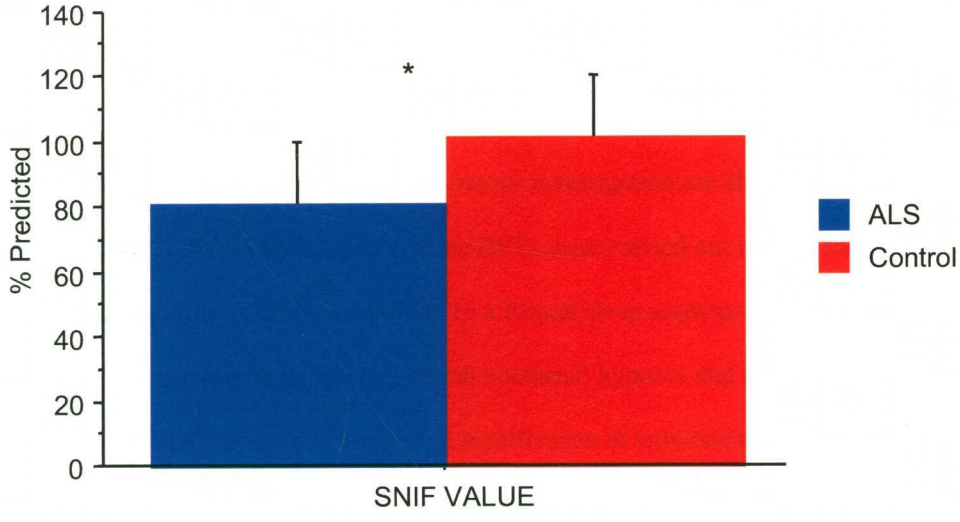

Figure 2.3. Box plot of Sniff Nasal Inspiratory Force (SNIF) in the ALS and Control group. SNIF was significantly lower in the ALS group ($p<0.05$) the error bars represent ±1 SD .

2.4 Discussion

Nocturnal Hypoventilation

From clinical experience, nocturnal hypoventilation (NH) is a phenomenon that can occur early in the course of ALS in patients that have no symptoms of diurnal respiratory insufficiency, and no symptoms consistent with nocturnal hypoxia. To assess whether standard respiratory investigation are able to detect the presence of NH in ALS, an array of routine RFTs were carried out in 16 ALS patients and 9 healthy controls in addition to a formal sleep assessment. Fifty percent of ALS patients were identified with nocturnal hypoxia and none in the control group. While there was borderline significance in only one respiratory parameter, maximal inspiratory pressure between the ALSNH+ patients and controls, the MEP value in isolation was not able to predict the presence of NH. These results suggest that standard clinical respiratory function tests, cannot reliably predict the presence of NH.

This study highlights the need to measure overnight oximetry in ALS patients for the presence of NH, which occurs independent of voluntary maximal respiratory effort measured in routine respiratory tests. Furthermore, the absence of change in standard respiratory function tests suggests a putative role for an abnormality in the central control of breathing in the genesis of NH. The results suggest that a penetration of central nervous system control of respiration in sleep may be critical in the development of NH. While there is evidence of the involvement of brainstem disturbances in the maintenance of respiration during sleep[194], no published data exists on the control of respiration during sleep in ALS or other form of motor neurone disease.

Our clinical observation demonstrated pathological UMN features are more common in the ALSNH+ group, raises the possibility that corticospinal and corticobulbar projections may be involved in the coordination of respiration during sleep. The aim of this study was to undertake dynamic sleep studies in patients with ALS, and to further investigate a second cohort of patients with quantitative measures of upper motor neuron dysfunction. This included clinical neurophysiological methods such as TMS and structural assessment of the CST using DTI. The hypothesis was that abnormalities of the UMN and CST would be more pronounced in ALS patients with NH.

In addition, it is of note that the routine RFTs used in this study were unable to predict the presence of NH, and are therefore unlikely to be helpful in determining the mechanism of NH. During the execution of the first study, it was apparent from the literature that FVC and other standard respiratory function measures are frequently used to monitor disease progression with mixed findings[181, 186, 195, 196]. FVC is commonly used as a predictor of survival in ALS[186, 197]. However, Velasco and colleagues (2002) recently demonstrated that FVC does not correlate with either NH or survival in ALS[172]. In addition, FEV1 is highly variable and does not correlate with disease progression or predict survival[198]. Similarly, MIP and MEP have a large range of normal values, with many technical variables[199].

The presence of NH is a potent predictor of survival in ALS. Unfortunately, the mechanisms that produce NH in ALS patients remain unknown. Studies in stroke patients reveal the complexity of the anatomy and physiology of the central control of respiration particularly during sleep[194].

If ALS patients have NH, Non-Invasive Positive-Pressure Ventilation (NIPPV) can be used as part of a multidisciplinary care approach[200], with a resultant significant improvement in sleep quality, daytime sleepiness, physical fatigue, and depression[201]. Not only can NIPPV assist lung function and exert a therapeutic effect on symptoms and quality of life, and have an impact on cognitive function[177], it can also delay the need for tracheostomy and prolong survival in patients with manifest respiratory failure[183]. It is not known whether patients with asymptomatic NH derive a survival benefit from the early institution of NIPPV, but in randomised controlled trial, NIPPV improves both quality of life and survival in patients with symptomatic respiratory failure[176].

The next goal in optimizing care and delivery of NIPPV for ALS patients requires accurate predictive tests of disease progression including the ability to detect NH in order to determine the best time to institute NIPPV. Clearly the goal is the development of a reliable and reproducible non-invasive tool that can accurately predict when desaturation is beginning to occur and which factors (including those outside diaphragmatic weakness) are important in its genesis. While SNIF is promising, routine respiratory function tests do not necessarily help the clinician with this decision. Routine surveillance oximetry is suggested in the management of patients with ALS to detect NH. SNIF could possibly be another useful tool to predict NH as it measures diaphragmatic strength which is jeopardized in NH patients.

Sniff Nasal Inspiratory Force and Forced Oscillation Technique

Recently, Sniff Nasal Inspiratory Force (SNIF) has been shown to be a predictive measure of survival, with improved sensitivity and specificity over conventional lung function tests [186]. There is a significant positive correlation between SNIF values and levels of nocturnal desaturation[186].

As part of the component of this project, SNIF was measured in addition to the routine RFTs with the simultaneous assessment of the UMN and CST in order to better understand the mechanisms involved in NH. There was opportunity to assess a novel measurement of lung mechanics, (Forced Oscillatory Technique - FOT) in patients with ALS and normal controls. SNIF was significantly different between the ALS and control group. Seated or supine FOT was not significantly different between the ALS and control group. FOT was chosen as a RFT as it investigates the upper airway resistance which is directly linked ti central control. The absence of an increase in upper airway resistance on assuming the supine position suggests that in the wakeful state a reduction in lung volume does not have a direct role in hypoventilation. It was hypothesised that there would be a difference between the two groups when supine but this may only be the case if patients suffer from NH. Unfortunately, at the time of this study this did not apply to any of the patients. There may be a difference in FOT during sleep that is not present during wakefulness. This may help to clarify the role of the involuntary muscles further.

The development of respiratory muscle weakness occurs in ALS is highly variable in terms of disease duration. Weakness of inspiratory muscles leads to hypercapnic respiratory failure, weakness of expiratory muscles impairs cough and airway clearance - both of which occur in ALS. There are simple, portable and

inexpensive ways by which respiratory function can be measured. These tests are dependent on maximal voluntary neuromuscular activation which may be difficult to ascertain. Invasive techniques such as phrenic nerve magnetic stimulation gives more reliable data on diaphragm strength[202] but the value may be overestimated if the patient suffers from significant upper motor neuron involvement[203].

One of the most common and useful non-invasive tests for inspiratory muscle strength is maximal inspiratory pressure (MIP). However, this may be difficult to measure accurately in "bulbar onset"(patients with significant bulbar function impairment) patients as an air tight seal around the mouthpiece is required. The SNIF procedure is a considerably preferable alternative as the manoeuvre triggers involuntary muscles as opposed to the MIP which, like all other lung function tests, is effort dependent on voluntary muscle. However, there are some of limitations to the SNIF technique such as severe nasal congestion and problems with the learning effect[204]. Previous groups have found SNIF to be more feasible than MIP in advanced ALS [185, 186] but not as useful in "bulbar onset" disease[205]. SNIF shows a linear decline with disease progression [185] and is more useful in predicting hypercapnia[203, 205]. Correlations with SNIF and quality of life are moderate to strong[173]. More importantly, SNIF can be used as a predictive tool for patients survival. A SNIF value <40cm H_2O is associated with a median survival of six months and <30cm H_2O median of three months[186]. Our study employed a control group to establish if there was a difference between early onset ALS patients and controls. The purpose of this study was to explore if SNIF could determine the difference between the ALS and control group early in the disease as this may be

useful as a diagnostic marker. There is no data on using FOT in ALS in the literature.

While searching for ALS patients with NH, ALS patients without NH were required as a positive control group along side a healthy control group. Unfortunately, no suitable ALS patients that suffered with NH were recruited but data already obtained in the ALS group not suffering with NH was analysed and compared to the control group. The original study hypothesis was that NH in early ALS was a manifestation of UMN involvement. The findings earlier in this chapter, demonstrated that NH was not predicted by routine respiratory function tests. This led to the hypothesis that there is a central mechanism reflected by abnormalities of involuntary pathways involved in the genesis of NH. Another significant finding was there were hardly any differences in respiratory function between the early disease onset ALS group and control group. The progression of respiratory failure is clearly dependent (in part) on involuntary muscles therefore tests that are able to selectively determine the integrity of the involuntary pathways are going to have a significantly better predictability. Hence there is a clear need to focus on developing an instrument to measure early change in the UMN.

Diffusion Tensor Imaging (DTI) and Transcranial Magnetic Stimulation (TMS) were chosen as measures of upper motor neuron pathology in ALS and are described in Chapter 3. Unfortunately, no suitable ALS patients with NH were admitted to our ALS clinic during the recruitment period, and thus the focus for the remainder of the thesis was on measuring UMN pathology in ALS using DTI and TMS.

3. Measurement of Upper Motor Neuron Involvement in Amyotrophic Lateral Sclerosis (ALS) using Transcranial Magnetic Stimulation (TMS) and Diffusion Tensor Imaging (DTI)

Aim

The aim of this study was to use two novel methods to interrogate simultaneously the UMN and CST in ALS patients and compare normal control subjects. These methods were then combined to develop an alternative, objective mechanism to determine the UMN involvement in ALS.

3.1 Introduction

In Chapter 2 it was demonstrated that standard respiratory function tests cannot distinguish between ALS patients who suffer from NH and those who do not. It is hypothesised that NH may be due to a central mechanism involving UMNs, at least in part. At the MND clinic at Royal North Shore Hospital, it was observed that patients with ALS who develop early, severe NH have a combined upper and lower motor neurone phenotype. Currently, the only clinical method to assess UMN involvement is the individual clinician's assessment of the tone and deep tendon reflexes etc as elicited with a tendon hammer. Furthermore, pathological studies have demonstrated the presence of UMN pathology in 75% of patients at post mortem examination even when no UMN signs are detectable by experienced clinicians during life[206]. There are limited techniques available to objectively assess UMN dysfunction in patients with ALS, and the search for such a tool is an area of intense interest[207, 208]. Such a tool could be important in gaining a better

understanding of ALS, in monitoring disease progression and potentially as a marker of drug effect in clinical trials.

An additional area where such a tool would be valuable is in helping determine the site of pathological onset in ALS, as this is currently unknown. Some authorities believe that the degeneration of motor neurons start in the cortex, while others believe it starts in the neuromuscular junction. Charcot himself believed that the degeneration of motor neurons was due to an anterograde process, even though the loss of motor neurons is most prominent below the medullary pyramids suggesting a "dying back" (retrograde) axonopathy[2].

The mechanism(s) of motor neuronal cell death in ALS are unknown. One prominent theory is cortical hyperexcitability and death of motor neurons due to glutamate excitotoxicity[209-211]. This theory is supported in part by the improved survival of ALS patients treated with riluzole, an inhibitor of glutamate release[95, 212-214].

The 'dying forward' hypothesis is also supported by Eisen and colleagues (1992) who suggested that ALS is a disorder of corticomotoneurons (UMN) causing excitotoxic anterograde degeneration of anterior horn cells (LMN) (AHC)[215].

Numerous transcranial magnetic studies support the 'dying forward' hypothesis with the demonstration of increased excitability early in the course of ALS[216-222].

Neuropathological studies also support evidence of early changes in the motor cortex, including the changes in Betz cells and loss of specific inhibitory cortical interneurons[223-225].

There is also evidence arguing against a dying forward process. Studies found that cortical hyperexcitability increases with disease duration[226], is unrelated to the disease duration[227], and that cortical and LMN degeneration occur independently[228, 229].

An alternative hypothesis suggests that LMN die due to the retrograde transport of pathogens from the neuromuscular junction, which then spread to the UMN's[230]. Other primary AHC disorders, such as poliomyelitis and spinal muscular atrophy do not share the same type of neurofilament cytoskeletal abnormalities as ALS[231]. The complexity of the anatomical and functional organization of the cortical motoneuronal system in humans cannot be underestimated.

After nearly 150 years since the first modern description of ALS the site of disease onset remains unknown. This may be due to the fact that until relatively recently there was little research considering UMN involvement in ALS.

This chapter will focus on the combination of two novel techniques involving TMS and DTI as to technique for measure UMN pathology in ALS.

3.1(i) TMS

TMS involves the generation of a large excitatory stimulus in the cortex, using single, paired, or multiple pulse stimuli. The pulse, or pulses, cause the selected population of neurons in the cortex to depolarise and discharge an action potential.

TMS uses non-invasive magnetic impulses to investigate UMN function and cortical abnormalities in ALS. It gives insight into the discharge characteristics of single motor units and/or the compound response of a muscle, or group of muscles.

The influence of cortical motoneurons on single voluntary activated lower motor neurons can be studied by TMS. This technique can also be used to try to elucidate the initial site of involvement of motor pathways in the development of ALS[223].

The paired-pulse test involves a sub-threshold transcranial magnetic stimulus to condition the electromyography (EMG) response to a larger test stimulus. In the paired-pulse technique, these conditioning and test stimuli are kept at a constant intensity while changes in the MEP amplitude are measured. This may be considered to have limited use due to the fluctuations in the MEP amplitude with repeated stimuli[232]. However, in the threshold tracking technique, the amplitude of the MEP response is fixed whilst the changes in the test stimulus required to generate this target response - when preceded by either sub- or supra-threshold conditioning stimuli - are measured. When transcranial magnetic threshold tracking is applied to the paired-pulse test, it effectively measures inhibition.

3.1(ii) DTI

DTI is a MR technique sensitized to the diffusion of water molecules[151] and is able to detect abnormalities in tissue earlier than conventional imaging techniques, that are often dependant on structural changes[153]. DTI is able to characterize the diffusion properties of water molecules in biological tissues. Water diffusion is not the same in all directions in brain white matter (termed anisotropic tissue)[154] and is expressed by the diffusion tensor $\boldsymbol{D}$. Diffusion refers to Brownian motion (random translational motion of molecules) resulting from the molecule's thermal energy. DTI measures the diffusion tensor $\boldsymbol{D}$ to give information about the state of the tissue.

Diffusion may not be the same in all directions due to the presence of membranes and various subcellular structures. These structures impose a directional

bias and hence the diffusion is anisotropic. In white matter tracts, there is high anisotropy since water diffusion is faster along the direction of nerve fibers. Changes are measured in the magnetic resonance signal along at least six non-collinear directions, resulting in the diffusion tensor. The diffusion tensor is a mathematical representation of water diffusion in the form of a three by three matrix[233] from which the indices of anisotropy and diffusivity are calculated[170].

The technique of DTI is able to detect very early changes in ischemia in both animals[157] and humans[234]. It is also able to detect lesions in MS animal models when conventional images are normal[235]. DTI permits the investigation of white matter architecture affected by pathology such as stroke[169, 236], tumour[237] and trauma[237, 238]; showing a reduced FA in the affected white matter tracts and a less consistent increase in trace ADC. FA is used to evaluate white matter in numerous conditions such as MS[239, 240], Wallerian degeneration, aging[241], schizophrenia[242] and ALS[161, 165].

There have been several publications utilising DTI in the investigation of UMN pathology in ALS. Some publications report that there is reduced anisotropy in the CST in patients with ALS[161, 162], which may occur early in the disease[163, 164]. Some authors claim that DTI relates to disease severity[161] and correlates with disease progression[165]. However, these studies used a small number of gradient directions[155] which could cause technical imprecision[243], making conclusions difficult.

Indeed, not all studies have found a correlation between anisotropy and disease severity[162, 244]. This may reflect the different methods employed in the studies, with differing field strengths, pulse sequence design and measurement

algorithms. Hence, despite promise, DTI methods are not routinely used in the assessment of UMN damage in ALS.

The use of DTI techniques in ALS, has provided preliminary evidence that the neurodegenerative process is not exclusive to the motor pathways, but may involve the basal ganglia, limbic system, spinal cord[166] thalamus, corpus callosum[164, 167]and frontal lobes, underneath the medial frontal gyrus[110, 142, 164].

DTI may eventually enable interrogation of the site of disease onset and may aid in elucidating the pathogenesis of ALS. Higher values of trace ADC and lower values of FA are reported in ALS patients with UMN involvement of the internal capsule and the pons. This supports a "dying back" mechanism of CST degeneration in ALS patients with UMN involvement[245].

According to the dying forward theory, the degeneration of UMN starts in the primary motor cortex with secondary degeneration along the CST. This may be demonstrated by the quality and density of orientated structures in the tissue[246] and is expressed as a change in diffusion tensor anisotropy. Studies have shown a decrease in FA in the non-pyramidal structures such as the thalamus and corpus callosum, as well as the pyramidal tract[164]. Disadvantages with DTI techniques include crossing fibers within the same voxel that may be contaminated with tracts from other parts of the brain[170, 247-249].

3.1 (iii) Tractography

Tractography is a method to calculate the position of white matter tracts within the brain and spinal cord. It infers continuity of fibers from voxel to voxel and reconstructs a putative white matter pathway based on probability[160]. There are numerous tractography algorithms able to generate probabilistic maps of fiber

connectivity between brain regions[250]. Using the technique of tractography, the CST is easily identifiable from motor cortex, as it runs through the internal capsule to the brainstem[160].

3.2 Methods

TMS and DTI studies were conducted in ten patients with clinically definite ALS,(as defined by the El Escorial criteria[105]), and in ten healthy controls (4 female and 6 male). There were 7 male and 3 female ALS patients all of whom were referred from the ALS multidisciplinary clinic at Royal North Shore Hospital. All patients were taking riluzole at 50mg twice daily. Eight of the patients had sporadic ALS and two patients had the familial variant.

The mean age of the patients was 58.7, ranging from 33 to 79 years. The mean time from diagnosis to the time of scanning, was 4.7 months ranging from two to seven months. None of the patients had dementia. Onset of disease was bulbar in two patients and limb in eight patients. All patients had upper motor neuron signs. There is no reproducible, reliable instrument to measure UMN features. All patients had UMN features include at least one of the following; brisk jaw jerk, spasticity, increase in deep tendon reflexes or extensor plantar responses as recorded by an experienced neurologist. In all patients, disease severity was measured using the Appel scale, a validated compound measure of disease disability[89]. The Appel scale comprises of five subsections: bulbar (maximum score = 30), respiratory (maximum score = 30), muscle strength (maximum score = 22), lower extremity function (maximum score = 35) and upper extremity function (maximum score = 33).

The mean Appel score was 57.6,+/-1SD (range 36-98), indicating moderate severity. No patients were taking any other psychoactive drugs. The patient's clinical characteristics are summarized in Table 3.1.

The mean age for the control group was 55.7, ranging from 34 to 72 years. There were four females and six males in the control group. Informed consent was ratified from all study participants and the study was approved by the North Sydney Area Health Service Human Research Ethics Committee. There was no significant difference in age between the ALS and control group ($p=0.65$).

Statistics

Each neurophysiological TMS and DTI parameter was compared between the ALS group and the control group applying the Mann-Whitney U test as appropriate for non-parametric data. The relationship between TMS and DTI parameters were analysed by Spearman's rank correlation test. A probability value of <0.05 was considered statistically significant.

Patient Number	Sex	Age	Disease duration (months)	Total Appel Score	Onset
1	F	33	2	44	Limb
2	M	44	7	66	Limb
3	M	79	4	78	Limb
4	M	54	3	41	Limb
5	M	55	6	70	Bulbar
6	F	54	4	68	Limb
7	F	71	6	53	Bulbar
8	M	53	7	46	Limb
9	M	73	3	43	Limb
10	M	71	5	40	Limb
Mean	**3 F, 7 M**	**58.7**	**4.7**	**54.9**	**2 B, 8 L**
Control Mean	**4 F, 6 M**	**55.7**			

Table 3.1. The disease onset was classified as either limb or bulbar. Disease duration refers to the period of diagnosis to the date of testing. The patients were clinically graded using the Appel scale (range 0-150).

3.2(i) TMS methods

Nerve Excitability Tests

The median nerve was first stimulated electrically at the wrist. The cathode was placed at the wrist crease and the anode located on the mid-forearm. A stimulus of 0.2ms and 1ms duration were delivered via 5-mm Ag-AgCl surface electrodes (ConMed, Utica, New York). The recording electrode was positioned over the motor point of the Abductor Pollicis Brevis (APB) with the reference electrode placed 4cm distally[251]. CMAPs were recorded via surface electrodes. Peak-to-peak amplitude and onset latency for the CMAP were determined and the Stimulus Response (SR) curves recorded separately for both stimuli. This data was used to estimate the strength duration time constant. This was achieved by comparing the ratio between the 0.2ms and 1ms stimuli required to evoke the same response using the Weiss's formula[232, 252]. NPI was calculated according to an established formula[253, 254]. The RMT was defined as the unconditioned stimulus intensity, expressed as a percentage of Maximum Stimulator Output (MSO%), required to maintain a target of 0.2mV. MEP amplitude was also recorded from the APB. CMCT was calculated according to the f wave method[255-257].

Cortical Excitability

TMS was applied to the motor cortex by a 90mm circular coil oriented to induce a current flow in a posterior-anterior direction, according to previously published methods[222]. Initially the coil was centred over the vertex and then moved in an antero-posterior and medial-lateral direction to find the optimal position to evoke maximal amplitude from the right APB muscle. These currents were generated by two high-power magnetic stimulators connected via a Magstim Bistim system (Magstim, Whitland, South West Wales, UK). This ensured that the conditioning and test stimuli could be independently set and delivered through one coil[232].

CMAP and MEP recordings were amplified and filtered (3HZ-3kHZ) using a Grass ICP511 A.C. amplifier (Grass-Telefactor, Astro-Med, West Warwick, Rhode Island) and sampled at 10kHZ using a 16-bit data acquisition card (National Instruments, Austin, Texas; PCI-MIO-16E-4). Data acquisition and stimulation delivery were controlled by QTRAC software (copyright Prof. Hugh Bostock, Institute of Neurology, Queen Square, London, UK).

Threshold Tracking

A paired-pulse paradigm was employed where a conditioning stimulus was delivered at intervals before a suprathreshold test stimulus was applied, again according to previously published methods[232, 258, 259].

The conditioning and test stimuli were kept at constant intensities in conventional paired-pulse technique and the changes in the MEP amplitude were measured. The MEP response (output) was fixed and changes in the test stimulus intensity required to generate this target response (i.e. when preceded by either sub- or supra-threshold conditioning stimuli), was measured.

Previous studies have demonstrated that if the ISI is between 1-5ms, the test response is inhibited, whereas at 7-20ms the test response is facilitated[232, 258-261].

The relationship between the logarithm of the MEP amplitude and the stimulus is close to linear over a 100-fold range of responses, from 0.02 to 2 mV[84]. Based on this finding, a small target response of 0.2mV (+/- 20%) was selected for the present study and subsequently tracked. The RMT was defined as the stimulus intensity to produce and maintain the target MEP response of 0.2mV peak-to-peak.

The intensity was then varied to: 60, 70, 80, 90, 100, 110, 120, 130, 140 and 150% RMT to determine the Stimulus Response (SR) curve for cortical stimulation of each subject. At each level of intensity three stimuli were delivered. Maximum MEP amplitude (mV) and MEP onset latency (ms) were recorded for each stimulus. Patients were asked to perform a weak voluntary contraction, estimated to represent 10%-30% of maximum voluntary contraction, during single pulse TMS to record the CSP. CSP duration was measured from the beginning of MEP to the return of EMG activity[262].

In brief, short-interval intracortical inhibition (SICI) and long intracortical inhibition (LICI) were investigated using two different paired pulse paradigms, adapted from previous studies[226, 258, 259]. In the first paradigm, measuring SICI, a subthreshold conditioning stimulus of 70% RMT (which did not evoke a MEP response) preceded a test stimulus at increasing Interstimulus Intervals (ISIs). The stimuli were delivered sequentially as a series of 3 channels (1st channel tracked the stimulus intensity required to produce the desired response, 2nd channel monitored the subthreshold conditioning stimulus and the 3rd tracked the stimulus required to produce the target MEP response. When the test stimulus produced two consecutive MEP responses within 20% of the target MEP response (0.2mV) tracking was deemed acceptable. Stimuli were delivered every 5-10 seconds. In the second paradigm, measuring LICI, a suprathreshold conditioning stimulus (120% RMT) preceded the suprathreshold test stimulus at increasing ISIs. In this instance, channel 1 tracked the stimulus intensity required to produce the unconditional test response and channel 2 tracked the stimulus required to produce the target MEP[222, 232].

The inhibition induced by a conditioning stimulus was measured as an increase in the test stimulus intensity required to evoke the target MEP. Inhibition was calculated using the following formula derived by Fisher[84]:

Inhibition = (conditioned test stimulus intensity – RMT)/RMT*100

Facilitation was measured as a decrease in the conditioned test stimulus intensity required to evoke the target MEP.

Reliability

Intra-class correlation coefficients of inter-rater reliability of these techniques are published[232].

3.2(ii) DTI Methods

3.2(ii)a Image Acquisition

All studies were performed using a 3 Tesla Philips Intera System (Philips Medical Systems, Best, The Netherlands) with an eight channel, phased array head coil and gradient coils (0-33mT/m). Head motion was restricted by placing pads on both sides of the subject's head. A single shot spin echo- EPI (Echo Planar Imaging) diffusion weighted sequence was performed for DTI acquisition.

Fifteen directional scans were used with an isotropic voxel resolution of 2.5mm (field of view 240mm, matrix of 96 x 96, slice thickness of 2.5mm, no gap). Fifty five slices were collected with an echo time of 110ms: repetition time of 8404ms and a b value of 1000s/mm^2, additionally one set of images with no diffusion weighting (b=0 s/mm^2) was acquired. The identical sequence was acquired six times and averaged after reconstruction to improve signal to noise ratios, with a total scan time of 30 minutes. To exclude other pathologies, two whole brain inversion recovery and T1-weighted fast spin echo whole brain volumes were acquired. No other pathologies were identified in any control or ALS patients, with all studies reviewed and reported by an independent expert neuroradiologist. Each scan was studied for head movement twice using DTIStudio.

Diffusion Tensor Image Data Processing

DTIstudio (Dr Susumu Mori, Johns Hopkins University, Baltimore, MD) was used to post-process the DTI sequences. Quantitative diffusion parameter maps were created including: FA, trace ADC, Colour maps, Parallel Diffusion (Para D - Ev1), and Perpendicular Diffusion (Perp D - [Ev2+Ev3]/2).

Regions of Interest and Tractography

Unlike conventional MRI, DTI requires further post-processing (tensor calculation) to produce measurements. Derivation of DTI allows calculation of various parameters including: Apparent Diffusion Coefficient (ADC) maps, anisotropy maps, principal eigenvalue maps, eigenvector images, colour maps and 3-D tract reconstruction.

DtiStudio is a versatile open source program for DTI computation and fiber tracking. Tensor elements, eigenvalues (Ev), eigenvectors, diffusion anisotropy, diffusion constants and colour-coded orientations can be calculated using this program. Interactive results can then be viewed interactively in orthogonal and three dimensional views. A Fiber Assignment by Continuous Tracking (FACT) algorithm and brute-force reconstruction enables the generation of three dimensional fiber tracts[263]. In the tracking algorithm, voxels with FA-values lower than 0.25 were excluded to avoid inclusion of grey matter and CSF[264]. The reconstruction angle for the tract was set at 70% (default setting for DTIStudio). These settings remained the same for all patients and controls.

Reliability

Intra-class correlation coefficients of inter-rater reliability were determined by repeating the placement of ROIs a second time on all of the datasets, after an interval of at least one week. Intra-observer reliability was high (kappa >0.9)

DTI Analysis

The axial slice was viewed on both colour-coded and FA maps and was selected for ROI placement. Two programs were used to analyse the DTI images: Fiber tracking in DTIStudio and Stereotaxic White matter Atlas in Talairach Coordinate (SWAT) in ROIEditor. (I wrote an instructions for these programs manual in collaboration with Dr. S. Mori, please see Appendix B).

Fiber tracking in DTIStudio

Fiber tracking was carried out using DTIStudio, colour maps were used to locate the cerebral peduncle and the internal capsule. An oval Region of Interest (ROI) was used and the first ROI was placed on the internal capsule, around slice 21, which then highlighted all of the fibers that penetrate it. A second ROI was then placed on the internal capsule, around slice 36, using the "AND' function (Figure 3.1.) Any fibers that were selected and were not part of the CST were removed using the "NOT" function. Whole CST statistics were generated including: FA, trace ADC, Ev1, Ev2 and Ev3 values in both the left and right CST, these were then recorded.

A manual circular ROI was then placed on slice 21, 26, 31 and 36 (Figure 3.2) size between 8-12 voxels within the fiber tracking region, and the FA, Trace

ADC, Ev1, Ev2 and Ev3 values were recorded for each ROI within the CST. This enabled measurement not only for the whole CST in each hemisphere but also at individual places within the CST as defined by tractography. The advantage of this method was that ROI measurements were obtained directly from the CST, as defined by tractography and not by a 'best guess' method of where the CST should be within the white matter. Most previous studies in this field have employed a 'best guess' method for identifying the CST ROIs. Fiber tracking enabled the CST to be located, and from this data, regions of interest drawn along the CST. This technique is theoretically more accurate than a 'best guess' method and hence the values obtained more likely to be representative of the CST (refer to the Appendix B for the instructions on using DTIStudio).

Eighteen months was spent on optimizing image protocols. Our protocol is derived from previously published methods together with modulation of local parameters in order to obtain best data. These parameters published in the thesis are applicable to most scanners as the examiner would agree differences between commercial DTI scan protocols and pulse sequence design are often proprietary and hence not accessible.

We sought to develop the technique on a clinical magnet that can be applied by anyone. We don't yet know if it is valid as we need to use it on a Siemens and GE scanner.

It is important to highlight the strength of the study in multiple acquisitions, signal to noise ratio. This technique is performed by few others and was suggested by Susumu Mori, Johns Hopkins Baltimore.

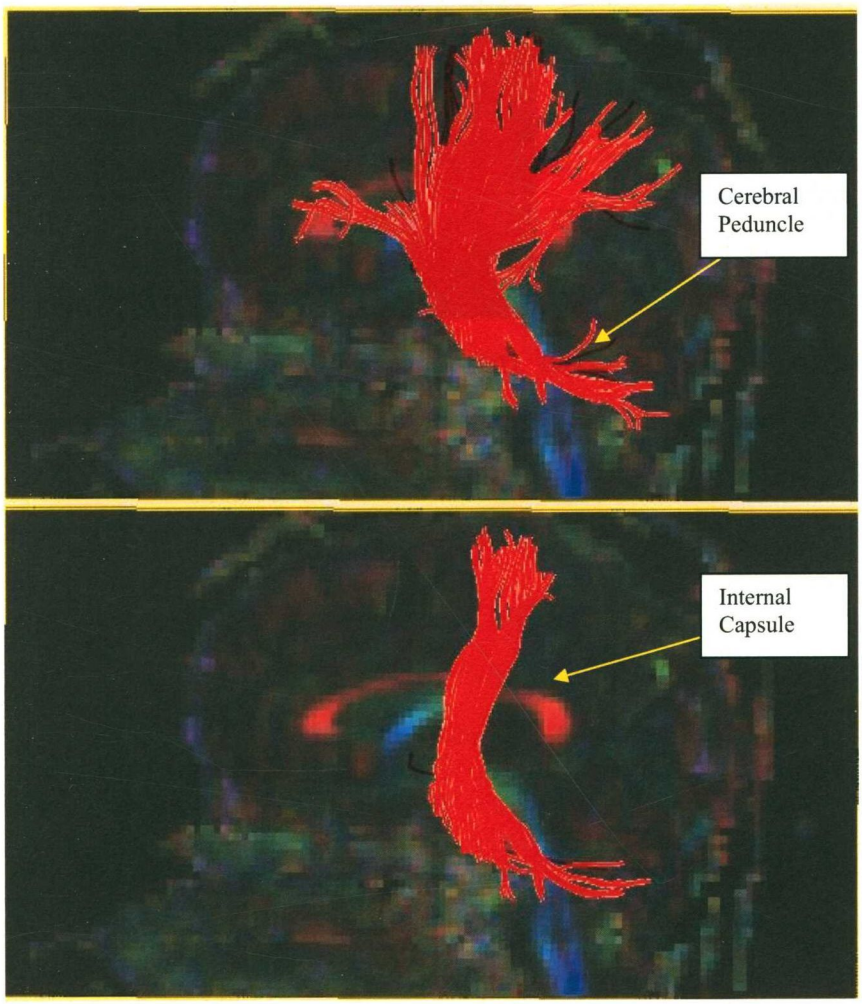

Figure 3.1. Selecting the CST.

Using DtiStudio, a ROI was placed on the cerebral peduncle and all of the fibers that penetrate this region were illuminated in red (top picture). Then a second ROI was placed in the internal capsule to obtain the fibers that run through the CST (bottom picture).

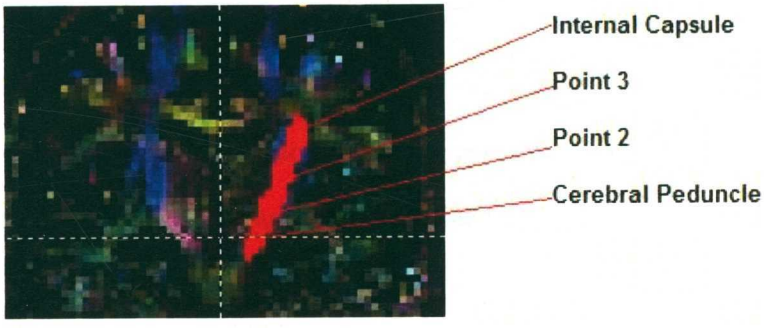

Figure 3.2. This is a colour map of the CST using DTI. The CST was selected by placing two regions of interest on the cerebral peduncle and the internal capsule. Once the corticospinal tract (in red) was located, four regions of interest were placed along the CST in each hemisphere. Point 1 – Cerebral peduncle (slice 21), Point 4 – Internal capsule (slice 36), Points 2 & 3 – slices (26 & 31) exactly in between these points.

Stereotaxic White matter Atlas in Talairach Coordinate (SWAT)

In addition to fiber tracking, a program termed SWAT was used to collect data relating to the CST (as developed by Professor S. Mori, Johns Hopkins University). SWAT is a program that can normalize DTI data to Talairach space. It accepts standard landmarks used to normalize brains in the Talairach spaces as well as user-defined landmarks. After the landmark-based normalization, the transformation is applied to tensor fields and various DTI-derived contrasts are recalculated. This allows population-based voxel-based analyses of DTI data.

This program performs brain rotation and normalisation to the Anterior Cingulate (AC) and Posterior Cingulate (PC) orientations. SWAT was used to process the data set before using ROI Editor to obtain values.

ROI Editor performs manual and automated parcellation of brains previously normalized by SWAT, allowing the user to place ROIs anywhere on the image and give values for each point selected. This is equivalent to processing DTIStudio conducts for FT. It can be used on all of images provided they are loaded at the same time.

3.3 Results

Ten ALS patients and ten controls underwent TMS and DTI. The TMS and DTI studies were performed on the same day. The clinical features and rating scores for the ten ALS patients are summarized in Table 3.1 and the conventional neurophysiological indices are in Table 3.2. The motor cortex was inexcitable in two ALS patients. All DTI scans were used, none having significant artefact.

3.3(i) Significant findings from TMS studies

The minimum F wave latency was significantly longer in the ALS group (32.2+/-0.78 ms) compared to the control group (28.5+/-0.53 ms) $p<0.01$. This is not a novel finding and is presumably due to anterior horn cell loss in the ALS patient group[265].

ALS patients had significantly lower CMAP amplitudes (4.7+/-1.41mV) compared to the controls (8.7+/-0.89mV, $p<0.01$). CMAP amplitude can be used as a broad marker of disease severity[266]. Vucic et al. has used a value of <4mV CMAP amplitude, in the absence of other causes, as a cut-off for more severe disease involvement[232]. Again this result is in keeping with the ALS disease state.

Stimulus response curves were generated with the MEP amplitude expressed as a percentage of CMAP amplitude recorded following electrical stimulation. The MEP:CMAP ratio was higher at all stimulus intervals in the ALS group reaching statistical significance at stimulus intensities 60% ($p=0.01$), 80% ($p<0.05$) & 90% ($p<0.05$). The CSP was lower at all stimulus intensities in the ALS group (Figure 3.3), reaching statistical significance at stimulus 140% ($p<0.05$), this is another feature indicative of hyperexcitability. The NPI was significantly lower in the ALS group (0.8+/-0.32) in comparison to the control group (2.1+/-0.23) ($p<0.01$).

SICI was significantly reduced in ALS patients compared to controls as shown in Figure 3.4 (ALS group = -1.7+/-2.19: Control group = 7.2+/-1.86, $P<0.05$). There was no correlation between any of the TMS parameters and the Appel score.

Patient #	Gender (M/F)	RMT (MSO%)	MEP Amplitude (mV)	CMAP Amplitude (mV)	F WAVE Latency (ms)	CMCT (ms)	MEP: CMAP Ratio	NPI	SICI
1	Female	61	1.1	5.9	33.9	3.5	0.2	1.2	-2.1
2	Male	N/A	N/A	0	N/A	N/A	N/A	0	N/A
3	Male	60.4	3	6	30.8	3	0.5	0.1	-3.4
4	Female	N/A	N/A	0	N/A	N/A	N/A	0	N/A
5	Male	50.3	1.5	15.2	34.3	3.2	0.1	3	4.9
6	Male	64	4.7	7.5	34.5	4.4	0.6	1.6	-12.8
7	Male	58	0.2	3.7	33.5	4.9	0.1	0.5	-6.8
8	Female	58	0.4	3	28	8.3	0.1	0.1	3.0
9	Male	46	0.6	2	N/A	N/A	N/A	N/A	-5
10	Male	48	2.7	3.6	30.6	5.4	0.8	0.3	8.7
11	Female	68	0.7	14	28.8	3.6	0.1	3.3	12.1
12	Male	54.3	5	9.5	31.1	8	0.5	2.3	2.5
13	Female	62.6	0.4	7.1	28.7	4.2	0.1	2.2	14.4
14	Male	37	4.3	8.6	27	4.6	0.5	2.1	-2.2
15	Female	67	2.9	7.5	26.2	3.6	0.4	1.8	13.1
16	Male	59	2.2	7.5	28.7	7.2	0.3	1.7	7.3
17	Female	63	1.1	10.2	26.8	5.8	0.1	2.4	10.0
18	Male	54.5	4.9	11	29.3	5.4	0.4	2.2	5.3
19	Male	62.9	5.7	6.7	30.5	6.4	0.9	2	-0.11
20	Male	58.9	1.2	5.3	27.4	4.4	0.2	1.2	11.
ALS Mean		55.7	1.8	4.7	32.2	4.7	0.3	0.8	-1.7
ALS SD±1		6.7	1.6	4.4	2.5	1.8	0.3	1.0	6.9
Control Mean		58.7	2.8	8.7	28.5	5.3	0.3	2.1	7.3
Control SD±1		8.9	2.0	2.5	1.6	1.5	0.3	0.5	5.8
Stat.Sig.		ns	ns	**<0.01**	**<0.01**	ns	ns	**<0.01**	**<0.05**

Table 3.2. Table of Clinical Neurophysiological Indicies

The TMS indicies for the ten ALS patients (in blue font) and ten normal controls (in red font). Two ALS patients were inexcitable (numbers two and four) and no F-waves were present for a further ALS patient (number eight). The CMAP amplitude was recorded from the Abductor Pollicis Brevis (APB). The CMAP response was absent in two patients making the rest of their TMS indicies unrecordable. NPI – Neurophysiological Index, RMT – Resting Motor Threshold, MEP – Motor Evoked Potential, CMCT – Central Motor Conduction Time.

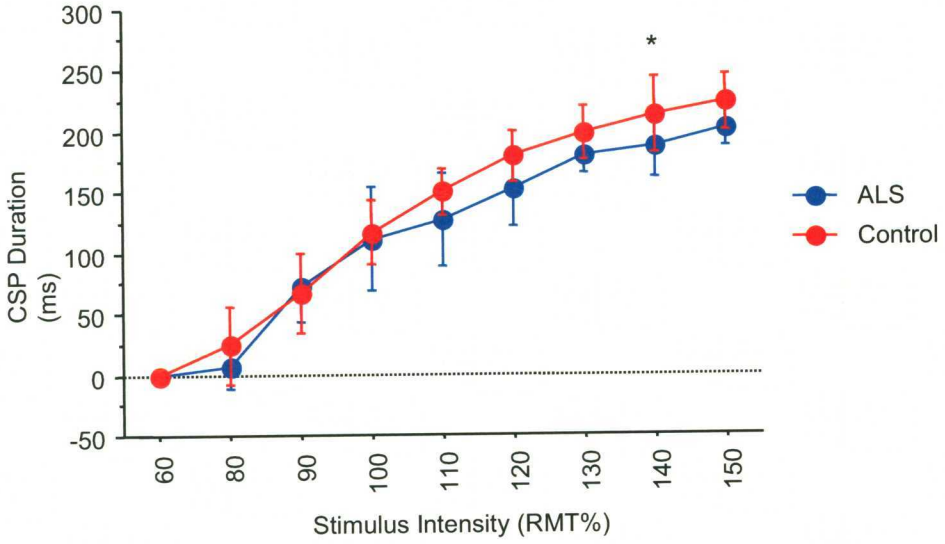

Figure 3.3. Cortical Silent Period (CSP) duration, measured from the onset of MEP to the beginning of EMG activity. The ALS group had a reduced CSP duration compared to the control group (Statistically significant at 140%, $p<0.05$), the error bars represent ±1 SD.

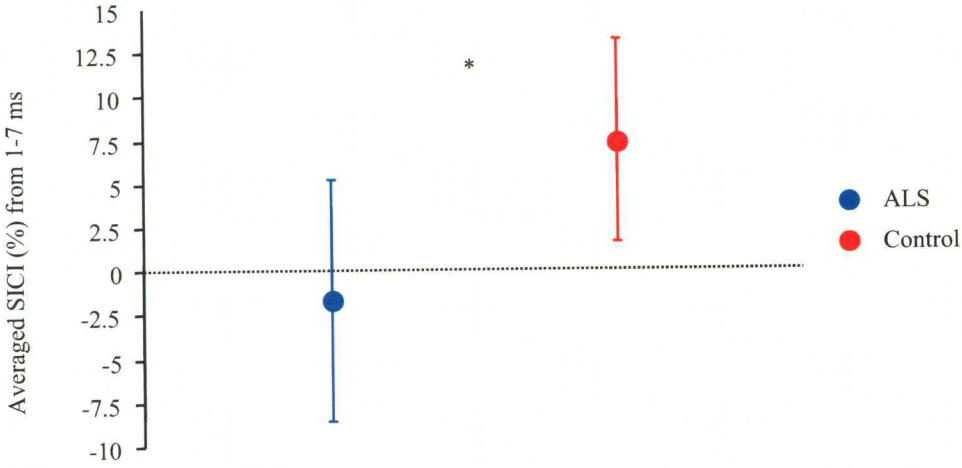

Figure 3.4. Point plot demonstrating the mean Short-Interval Intracortical Inhibition (SICI), defined as the stimulus intensity required to maintain a target output of 0.2mV. In the ALS group there was an absence of SICI and this group demonstrated facilitation ($p<0.02$). The error bars represent ±1 SD.

3.3(ii) DTI Results

Fiber-Tracking in DTI Studio

Fiber-tracking of the CST was performed in both hemispheres, and mean FA, trace ADC and eigenvalues in each CST recorded at the same four points along the CST in all subjects: Point 1 the cerebral peduncle: Point 4 in the internal capsule: And points 2 and 3 half way in between these points (Figure 3.2).

Two regions of interest were used to locate the CST by using the fiber tracking function in the DTI studio program. Once performed, individual regions of interest were placed along the CST on both sides (left and right) and an average value was obtained for a region of interest (between 8-12 pixels).

Further analysis demonstrated significant differences between the ALS and control groups. These differences were in FA, trace ADC and in PerpD mostly located on the whole of the tract.

The PerpD ([Ev2 + Ev3]/2) was higher at all points of the CST in both hemispheres in the ALS group. This reached a statistical significance on the whole left tract value ($p<0.01$), the whole right tract value ($p<0.02$) and at the right internal capsule ($p<0.05$). FA was lower in the ALS group in both hemispheres at all points along the CST. This difference in FA reached statistical significance in whole left tract value ($p<0.002$) and whole right tract value ($p<0.001$). The trace ADC value was higher at all points in both hemispheres along the CST in the ALS group and reached statistical significance in the left CST at point 2 ($p<0.02$). These findings are given in Table 3.3.

Fiber Tracking	Average Tract			Point 2			Internal Capsule		
	ALS	Control	P Value	ALS	Control	P Value	ALS	Control	P Value
FA Left	0.58	0.62	**<0.01**	0.62	0.65	NS	0.48	0.50	NS
FA Right	0.57	0.60	**<0.01**	0.56	0.61	NS	0.45	0.50	NS
ADC Left	0.22	0.22	NS	0.22	0.20	**<0.05**	0.21	0.20	NS
ADC Right	0.23	0.22	NS	0.21	0.21	NS	0.22	0.20	NS
PerpD Left	0.48	0.44	**<0.01**	0.43	0.37	NS	0.51	0.47	NS
PerpD Right	0.50	0.45	**<0.05**	0.46	0.42	NS	0.55	0.46	**<0.05**
Unit of ADC values: x 10^{-2} mm^2/s and perpendicular diffusivity: x 10^{-3} mm^2/s									
P values were obtained in Mann-Whitney U tests and are considered significant when printed in bold.									
NS – Not significant									

Table 3.3. Table of results from the Fiber Tracking Analysis

There was a significant difference between the ALS and control group along the whole CST on both the left and right hemispheres in PerpD and FA. PerpD ([Ev2 + Ev3]/2) was higher in ALS group at all points of the CST in both hemispheres this reached a statistical significance at the whole L CST ($p<0.01$), whole R CST ($p<0.02$) and at the right internal capsule ($p<0.05$). This was the predicted result as there is less restriction in UMN degeneration. FA values in the CST was lower at all points in both hemispheres in the ALS group this reached a statistical significance in the whole left tract value ($P<0.002$) and whole right tract value ($P<0.001$). This result may be due to less structural organization within the axon. Trace ADC values in the CST were higher at all points in both hemispheres in the ALS group, this reached a statistical significance at left point 2 ($P<0.02$). NS = not significant.

Stereotaxic White matter Atlas (SWAT)

The CST was located using the colour maps in the SWAT program. Four ROIs were placed consistently along both the right and left CST. There were significant differences between the ALS and control group. These differences were in perpendicular diffusion, FA & Trace ADC, and were primarily located on the whole of the CST value. PerpD was higher at all of the CST points in both hemispheres in the ALS group. This reached statistical significance in the whole left and right cerebral peduncle and in the right internal capsule ($p<0.01$).

FA values were lower in the ALS group at all points in both hemispheres, reaching statistical significance in the left cerebral peduncle ($p<0.01$). The trace ADC values were significantly higher in the ALS group in the left cerebral peduncle ($p<0.05$) and in the left internal capsule ($p<0.05$). For a summary of the findings refer to Table 3.4.

SWAT	Cerebral Peduncle			Point 3			Internal Capsule		
	ALS	Control	P Value	ALS	Control	P Value	ALS	Control	P Value
FA Left	0.62	0.69	**<0.01**	0.71	0.74	NS	0.70	0.71	NS
FA Right	0.68	0.73	NS	0.61	0.64	NS	0.61	0.63	NS
ADC Left	0.24	0.21	**<0.01**	0.21	0.22	**<0.05**	0.22	0.23	NS
ADC Right	0.20	0.20	NS	0.22	0.21	NS	0.24	0.21	**<0.05**
PerpD Left	0.52	0.39	**<0.05**	0.36	0.35	NS	0.39	0.31	NS
PerpD Right	0.36	0.31	**<0.05**	0.45	0.41	NS	0.50	0.41	**<0.05**
Unit of ADC values: x 10^{-2} mm^2/s and perpendicular diffusivity: x 10^{-3} mm^2/s.									
P values were obtained in Mann-Whitney U tests and are considered significant when printed in bold.									
NS – Not Significant									

Table 3.4. Table of Results from the SWAT analysis

PerpD was higher in the ALS group at all points of the CST in both hemispheres. This reached a statistical significance in the whole left and right Cerebral Peduncle (L CP, $p<0.01$, R CP, $p<0.05$) and in the Right Internal Capsule (R IC, $p<0.05$). The ALS group had a lower FA value at all points, in both hemispheres, which reached statistical significance in the left cerebral peduncle ($P<0.01$). The ALS group had a statistically higher value of trace ADC than the control group in the left cerebral peduncle ($P<0.01$), left point 3 ($p<0.05$) and in the right internal capsule ($P<0.05$). NS = not significant.

Summary for both FT and SWAT

There were significantly different values in FA, PerpD and Trace ADC between the ALS and control group using both programs i.e. FT and SWAT (Figure 3.5). The two programs consistently found that the PerpD was higher at all points of the CST bilaterally and that the FA was lower at all points of the CST bilaterally in the ALS group. However, the location within the CST, where this difference reached statistical significance, varied between the two programs used. The FT program found that the most likely place on the CST to be statistically different between ALS and controls was the whole tract value (4/7 significant findings). This is calculated by DTIStudio. This function does not exist in SWAT. The other significant findings using FT was at point 2 and in the internal capsule. In the SWAT program, four out of the six significant findings were in the cerebral peduncle, one significant finding at point 3 and two significant findings in the internal capsule. The most likely explanation for this difference in statistical significance is the variance in the mathematical calculations used by the two programs to analyse data.

The important fact is that the two programs concurred on the trends between ALS patients and the control group. These two programs complement one another and should/could be used together. Interestingly, there was no correlation between any of the DTI parameters and the Appel score, nor with the disease duration.

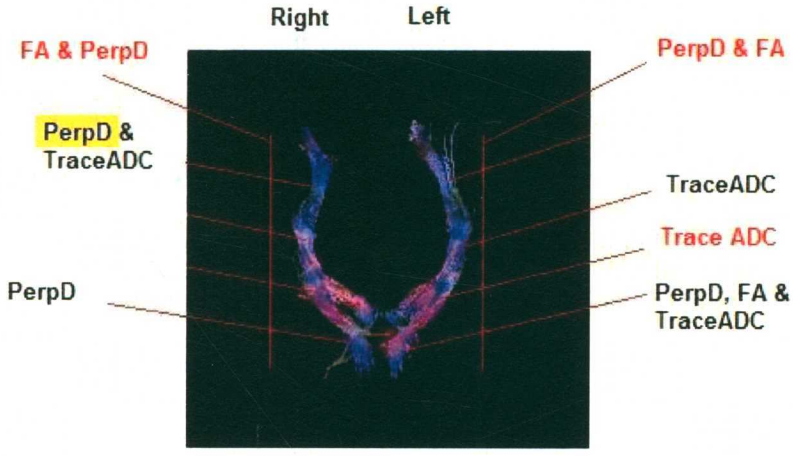

Figure 3.5. This is an image of CST produced by the Fiber tracking program. It illustrates the left and right CST with graphical representation of the areas and DTI parameters that were different between the ALS and control group. The red text illustrates the significant findings between the ALS and control group using the FT program results. The black text illustrates the significant findings using the SWAT program results. The yellow highlighted box is where there is a significance using both FT and SWAT program results. FA – Fractional Anisotropy, PerpD – Perpendicular Diffusivity & Trace ADC - apparent diffusion coefficient.

3.3(iii) Correlations between DTI & TMS

The DTI and TMS results show a significant difference between the ALS and control group. In order to better understand these two techniques, a correlation analysis for the two methods was performed. The correlation studies between the TMS and DTI tractography parameters were performed to understand the relationship between them. TMS parameters were correlated with different DTI parameters using results from both the FT program and SWAT program. As only the left hemisphere was used in TMS, only the left hemisphere DTI results were used. Using the data obtained from the correlation study, an algorithm utilising both the TMS and DTI parameters was developed.

Firstly, the FT results were correlated with the TMS parameters as a whole tract (compact data) and subsequently as individual points along the CST. Then the same process was repeated using the SWAT program results. These correlations were then tabulated to illustrate the potential for an algorithm to measure UMN involvement in ALS. All of the individual correlation tables are included in Appendix C.

The data from both of the DTI programs were added together into a colour coded Table (Table 3.5). This Table demonstrates that there are both differences and similarities in the programs with relation to the correlation of TMS parameters with DTI parameters. All of the DTI parameters were found to correlate with at least one TMS parameter using both of the programs. The DTI parameter that correlated most strongly in both DTI programs was Trace ADC, followed by PerpD, FA and ParaD. The largest difference between the two DTI programs are that the SWAT program

correlated with SICI in all of the DTI parameters whereas this was not found to correlate using the results from the fiber tracking program.

The TMS parameters that correlated with all of the DTI parameters were SICI, CMAP latency, F Wave latency, MEP/CMAP and MEP amplitude. There were 32 significant correlations in total: nine were SWAT only, ten were fiber tracking only and 13 involved both programs. This suggests that, overall, the programs complemented each other.

An example of these correlations is demonstrated in Figures 3.6-3.10. Some of these significant findings occurred in the cerebral peduncle: there was a negative correlation between SICI and PerpD (Figure 3.6, $p<0.05$), and between SICI and Trace ADC (Figure 3.7, $p<0.02$). There were positive correlations between SICI and FA (Figure 3.8 $p<0.05$), F Wave latency and ParaD (Figure 3.9, $p<0.02$) and F Wave latency and Trace ADC (Figure 3.10, $p<0.05$).

	ParaD	PerpD	TraceADC	FA
SICI				
MEP amplitude				
MEP/latency				
MEP/CMAP				
CMT				
RT				
F Wave latency				
CMAP amplitude				
CMAP latency				
NPI				

Table 3.5. Colour coded representation of all of the significant correlations in DTI and TMS parameters, when combining both the compact and individual tracts in the fiber tracking and SWAT results (Black-SWAT, Red-FT, Yellow-both programs). SICI – Short-Interval Intracortical Inhibition, MEP – Motor Evoked Potential, CMAP – Compound Muscle Action Potential, CMT – Cortical Motor Threshold, RT – Resting Threshold, NPI – Neurophysiological Index

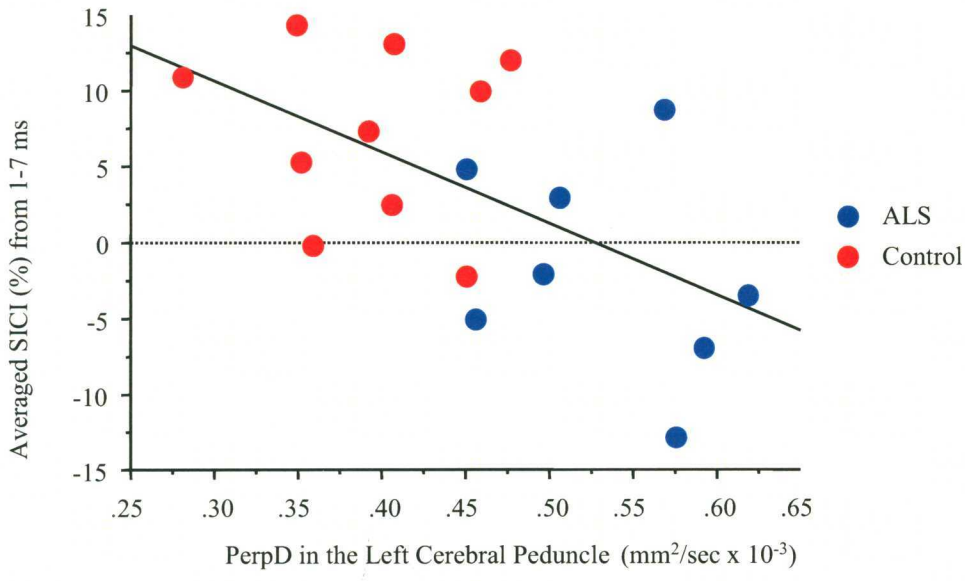

Figure 3.6. There was a negative correlation with SICI and the PerpD in the cerebral peduncle ($p<0.05$). The ALS group is clustered towards the bottom right corner of the graph as their average SICI value was low and their PerpD values were high in comparison to the control group. In ALS there is an increase in the PerpD value and a decrease in SICI.

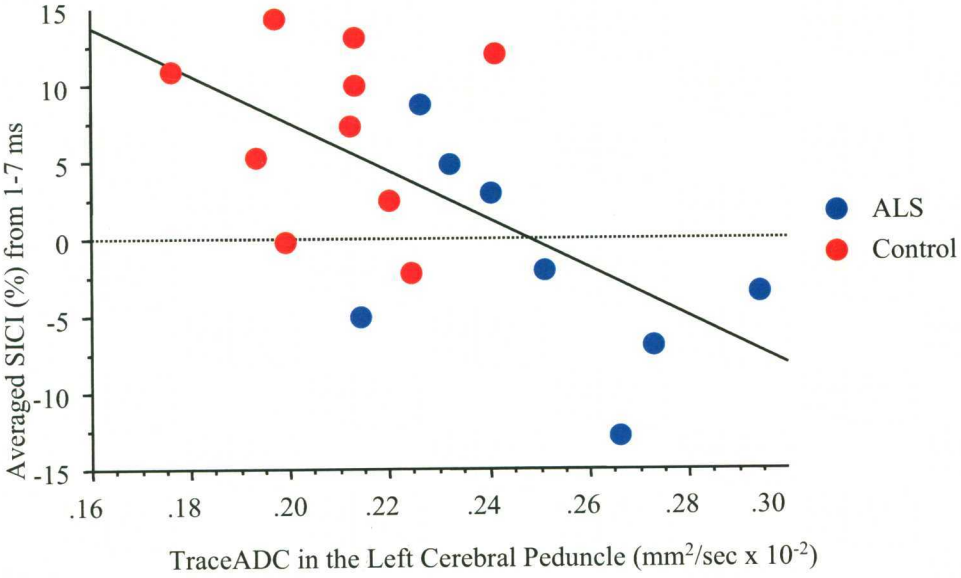

Figure 3.7. There was a negative correlation with SICI and Trace ADC values in the cerebral peduncle ($p<0.02$). The ALS group is clustered towards the bottom right corner of the graph, since their average SICI values were low and their Trace ADC values were high compared to the control group.

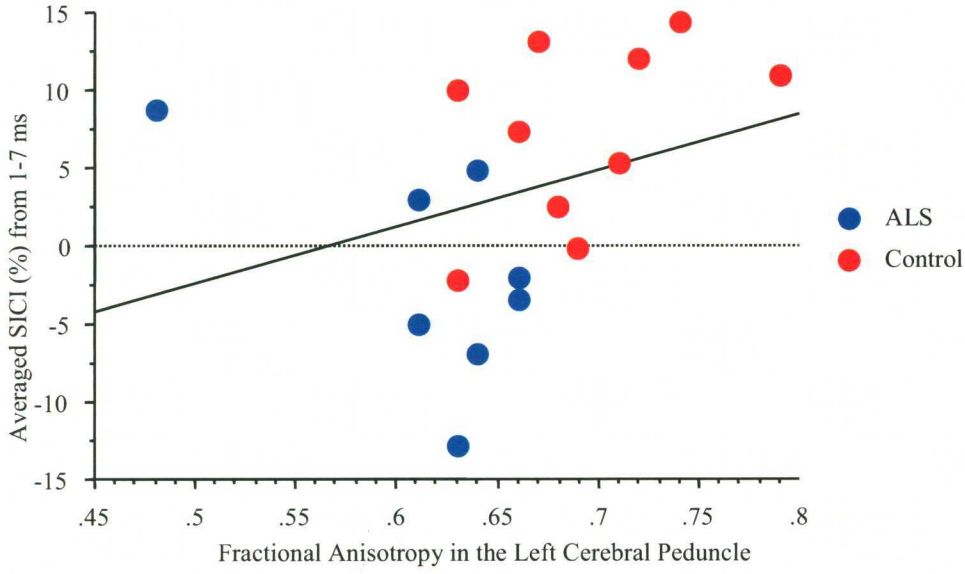

Figure 3.8. There was a positive correlation with SICI and FA values in the cerebral peduncle ($p<0.05$). The ALS group is clustered towards the bottom left corner of the graph as their average SICI values were low as were their FA values in comparison to the control group.

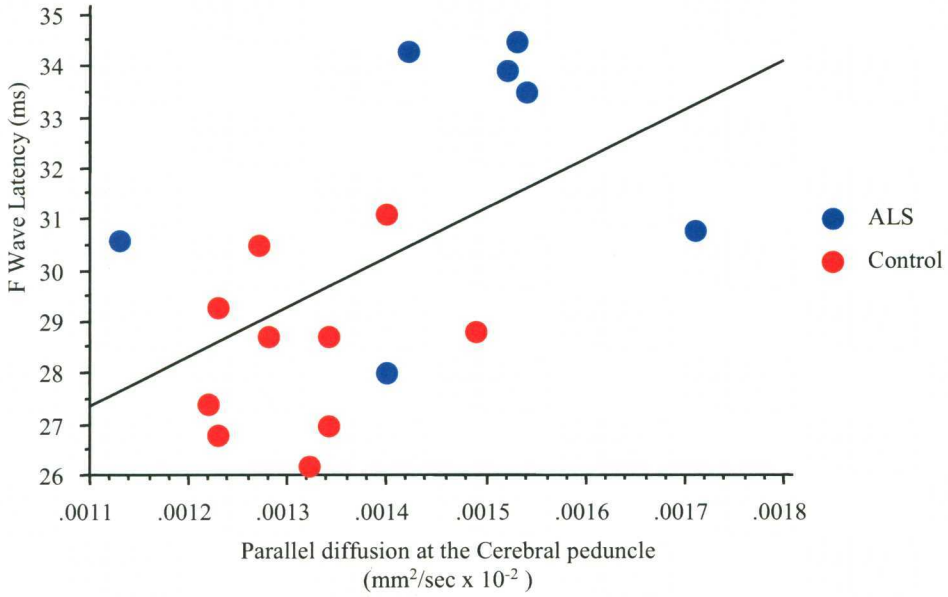

Figure 3.9. There was a positive correlation between the F Wave latency and the ParaD values in the cerebral peduncle ($p \leq 0.02$). The ALS group is clustered towards the top right corner of the graph since their average F Wave latency and ParaD values were high in comparison to the control group.

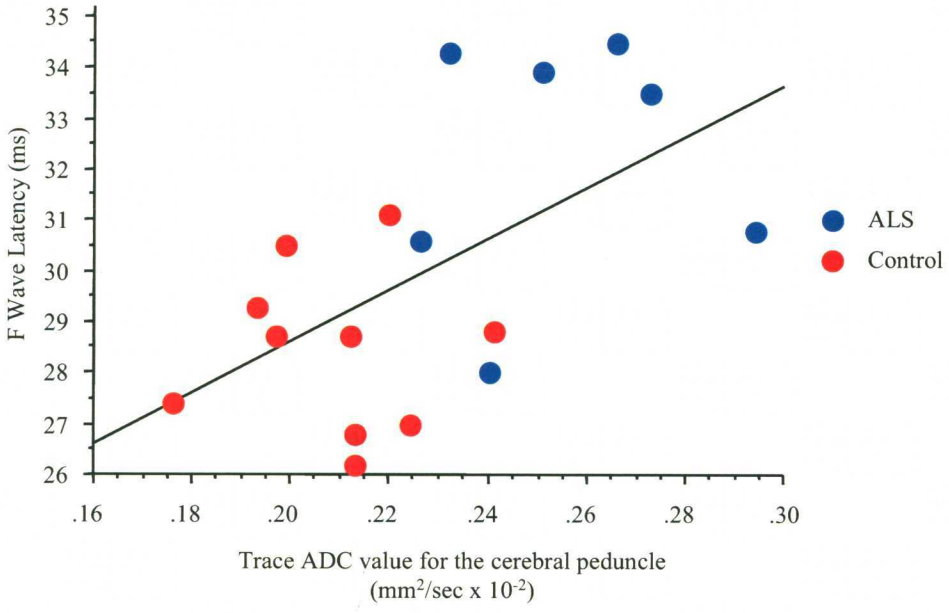

Figure 3.10. There was a positive correlation between the F Wave latency and the Trace ADC values in the cerebral peduncle ($p<0.05$). The ALS group is clustered towards the top right corner of the graph as their average F Wave latency and Trace ADC value was higher than the control group.

3.3(iv) Algorithm to calculate UMN pathology

Given the concordance between the DTI results and the multiple significant correlations of the DTI values with the TMS values, a mathematical model of UMN damage as a derivative from both instruments was attempted. There were many correlations between the DTI and TMS parameters, as demonstrated in the previous section. Multiple interactions exist within the TMS and DTI data such as the TraceADC/CMAPamp ratio. However, the CMAPamp investigates peripheral disturbances in ALS and is not an UMN measurement, thus the focus shifted to other TMS parameters.

The optimal TMS parameter that was able to distinguish between the ALS and the control groups, with the strongest interaction with TMS parameters, was SICI. The more negative the SICI value the more hyperexcitable the cortex, and the greater the abnormality in the CST as determined by DTI. SICI is expressed as a continuous variable, with the more abnormal SICI in ALS trending from a positive integer to a more negative integer: DTI variables are generally expressed as values between zero and one. Ratios with SICI as the numerator and various TMS parameters as the denominator, were therefore derived.

UMN Index = SICI/DTI parameter

There were significant interactions at all points of the CST with all of the DTI parameters and SICI with both SWAT and FT (Table 3.6). This is demonstrated graphically in Figures 3.14-17. This simple algorithm is therefore able to determine the amount of UMN involvement in the ALS group compared with the control group.

SICI/ParaD	ALS	Control	p value
Whole	-1.4E+03	5.6E+03	**<0.01**
CP	-8.6E+02	5.5E+03	**<0.05**
CP	-1.2E+03	4.7E+03	**<0.05**
Pt 2	-1.0E+03	4.9E+03	**<0.05**
Pt 2	-1.2E+03	5.6E+03	**<0.05**
Pt 3	-1.2E+03	5.5E+03	**<0.05**
Pt 3	-1.4E+03	5.8E+03	**<0.05**
IC	-1.3E+03	5.8E+03	**<0.01**
IC	-1.6E+03	6.8E+03	**<0.05**

SICI/FA	ALS	Control	p value
Whole	-2.6E+00	1.2E+01	**<0.05**
CP	-2.1E+00	1.0E+01	**<0.05**
CP	-2.1E+00	1.1E+01	**<0.05**
Pt 2	-2.0E+00	9.9E+00	**<0.05**
Pt 2	-2.4E+00	1.1E+01	**<0.05**
Pt 3	-2.3E+00	9.9E+00	**<0.05**
Pt 3	-2.3E+00	1.2E+01	**<0.05**
IC	-2.2E+00	1.1E+01	**<0.05**
IC	-2.8E+00	1.4E+01	**<0.05**

SICI/PerpD	ALS	Control	p value
Whole	-4.2E+03	1.7E+04	**<0.01**
CP	-2.8E+03	1.9E+04	**<0.01**
CP	-4.2E+03	1.6E+04	**<0.01**
Pt 2	-5.3E+03	2.1E+04	**<0.05**
Pt 2	-4.9E+03	1.9E+04	**<0.01**
Pt 3	-5.0E+03	2.4E+04	**<0.05**
Pt 3	-4.5E+03	1.8E+04	**<0.01**
IC	-4.9E+03	1.9E+04	**<0.05**
IC	-3.6E+03	1.6E+04	**<0.05**

SICI/ADC	ALS	Control	p value
Whole	-8.0E+02	3.4E+03	**<0.05**
CP	-5.5E+02	3.5E+03	**<0.05**
CP	-7.9E+02	2.9E+03	**<0.01**
Pt 2	-7.6E+02	3.3E+03	**<0.05**
Pt 2	-8.5E+02	3.6E+03	**<0.01**
Pt 3	-8.3E+02	3.8E+03	**<0.05**
Pt 3	-8.8E+02	3.5E+03	**<0.01**
IC	-8.6E+02	3.6E+03	**<0.05**
IC	-8.4E+02	3.6E+03	**<0.05**

Table 3.6. Mean Ratios of control and ALS SICI divided by any given DTI parameter

All of the ratios are significantly different between the ALS and control groups. The black font signifies a finding using the SWAT DTI results and the red font signifies a finding using the FT DTI results. For every DTI parameter, the ratio was significantly different between the two groups. ParaD – Parallel diffusion, ADC – Trace ADC, PerpD – Perpendicular diffusion. Whole – Whole tract, CP – Cerebral Peduncle, Pt 2 – Point 2, Pt 3 – Point 3 & IC – Internal Capsule.

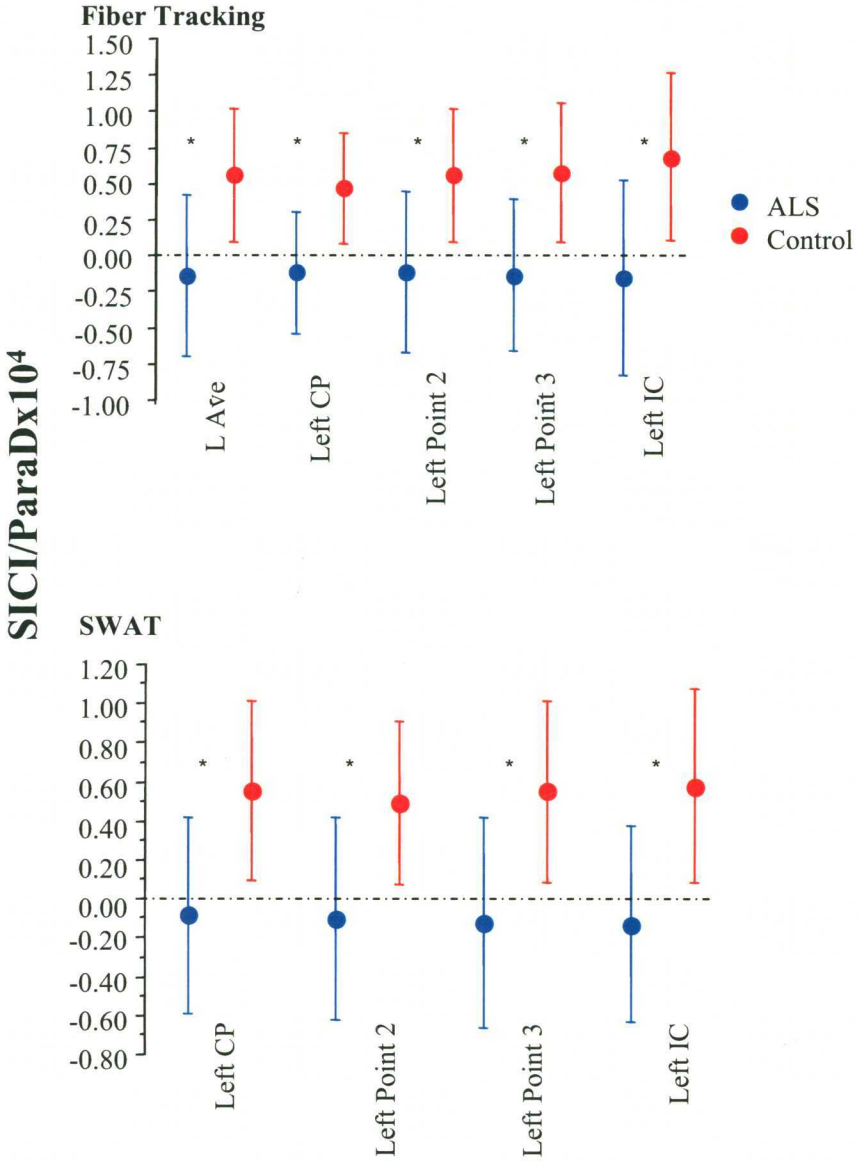

Figure 3.11. Mean values of the ratio of SICI/ParaD ±1 SD for Fiber Tracking and SWAT DTI measurements. The ratio of SICI/ParaD was significantly different at all levels of the CST, between the ALS and control groups using either analysis program. The asterisk represents statistical significance at a level of $p<0.05$.

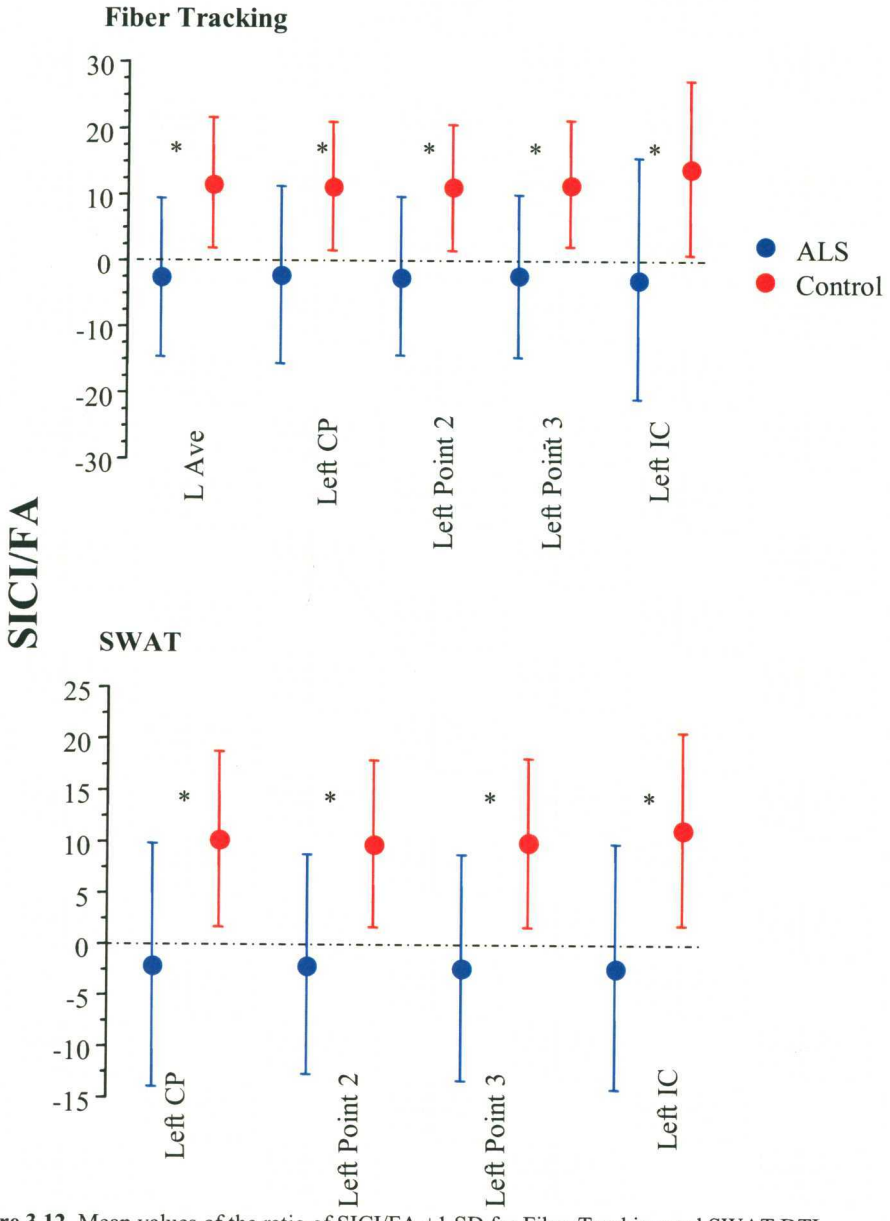

Figure 3.12. Mean values of the ratio of SICI/FA ±1 SD for Fiber Tracking and SWAT DTI measurements. The ratio of SICI/FA was significantly different at all levels of the CST, between the ALS and control groups using either analysis program. The asterisk represents statistical significance at a level of $p<0.05$.

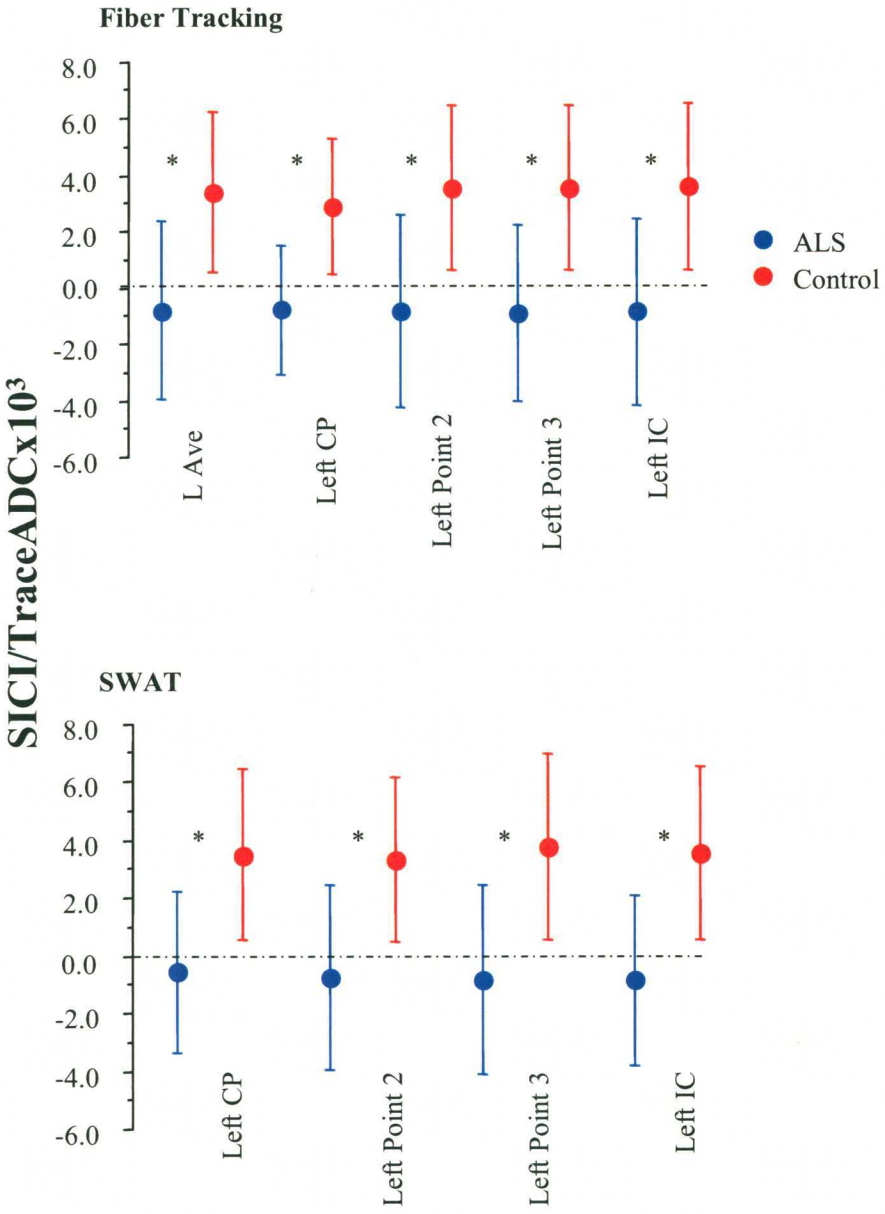

Figure 3.13. Mean values of the ratio of SICI/TraceADC ±1 SD for Fiber Tracking and SWAT DTI measurements. The ratio of SICI/TraceADC was significantly different at all levels of the CST, between the ALS and control groups using either analysis program. The asterisk represents statistical significance at a level of $p<0.05$.

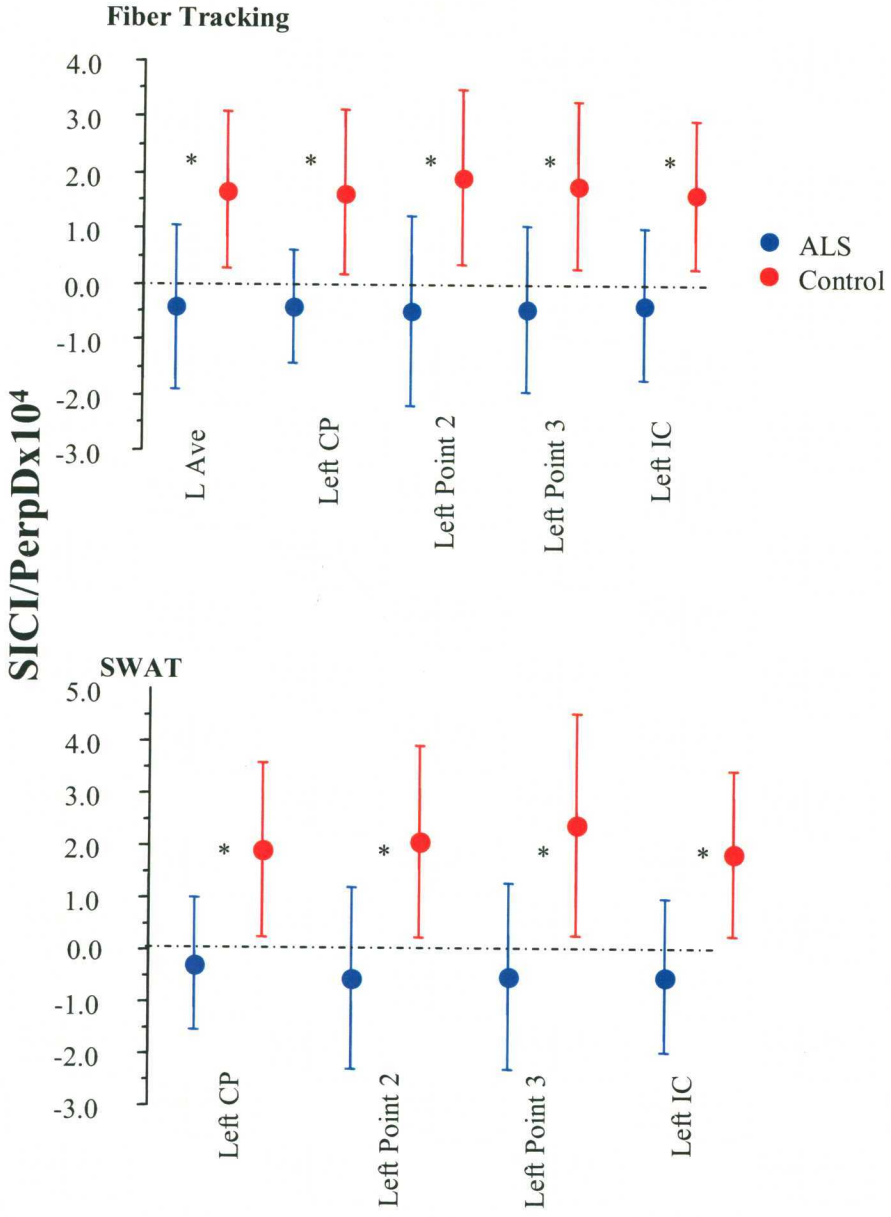

Figure 3.14. Mean values of the ratio of SICI/PerpD ±1 SD for Fiber Tracking and SWAT DTI measurements. The ratio of SICI/PerpD was significantly different at all levels of the CST, between the ALS and control groups using either analysis program. The asterisk represents statistical significance at a level of $p<0.05$.

3.4 Discussion

TMS studies were undertaken in ten newly diagnosed ALS patients, all with UMN involvement, and ten healthy controls to ascertain if there was evidence of cortical hyperexcitability in the ALS patients and to replicate the previously published method of Vucic and Kiernan 2006[222]. The same group of subjects then underwent DTI and the data was analysed using two different techniques: SWAT and FT. The data from the TMS and DTI was analysed to ascertain whether there was any difference between the ALS and the control group and then used for a correlation study between the TMS and DTI parameters, to develop an algorithm to determine the amount of UMN involvement in ALS. There was no significant difference in age between the ALS and control group ($p=0.65$).

Transcranial Magnetic Stimulation

The TMS study confirmed that ALS patients have abnormalities throughout the neural axis that are measurable via threshold tracking techniques. The ALS group had, statistically, significantly lower CMAP and NPI values than the control group, consistent with other studies[253, 267]. There was also significantly lower SICI and CSP duration, together with increases in the MEP:CMAP ratio and the SR curve gradient, all of which suggested cortical hyperexcitability[222, 226, 227, 268-270].

The Mechanisms of SICI

Obtaining a better understanding of SICI may shed light on the mechanisms that mediate intracortical inhibition and facilitation abnormalities. It was first demonstrated by Kujirai et al.(1993) that a subthreshold conditioning stimulus could suppress the response to a later suprathreshold test stimulus when the ISI was <5ms. Now it is known that there are two distinct phases of SICI[84, 232, 258, 271]. The

mechanism of the first phase of SICI remains unclear but the second phase is believed to be cortical in origin, mediated by GABA-secreting inhibitory cortical interneurons via $GABA_A$ receptors[272]. The reduction in SICI could be due to a loss of inhibitory cortical interneurons, as demonstrated by neuropathological studies[225].

SICI is partially restored in ALS patients who are treated with riluzole[270, 272], suggesting a down regulation of excitable cortex and possible involvement of glutamatergic mechanisms. Riluzole also inhibits persistent sodium currents and decreases intracortical facilitation[273, 274]. All of our ALS patients were on riluzole during the study, which perhaps reduced the magnitude of our findings. It was not considered appropriate or ethical to withdraw riluzole therapy during the study. Nevertheless, a clear distinction on these neurophysiological parameters was found between ALS and control subjects, suggesting an abnormality of significantly greater amplitude than that which may not be conveyed (or masked) by Riluzole.

In addition to reduction of SICI, the CSP duration was reduced in ALS. Given that the CSP duration is mediated by inhibition of anterior horn cells in the early phase [262, 275-277] and cortical processes, via $GABA_B$ receptors, in later segments [272, 275, 278-280], this finding is in keeping with previous studies documenting both disinhibition at the anterior horn cell level [281, 282] and of dysfunction of cortical inhibitory intreneurons acting via $GABA_B$ receptors [226].

Diffusion Tensor Imaging

The second tool used to investigate UMN involvement in this study was DTI. DTI investigates brain structures and assesses axonal fiber architectures in vivo. The following parameters were analysed: diffusion tensor eigenvalues (parallel

diffusivity and perpendicular diffusivity), fractional anisotropy and trace ADC values in the CST.

DTI parameters were examined using two different programs to analyse the source data, FT using DTIstudio and SWAT. Both of the programs highlighted congruent results and each technique revealed specific detail of the changes between the ALS and control group. The different analyses are discussed in the following paragraphs.

Fiber tractography ("fiber tracking"), allows three-dimensional pathways of white matter tracts to be reconstructed by sequentially piecing together spaced estimates of fiber orientation to form continuous fiber trajectories[283, 284]. The algorithm for fiber tracking is based on the Fiber Assignment by Continuous Tracking (FACT) approach. This means that the tracking is performed using a continuous coordinate system rather than a discrete voxel-based matrix grid[283, 285]. In brief, a line was propagated in both retrograde and orthograde directions according to v1 at each pixel from a seed pixel. If the FA was lower than a threshold of 0.25 within a pixel, the tracking would be terminated. Fibers that penetrated the ROIs, defined by anatomical landmarks were retained. In the fiber tracking analysis, the CSTs were constructed using multiple regions of interest. Neuroanatomical knowledge of the approximate location of the CST was used to define reference ROIs through which the tracts must pass.

The other program that was used to analyse the DTI data was Stereotaxic White matter Atlas in Talairach coordinate (SWAT). This program normalizes DTI data to the Talairach space by brain rotation and normalisation to the Anterior Cingulate (AC) and Posterior Cingulated (PC) orientation. Once the landmark-based

normalization is completed, the transformation is applied to tensor fields and the various DTI-derived contrasts are recalculated. SWAT allows population-based voxel-based analysis of the DTI data. Once the data was processed by the SWAT program it was analysed using the ROI editor program.

Quantitative statistical comparison of DTI parameters showed a significant decrease in FA, a significant increase in perpendicular diffusion and a significant increase in the trace ADC value, using both DTIstudio and ROI editor. Previous studies have shown a decrease in FA along the CST in ALS patients[113, 129, 161-165, 244, 245, 286], some of which believe that the magnitude of diffusion was reported to be unchanged[163, 286], or increased[161, 162], while others believe that the anisotropy changes result from a loss of fiber integrity caused by axonal degeneration[164, 287].

Sage et al. (2006), studied quantitative DTI in ALS with an aim to evaluate the changes in DTI parameters in the whole brain of ALS patients using fiber tracking and voxel-based analysis. Using fiber tracking they found that the precentral part of the CST was impaired[264]. Voxel-based analysis show that changes of diffusion also occur throughout the brain and are not limited to the CST in ALS patients[113]. At the time when our research was being conducted, no other report had investigated the role of eigenvalues in ALS. A recently published paper did observe changes in eigenvalues along the CST, mainly reporting significance in ParaD, not PerpD, supporting our study[288]. This paper did not use fiber tracking and used the coronal slice to place a ROI (which is different to our study as this study observed the axial slice). Using fiber tracking, there was a significant difference between the ALS and control group mostly along the whole of the CST on both the left and right side in the perpendicular diffusion and FA.

The SWAT program demonstrated an increase in the PerpD along most of the regions of the CST. This reached statistical significance on the left cerebral peduncle, right cerebral peduncle and at the right internal capsule.

The ALS group had lower FA values along the whole CST in both hemispheres which reached significance at the left cerebral peduncle. The ALS group had higher Trace ADC values along most of the right and left CST, the only point at which this is reversed is on left and right point 2 of the CST. The ALS group had a significantly higher value in the left cerebral peduncle, left and right internal capsule.

Explanation of higher diffusion in ALS

The PerpD and trace ADC were higher in the ALS group and the FA value was lower in the ALS group. Neuronal degeneration, inclusion bodies, cytoskeletal structural abnormalities and astrocytic gliosis, may be responsible for the observed abnormalities in the diffusion parameters in ALS. However, tight packing of axons and axonal membranes are the main determinants of anisotropic diffusion[289]. An increase in water diffusion perpendicularly, and therefore the PerpD value, could be due to increased membrane permeability secondary to axonal membrane injury and/or to axonal degeneration secondary to neuronal death.

Limitations in DTI

The FT and SWAT programs were not always concordant, probably due to mathematical post-processing. Both programs, however, highlighted differences between the groups in the same parameters along the CST. In summary then, there were significant differences between ALS and control groups when investigating

PerpD, FA and Trace ADC. These findings demonstrate a difference between ALS and control groups along the CST. The FT and SWAT program seem to complement each other as one method is able to detect differences along the entire SCT, whereas the other method identifies differences in ROIs along the CST.

The present study, using a combination of threshold tracking TMS techniques and diffusion tensor imaging to explore upper motor neuron dysfunction in ALS patients, has effectively quantified independent UMN abnormalities in ALS patients. Upper motor neuron dysfunction was evident in ALS patients with reductions in the resting motor threshold, short-interval intracortical inhibition and cortical silent period duration. In addition, structural abnormalities were evident by reduced fractional anisotropy, and increased trace ADC and perpendicular diffusivity. The reduction of SICI correlated with DTI abnormalities, thereby suggesting that the changes in SICI were associated with underlying structural abnormalities of axons within the central nervous system. Together, these findings confirmed the presence of UMN dysfunction in ALS and suggest that changes in SICI were associated with underlying structural abnormalities within the axons of the central nervous system. In addition, an objective measure of UMN involvement has been developed, that appeared to be more sensitive at detecting UMN abnormalities than conventional DTI parameters.

Correlations and potential Algorithm

There was no correlation between disease duration, total Appel score with any of the DTI or TMS parameters. The former is consistent with all of the patients having similar disease durations. The latter is not surprising either as domains

assessed by the Appel scale are dependent on strength, which is largely dependent on LMN integrity. There are no sub scores in the Appel Rating Scale that directly interrogate UMN symptoms or signs. Furthermore the clinical assessment of the severity of UMN abnormalities is difficult.

Correlations were carried out to determine the relationship between TMS parameters and the DTI parameters. DTI data was studied as whole tract (compact) data and also as individual points along the CST using results from both the SWAT and FT programs. Numerous correlations were found between the TMS and DTI parameters in both the compact and individual points data. From the correlation study, the TMS parameters that correlated with both DTI programs were tested to see if a new algorithm to measure UMN involvement in ALS could be generated. To our knowledge, there is no published algorithm to quantify UMN abnormalities using both DTI and TMS as independent measures. Such an algorithm could be of assistance in providing a measure of disease progression in clinical trials, or by gaining a better understanding of the mechanisms of this disease, and to possibly help in the development of a diagnostic tool.

There were many correlations between the DTI and TMS parameters. Other interactions exist within TMS and DTI such as the TraceADC/CMAPamp ratio. There was a significant difference between ALS and control groups at all points of the CST using both FT and SWAT results.

To narrow the focus in generating a potential algorithm, the TMS parameter SICI was compared with all of the DTI parameters. There was a significant difference in the SICI/DTI ratio for all of the parameters at all of the points in the CST using both programs in ALS patients and the control group. This is the first

algorithm to quantify UMN involvement in ALS using parameters from DTI and TMS. Unlike the neurophysiological index this ratio combines TMS and DTI, independent measures of UMN abnormality. It is possible that this ratio could be used in clinical trials to see if the drug tested has a positive or negative effect. Lastly such measures could offer an insight into the cause(s) of ALS, as research supports the proposed idea that ALS pathology may start in the cortex (the so-called, "anterograde disease process")[217, 222]. The benefits of performing DTI and TMS in ALS patients to determine UMN involvement may outweigh the cost and inconvenience of these tests.

4.0 General Discussion

Amyotrophic Lateral Sclerosis (ALS) is characterized by the progressive deterioration of the CST, anterior horn cells of the spinal cord and the brainstem. There is no pathognomonic test to confirm the diagnosis of ALS, and physicians rely on clinical criteria – upper and lower motor neuron signs – supported by electrophysiological studies for diagnosis[290]. Commonly, the diagnosis of ALS is a process of elimination which can take a long time. The estimated incidence of ALS is approximately two per 100,000 persons per year, and the prevalence is approximately six per 100,000 persons[291].

The presentations, clinical phenotypes and outcomes of ALS are diverse and a marker of disease progression is not available to date. No single algorithm combines the findings of functional assessments and rating scales, such as those that assess quality of life, with biological markers of disease activity and findings from imaging and neurophysiological assessments.

There are numerous theories attempting to explain the cause(s) of ALS but unfortunately none are as yet proven. It is conceivable that ALS is a heterogeneous disease with common characteristic biological, pathological and clinical features. One difficulty in understanding the ALS disease process is that at the time of diagnosis a large percentage of the motor neurons have already degenerated. It is also difficult to determine where the pathological process starts. It is not known if the pathological process starts at the neuromuscular junction, spreading in a retrograde direction toward the UMNs: or if the process starts in the motor cortex, spreading anterogradely down the CST to the anterior horn cell. The process of

studying disease pathology would be easier if there was an investigational tool to study the motor system for early changes.

The initial aim of this thesis was to examine why a proportion newly diagnosed ALS patients develop severe NH and others do not. This is an important question as patients who suffer from NH have a significantly shorter survival without early intervention with non-invasive ventilation, than do patients without NH. A cohort of patients from the ALS clinic at Royal North Shore, with NH, who did not have any disturbance or daytime respiratory function was identified. This thesis started with a retrospective study to better categorize respiratory function in this cohort., and examine the relationship between daytime respiratory function and NH. Analysis of RFT data revealed that no routine respiratory function tests was distinguished NH from non-NH patients(Chapter 2 and Appendix D). This led to the hypothesis of a central mechanism(s) in the development of NH, as patients found to have early evolution of NH demonstrated a combination of UMN and LMN signs clinically.

Diffusion Tensor Imaging (DTI) and Transcranial Magnetic Stimulation (TMS) were chosen to study UMN involvement in ALS with the hypothesis that a combination of these two techniques might distinguish between NH and non-NH suffers, as well as providing a better understanding of the nature and pattern of UMN involvement in ALS. Unfortunately, no ALS patients with early NH were identified during the study period, so this thesis focused on the development of a TMS/DTI algorithm to determine or quantify UMN involvement in ALS. The results reported in Chapter 3 demonstrated extensive UMN involvement in newly diagnosed ALS

patients using TMS and DTI. Subsequently both techniques were combined into a ratio of UMN damage. This is discussed in more detail later.

In Chapter 2, data was collected from 16 consecutive ALS patients with early limb-onset ALS, but without any bulbar dysfunction or signs of NH. These patients underwent standard respiratory function tests and formal sleep studies. All patients and controls underwent standard respiratory function tests which included: spirometry, vital capacity, lung volumes, diffusion for carbon monoxide, measurement of Maximal Expiratory Pressure (MEP) and Maximal Inspiratory Pressure (MIP). The results contained were compared to that of nine healthy control patients (age/sex matched) who underwent a similar assessment. Patients who suffered from NH had clear evidence of oxygen desaturation to 90% or less for a period of more than 2 minutes while asleep at night. All NH patients showed poor resaturation and had a fall from the baseline saturation of $\geq 4\%$. This, together with the absence of coexistent obesity, was considered sufficient to exclude obstructive sleep.

NH was identified in 50% of ALS patients. There was no significant difference in any of the standard respiratory parameters between ALS patients and the control group. The only borderline significant result was MEP between ALS patients who suffered from NH and the control group. However, the MEP value was not a predictor of the presence of NH when analysed in isolation.

This study highlights the importance of measuring overnight oximetry in all patients with ALS to screen for the presence of NH, as this important feature appears to be occur independent of voluntary maximal respiratory effort measured in routine

respiratory tests. More importantly, if patients with ALS are found to suffer from NH, they can be offered early access to Non-Invasive Positive-Pressure Ventilation (NIPPV), with a resultant and highly significant improvement in sleep quality, daytime sleepiness, physical fatigue and depression[201].

Furthermore, the absence of change in standard respiratory function tests at the onset of NH suggests the involvement of additional mechanisms, such as the involvement of central respiratory control. Future studies could interrogate this further by correlating the findings of dynamic sleep studies in ALS patients who demonstrate NH, with the investigation of UMN function by clinical neurophysiological techniques such as TMS, and structural assessment of the Corticospinal Tract (CST) using DTI.

As there was only a marginally significant difference in the MEP measurement between ALS and control groups it lead to the investigation of Sniff Nasal Inspiratory Force (SNIF) as a tool to distinguish early onset ALS patients from healthy controls. We decided to investigate the Forced Oscillation Technique (FOT) in ALS patients to see if this respiratory function test could distinguish ALS patients who suffer from NH from those who did not. There are no published data on the use of this technique in ALS patients. The ALS group had a significantly lower SNIF value than the control group. There was no significant difference in FOT values between ALS or control groups.

UMN dysfunction is difficult to quantify clinically in ALS, and may be impossible to detect in the presence of significant LMN involvement. Pathological studies have demonstrated the presence of UMN pathology in 75% of patients at post mortem examination, even when no UMN signs were detectable by experienced

clinicians during life[206]. Standard imaging techniques are of limited use in assessing ALS patients, as UMN dysfunction tends to be both variable and localised to small structures which may be below macroscopic resolution[292, 293]. Imaging studies often neglect the anterior horn cell and focus on the cerebral UMN's, and its outflow pathway - the Corticospinal Tract (CST)[149]. ALS selectively targets spinal anterior horn and brainstem motor neurons (Lower Motor Neurons, LMNs) and neurons of the primary motor cortex (UMN) that give rise to the CST . Any potential UMN assessment/measurement technique for ALS needs to be safe, reliable, without large measurement error, sensitive to disease progression and severity. DTI and TMS were used in the study to measure upper motor neuron damage in ALS in our patient population.

In Chapter 3, TMS studies were undertaken in 10 ALS patients and 10 controls, to assess cortical excitability via a paired pulse threshold tracking paradigm. This involved a conditioning stimulus that was delivered at time intervals before a suprathreshold test stimulus. The conditioning and test stimuli remained constant and the effects of the conditioning stimulus were measured by recording the changes in the amplitude of the test response. Inhibition and facilitation were measured using Interstimulus Interval (ISI). It is believed that intracortical inhibition and facilitation reflect changes in the cortical circuitry. Short-Interval Intracortical Inhibition (SICI) was first reported by Kujirai et al. (1993)[258]. The mechanism of this inhibition is believed to be of cortical origin, and such a proposition is supported by epidural recordings[84, 259]. There are two physiologically distinct phases of SICI[84, 271] with the first phase occurring at an ISI of </= 1ms and the second at ISI of 2.5ms. There

is debate regarding the first phase of SICI. Some believe it reflects local excitability properties of the cortical axon[84]. Whilst others believe it is best explained by the activation of inhibitory circuits different from those that mediate inhibition of the second phase[271]. The mechanism of the second phase is believed to be of cortical origin and mediated by GABA-secreting inhibitory cortical interneurons via $GABA_A$ receptors[272, 294].

In keeping with previous studies[226, 227, 268-270, 295], SICI was found to be significantly reduced in ALS patients in this study. The reduction of SICI may be explained by a loss of inhibitory cortical interneurons. Neuropathological studies reveal a loss of parvalbumin-positive inhibitory cortical interneurons in ALS patients[225]. However, SICI is rapidly restored in ALS patients when treated with pharmacological agents such as riluzole[270, 272] which means that loss of inhibitory cortical interneurons is not the only mechanism mediating SICI reduction. Glutamate-mediated down-regulation of SICI may be another mechanism responsible for this reduction of SICI in ALS. All our ALS patients were on riluzole, and yet still had demonstrable abnormalities in SICI. This study was able to reproduce the findings of Vucic and Kiernan, and establish the presence of cortical hyperexcitability in ALS patients.

DTI studies were then undertaken in the same subjects, on the same day, to gain a better understanding of the structural integrity of the neuronal fiber tracts in the CST. DTI quantifies the water diffusion characteristics along the CST. Fractional Anisotropy (FA) measures the coherence of diffusion, Apparent Diffusion Coefficient (ADC) measures bulk diffusion and the directionality of diffusion (parallel or perpendicular) to fiber tracts is measured by eignevalues[288]. Two

analysed/software programs were used, Stereotaxic White matter Atlas in Talairach Coordinate (SWAT) and fiber tracking to obtain data from the CST. The main difference between the two programs used to process the DTI data was that fiber tracking enabled accurate identification of the CST for further analysis, in contrast to previous published studies. Tractography enabled reconstruction of the CST by instructing the program to identify white matter tracts joining specific regions within the brain. Anatomically, the two points used to identify the CST were the cerebral peduncle and the posterior limb of the internal capsule. The fiber tracking program was instructed to draw the tract connecting these two specific regions, the CST. In the SWAT program, a 'best guess' approach is taken whereby no tract is generated, but anatomical knowledge allows for the placement of the regions of interest (ROIs), in reference to an idealized brain map. ROIs were placed along the CST at four standard points starting from the cerebral peduncle and finishing at the internal capsule. This was done to use a second method of analysis of the dataset, to determine whether the method of analysis was robust.

The main result arising from this was that there were significant differences between the ALS and control groups in all parameters, using both programs. In general, FA was lower in ALS, in concordance with previous studies[113, 129, 161-165, 244, 245, 286], ADC abnormalities were also a common finding[288] and abnormal eigenvalues[129, 163]. This study is the first, to our knowledge, to examine eigenvalues using fiber tracking and to compare and confirm these results with the SWAT results. Most of the abnormalities were found in the whole tract using FT and in the cerebral peduncle using the SWAT program. The programs showed the same trend between

ALS and control groups, but highlighted the significance to vary at different sites along the CST.

The FT program DTIStudio has the ability to calculate the selected tract statistics i.e. the average of the whole CST tract, not just the average of the points selected along the tract. This was significantly different between ALS and control groups for FA and PerpD, with the ALS group showing more perpendicular diffusivity and a lower fractional anisotropy bilaterally. This function does not exist in ROI editor (the program that analyses the SWAT data) but SWAT highlighted significant differences in the cerebral peduncle, with the ALS group having a significantly higher left ADC, bilaterally higher PerpD values and a lower left FA value than controls. Both programs showed abnormalities in the right internal capsule with regard to perpendicular diffusivity. The SWAT program also reported a significant difference between the ALS and control groups in the right internal capsule for the trace ADC value.

In the last section of this chapter, correlations were explored between the methods used to obtain a potential TMS/DTI algorithm to quantify UMN abnormalities. These data were analysed as both compact entities and individual points along the CST for the DTI findings and then correlated with the TMS parameters. This involved four correlation matrices and then a fifth summary correlation table added to highlight where the correlations were when looking at all of the results (compact and individual points using both FT and SWAT). The correlation studies were carried out looking at the data as a whole, irrespective of disease or non-disease state, and then for correlations within each group (ALS and control). Eighty percent of the DTI and TMS parameters correlated in the summary

Table. It was decided to further examine the parameters that correlated in both the FT and SWAT programs, to narrow the search for the DTI/TMS ratio. In the final part of this chapter a ratio between SICI/DTI parameters was found that gave statistically significant differences between the ALS and control group. This ratio was significant at all CST points bilaterally in both the FT and SWAT program. The current study can be improved by repeating and using different types of MND variants to see whether the UMN index is powerful enough to distinguish different phenotypes.

Prospect of future studies

This thesis has identified UMN involvement in ALS using both TMS and DTI. TMS is a well established research tool in ALS, whereas DTI is a relatively new technique in this context. The concept of studying white matter tracts within the brain of ALS patients is in its infancy. However, a significant problem for DTI studies is the lack of a gold standard for analysing images. However, this gold standard is currently being developed. Major centres, such as John Krieger at Johns Hopkins University in Baltimore, is developing programs that should prove to be more reliable analytical tools. Initially the DTI field studied FA and Mean diffusivity. However, the focus has now shifted to include eigenvalues, which allow a better understating of the potential location of water diffusivity. This is important, as it should enable a deeper understanding of the disease process.

Combining TMS data with DTI lead to the development of an algorithm that can measure UMN involvement in ALS. The SICI/DTI algorithm may be useful in determining the involvement of UMNs in ALS. More studies are needed using this algorithm in other ALS patients and control groups to determine the threshold and range of values found in healthy controls and ALS patients. This algorithm also needs to be tested longitudinally with MUNE to see how the UMN and LMN involvement differs throughout the course of ALS. This tool might prove to be a powerful addition or tool in the assessment of UMN abnormalities in ALS. More studies are needed to compare other UMN disorders such as primary lateral sclerosis, HSP and Parry Romberg syndrome, described in more detail in Appendix A.

Hopefully this thesis has described the new concept of combining two powerful techniques, TMS and DTI that are already in use in isolation, to study UMN involvement potentially in numerous disease states.

Abbreviations

AC – Anterior Cingulate

ADC – Apparent Diffusion Coefficient

AHC – Anterior Horn Cell

ALS – Amyotrophic Lateral Sclerosis

ALS FRS – Amyotrophic Lateral Sclerosis Functional Rating Scale

ALS FRS-r – Amyotrophic Lateral Sclerosis Functional Rating Scale Revised

ALSNH – Amyotrophic Lateral Sclerosis Nocturnal Hypoventilation

ANOVA – Analysis of Variance

APB – Abductor Pollicis Brevis

BDNF – Brain-Derived Neurotrophic Factor

BIPAP – Bi-Level Intermittent Positive Pressure

CMAP – Compound Muscle Action Potential

CMCT – Central Motor Conduction Time

CMT – Cortical Motor Threshold

CO – Carbon Monoxide

CP – Cerebral Peduncle

Cr - Creatine

CSP – Cortical Silent Period

CST – Corticospinal Tract

CTNF – Ciliary Neurotrophic Factor

D - Diffusion

DLCO – Carbon Monoxide Diffusing Capacity

DTI – Diffusion Tensor Imaging

EEc – El Escorial Criteria

EEG – Electroencephalogram

EMG – Electromyography

EOG – Electrooculography

EPI – Echo Planar Imaging

Ev – Eigenvalues

FA – Fractional Anisotropy

FACT – Fiber Assignment by Continuous Tracking

FEV1 – Forced Expiratory Volume in one second

FLAIR – Fluid Attenuated Inversion Recovery

FOT – Forced Oscillation Technique

FT – Fiber Tracking

FVC – Forced Vital Capacity

GCIC – Global Clinical Impression of Change

IGF – Insulin Growth Factor

IC – Internal Capsule

ISI – Interstimulus Intervals

LICI – Long Intracortical Inhibition

LMN – Lower Motor Neurons

MEP – Maximum Expiratory Pressure

MIP – Maximum Inspiratory Pressure

MND – Motor Neuron Disease

MRS – Magnetic Resonance Spectroscopy

MSO – Maximum Stimulation Output

MUNE – Motor Unit Number Estimation

NAA – N-Acetyl-Aspartate

NCS – Nerve Conduction Studies

NH – Nocturnal Hypoventilation

NIPPV – Non-Invasive Positive Pressure Ventilation

NIV – Non Invasive Ventilation

NPI – Neurophysiological Index

NS – Not significant

P – Pressure

ParaD – Parallel Diffusivity

PC – Posterior Cingulate

PEF – Peak Expiratory Force

PerpD – Perpendicular Diffusivity

PLS – Primary Lateral Sclerosis

PMA – Progressive Muscular Atrophy

PSG - Polysomnography

PSTH – Peristimulus Time Histogram

RDI – Respiratory Disturbance Index

REM – Rapid Eye Movement

RFT – Respiratory Function Test

RMT – Resting Motor Threshold

ROI – Region of Interest

Rrs - Resistance

RV – Residual Volume

SICI – Short-Interval Intracortical Inhibition

SMA – Spinal Muscular Atrophy

SNIF – Sniff Nasal Inspiratory Force

SOD – Super Oxidase Dismutase

SR – Stimulus Response

SWAT – Stereotaxic White Matter Atlas in Talairach Coordinate

TLC – Total Lung Capacity

TMS – Transcranial Magnetic Stimulation

UMN – Upper Motor Neuron

V – Flow

References

1. Bruijn LI, Miller TM, Cleveland DW. Unraveling the mechanisms involved in motor neuron degeneration in ALS. Annu Rev Neurosci 2004;27:723-49.

2. Charcot J JA. Deux cas d'astrophie musculaire progressive avec lesions de la substance grise et des faisceaux antero lateraux de la moelle epiniere. Arch Physiol Neurol Pathol 1869;2:744-754.

3. Davenport RJ, Swingler RJ, Chancellor AM, Warlow CP. Avoiding false positive diagnoses of motor neuron disease: lessons from the Scottish Motor Neuron Disease Register. J Neurol Neurosurg Psychiatry 1996;60(2):147-51.

4. Mitsumoto H, Chad, DA & Pioro EP. Terminology & Classification of AlS In Amyotrophic Lateral Sclerosis. In. philadelphia: FA Davis Company; 1998. p. 3-15.

5. Ringel SP, Murphy JR, Alderson MK, Bryan W, England JD, Miller RG, et al. The natural history of amyotrophic lateral sclerosis. Neurology 1993;43(7):1316-22.

6. Talman P, Mathers S, Mostert E, Forbes A. Evaluation of clinical patterns and rate of progression of motor neuron disease. ALS and other motor neuron disorders 2002;3(Suppl. 2):93.

7. Brooks BR. El Escorial World Federation of Neurology criteria for the diagnosis of amyotrophic lateral sclerosis. Subcommittee on Motor Neuron Diseases/Amyotrophic Lateral Sclerosis of the World Federation of Neurology Research Group on Neuromuscular Diseases and the El Escorial "Clinical limits of amyotrophic lateral sclerosis" workshop contributors. J Neurol Sci 1994;124 Suppl:96-107.

8. Miller RG, Munsat TL, Swash M, Brooks BR. Consensus guidelines for the design and implementation of clinical trials in ALS. World Federation of Neurology committee on Research. J Neurol Sci 1999;169(1-2):2-12.

9. Traynor BJ, Codd, M.b., Corr, B., Forde, C., Frost, E. & Hardiman, M. Clinical features of Amyotrophic Lateral Sclerosis According to the El Escorial and Airlie House Diagnostic Criteria. Arch Neurol. 2000;57:1171-1176.

10. Kiernan M. Motor neuron disease: a Pandora's box. MJA 2003;178:311-312.

11. Lewis RA. Neuropathies associated with conduction block. Curr Opin Neurol 2007;20(5):525-30.

12. Van den Berg-Vos RM, Franssen H, Wokke JH, Van Es HW, Van den Berg LH. Multifocal motor neuropathy: diagnostic criteria that predict the response to immunoglobulin treatment. Ann Neurol 2000;48(6):919-26.

13. aihw. In.

14. Rosen DR, Siddique T, Patterson D, Figlewicz DA, Sapp P, Hentati A, et al. Mutations in Cu/Zn superoxide dismutase gene are associated with familial amyotrophic lateral sclerosis. Nature 1993;362(6415):59-62.

15. Garber K. GENETICS: The Elusive ALS Genes. Science 2008;319(5859):20.

16. Aebischer P, Kato AC. Playing defense against Lou Gehrig's disease. Sci Am 2007;297(5):86-93.

17. Andersen PM, Nilsson P, Keranen ML, Forsgren L, Hagglund J, Karlsborg M, et al. Phenotypic heterogeneity in motor neuron disease patients with CuZn-superoxide dismutase mutations in Scandinavia. Brain 1997;120 (Pt 10):1723-37.

18. Al-Chalabi A, Andersen PM, Chioza B, Shaw C, Sham PC, Robberecht W, et al. Recessive amyotrophic lateral sclerosis families with the D90A SOD1 mutation

share a common founder: evidence for a linked protective factor. Hum Mol Genet 1998;7(13):2045-50.

19. Rowland LP. Molecular basis of genetic heterogeneity: role of the clinical neurologist. J Child Neurol 1998;13(3):122-32.

20. Cudkowicz ME, McKenna-Yasek D, Chen C, Hedley-Whyte ET, Brown RH, Jr. Limited corticospinal tract involvement in amyotrophic lateral sclerosis subjects with the A4V mutation in the copper/zinc superoxide dismutase gene. Ann Neurol 1998;43(6):703-10.

21. Hassan A, Erjavec, S., Winter, S. & Rowe, D. Anticipation in a pedigree with familial amyotrophic lateral sclerosis secondary to a mutation in superoxide dismutase type 1 (V148G). In: Swash M, editor. 18th International Symposium on ALS/MND; 2007; Toronto, Canada: Informa Healthcare; 2007. p. 198.

22. Chandran J, Ding J, Cai H. Alsin and the molecular pathways of amyotrophic lateral sclerosis. Mol Neurobiol 2007;36(3):224-31.

23. Greenway MJ, Andersen PM, Russ C, Ennis S, Cashman S, Donaghy C, et al. ANG mutations segregate with familial and 'sporadic' amyotrophic lateral sclerosis. Nat Genet 2006;38(4):411-3.

24. Hardiman O, Greenway M. The complex genetics of amyotrophic lateral sclerosis. Lancet Neurol 2007;6(4):291-2.

25. Simpson CL, Al-Chalabi A. Amyotrophic lateral sclerosis as a complex genetic disease. Biochim Biophys Acta 2006;1762(11-12):973-85.

26. Veldink JH, Van den Berg LH, Wokke JH. The future of motor neuron disease: the challenge is in the genes. J Neurol 2004;251(4):491-500.

27. Orrell RW. Understanding the causes of amyotrophic lateral sclerosis. N Engl J Med 2007;357(8):822-3.

28. Cole N, Siddique T. Genetic disorders of motor neurons. Semin Neurol 1999;19(4):407-18.

29. Cookson MR, Shaw PJ. Oxidative stress and motor neurone disease. Brain Pathol 1999;9(1):165-86.

30. Chou SM, Wang HS, Taniguchi A. Role of SOD-1 and nitric oxide/cyclic GMP cascade on neurofilament aggregation in ALS/MND. J Neurol Sci 1996;139 Suppl:16-26.

31. Leigh PN, Dodson A, Swash M, Brion JP, Anderton BH. Cytoskeletal abnormalities in motor neuron disease. An immunocytochemical study. Brain 1989;112 (Pt 2):521-35.

32. Gibson SJ, Polak JM, Katagiri T, Su H, Weller RO, Brownell DB, et al. A comparison of the distributions of eight peptides in spinal cord from normal controls and cases of motor neurone disease with special reference to Onuf's nucleus. Brain Res 1988;474(2):255-78.

33. Shaw PJ. Excitotoxicity and motor neurone disease: a review of the evidence. J Neurol Sci 1994;124 Suppl:6-13.

34. Livet J, Weissman TA, Kang H, Draft RW, Lu J, Bennis RA, et al. Transgenic strategies for combinatorial expression of fluorescent proteins in the nervous system. Nature 2007;450(7166):56-62.

35. Vucic S, Burke, D. & Kiernan, M.C. Diagnosis of motor neurone disease. In: Kiernan MC, editor. The Motor Neurone Disease Handbook. Pyrmont, Austalia: Austalasian Medical Publishing Company Limited; 2007. p. 89-104.

36. Barohn RJ, Kissel JT, Warmolts JR, Mendell JR. Chronic inflammatory demyelinating polyradiculoneuropathy. Clinical characteristics, course, and recommendations for diagnostic criteria. Arch Neurol 1989;46(8):878-84.

37. Bouchard C, Lacroix C, Plante V, Adams D, Chedru F, Guglielmi JM, et al. Clinicopathologic findings and prognosis of chronic inflammatory demyelinating polyneuropathy. Neurology 1999;52(3):498-503.

38. Rotta FT, Sussman AT, Bradley WG, Ram Ayyar D, Sharma KR, Shebert RT. The spectrum of chronic inflammatory demyelinating polyneuropathy. J Neurol Sci 2000;173(2):129-39.

39. Latov N. Diagnosis of CIDP. Neurology 2002;59(12 Suppl 6):S2-6.

40. Roth G, Rohr J, Magistris MR, Ochsner F. Motor neuropathy with proximal multifocal persistent conduction block, fasciculations and myokymia. Evolution to tetraplegia. Eur Neurol 1986;25(6):416-23.

41. Parry GJ, Clarke S. Multifocal acquired demyelinating neuropathy masquerading as motor neuron disease. Muscle Nerve 1988;11(2):103-7.

42. Pestronk A, Cornblath DR, Ilyas AA, Baba H, Quarles RH, Griffin JW, et al. A treatable multifocal motor neuropathy with antibodies to GM1 ganglioside. Ann Neurol 1988;24(1):73-8.

43. Pestronk A, Chaudhry V, Feldman EL, Griffin JW, Cornblath DR, Denys EH, et al. Lower motor neuron syndromes defined by patterns of weakness, nerve conduction abnormalities, and high titers of antiglycolipid antibodies. Ann Neurol 1990;27(3):316-26.

44. Bouche P, Moulonguet A, Younes-Chennoufi AB, Adams D, Baumann N, Meininger V, et al. Multifocal motor neuropathy with conduction block: a study of 24 patients. J Neurol Neurosurg Psychiatry 1995;59(1):38-44.

45. Taylor BV, Wright RA, Harper CM, Dyck PJ. Natural history of 46 patients with multifocal motor neuropathy with conduction block. Muscle Nerve 2000;23(6):900-8.

46. Kiernan MC, Guglielmi JM, Kaji R, Murray NM, Bostock H. Evidence for axonal membrane hyperpolarization in multifocal motor neuropathy with conduction block. Brain 2002;125(Pt 3):664-75.

47. Krishnan AV, Pamphlett R, Burke D, Kiernan MC. Ctoplasmic-body myopathy masquerading as motor neurone disease. Muscle Nerve 2004;In Press.

48. Hirayama K, Tsubaki T, Toyokura Y, Okinaka S. Juvenile muscular atrophy of unilateral upper extremity. Neurology 1963;13:373-80.

49. Colombo R, Mazzini L, Mora G, Parenzan R, Creola G, Pirali I, et al. Measurement of isometric muscle strength: a reproducibility study of maximal voluntary contraction in normal subjects and amyotrophic lateral sclerosis patients. Med Eng Phys 2000;22(3):167-74.

50. Bromberg MB, Forshew DA, Nau KL, Bromberg J, Simmons Z, Fries TJ. Motor unit number estimation, isometric strength, and electromyographic measures in amyotrophic lateral sclerosis. Muscle Nerve 1993;16(11):1213-9.

51. McComas AJ, Fawcett PR, Campbell MJ, Sica RE. Electrophysiological estimation of the number of motor units within a human muscle. J Neurol Neurosurg Psychiatry 1971;34(2):121-31.

52. Galea V, de Bruin H, Cavasin R, McComas AJ. The numbers and relative sizes of motor units estimated by computer. Muscle Nerve 1991;14(11):1123-30.

53. Stein RB, Yang JF. Methods for estimating the number of motor units in human muscles. Ann Neurol 1990;28(4):487-95.

54. Stashuk DW, Doherty TJ, Kassam A, Brown WF. Motor unit number estimates based on the automated analysis of F-responses. Muscle Nerve 1994;17(8):881-90.

55. Bromberg MB. Motor unit estimation: reproducibility of the spike-triggered averaging technique in normal and ALS subjects. Muscle Nerve 1993;16(5):466-71.

56. Felice KJ. Thenar motor unit number estimates using the multiple point stimulation technique: reproducibility studies in ALS patients and normal subjects. Muscle Nerve 1995;18(12):1412-6.

57. Wang FC, Delwaide PJ. Number and relative size of thenar motor units in ALS patients: application of the adapted multiple point stimulation method. Electroencephalogr Clin Neurophysiol 1998;109(1):36-43.

58. Neto HS, Filho JM, Passini R, Jr., Marques MJ. Number and size of motor units in thenar muscles. Clin Anat 2004;17(4):308-11.

59. Daube JR. Estimating the number of motor units in a muscle. J Clin Neurophysiol 1995;12(6):585-94.

60. Lomen-Hoerth C, Olney RK. Comparison of multiple point and statistical motor unit number estimation. Muscle Nerve 2000;23(10):1525-33.

61. Lomen-Hoerth C, Slawnych MP. Statistical motor unit number estimation: from theory to practice. Muscle Nerve 2003;28(3):263-72.

62. Shefner JM, Jillapalli D, Bradshaw DY. Reducing intersubject variability in motor unit number estimation. Muscle Nerve 1999;22(10):1457-60.

63. Henderson RD, McClelland R, Daube JR. Effect of changing data collection parameters on statistical motor unit number estimates. Muscle Nerve 2003;27(3):320-31.

64. Shefner JM, Cudkowicz ME, Zhang H, Schoenfeld D, Jillapalli D. The use of statistical MUNE in a multicenter clinical trial. Muscle Nerve 2004;30(4):463-9.

65. Armon C, Brandstater, M.E. Motor unit number estimate-based rates of progression of ALS predict patient survival. Muscle Nerve 1999;22(11):1571-5.

66. Felice KJ. A longitudinal study comparing thenar motor unit number estimates to other quantitative tests in patients with amyotrophic lateral sclerosis. Muscle Nerve 1997;20(2):179-85.

67. Henderson RD, McCombe PA, Ridall GR, Pettitt AN. Bayesian statistics for estimating motor unit numbers. Neurology 2004;62(Suppl5):455.

68. Burke D, Kiernan MC, Mogyoros I, Bostock H. Differences in the properties of human sensory and motor axons. In: Kimura J, Kaji R, editors. Physiology of ALS & Related Diseases. Amsterdam: Elsevier; 1997. p. 41-51.

69. Bostock H, Sharief MK, Reid G, Murray NM. Axonal ion channel dysfunction in amyotrophic lateral sclerosis. Brain 1995;118 (Pt 1):217-25.

70. Kodawa M KR, Kojima Y. Threshold electronus in patients with amyotrophic lateral sclerosis: further experience with Japanese subjects. Electroenceph Clin Neurophysiol 1995;97:S172.

71. Horn S, Quasthoff S, Grafe P, Bostock H, Renner R, Schrank B. Abnormal axonal inward rectification in diabetic neuropathy. Muscle Nerve 1996;19(10):1268-75.

72. Mogyoros I, Kiernan, M.C., Burke, D. & Bostock, H. Strength-duration properties of sensory and motor axons in amyotrophic lateral sclerosis. Brain 1998;121:851-859.

73. Burke D, Mogyoros I, Kiernan MC, Bostock H. Excitability of cutaneous afferents in Amyotrophic Lateral Sclerosis. In: Kimura J, Kaji R, editors. Physiology of ALS and Related Diseases. Amsterdam: Elsevier; 1997. p. 145-154.

74. Kiernan MC. Impulse Conduction. In: Aminoff MJDRB, editor. Encyclopedia of the Neurological Sciences. USA: Academic Press; 2003. p. 639-642.

75. Kiernan MC, Burke, D. Threshold electronus in the assessment of Motor Neuron Disease. In: F.Mauguiere JD, editor. Handbook of Clinical Neurophysiology. Amsterdam: Elsevier; 2004.

76. Kiernan MC, Burke D, Andersen KV, Bostock H. Multiple measures of axonal excitability: a new approach in clinical testing. Muscle Nerve 2000;23(3):399-409.

77. Kiernan MC, Hart IK, Bostock H. Excitability properties of motor axons in patients with spontaneous motor unit activity. J Neurol Neurosurg Psychiatry 2001;70(1):56-64.

78. Krishnan AV, Lin CS, Kiernan MC. Nerve excitability properties in lower-limb motor axons: evidence for a length-dependent gradient. Muscle Nerve 2004;29(5):645-55.

79. de Carvalho M, Evangelista T, Sales-Luis ML. The corticomotor threshold is not dependent on disease duration in amyotrophic lateral sclerosis (ALS). Amyotroph Lateral Scler Other Motor Neuron Disord 2002;3(1):39-42.

80. Olney RK. Transcranial Magnetic Stimulation: Pro. ALS and other motor neuron disorders 2002;Suppl 1:S111.

81. Siciliano G, Manca ML, Sagliocco L, Pastorini E, Pellegrinetti A, Sartucci F, et al. Cortical silent period in patients with amyotrophic lateral sclerosis. J Neurol Sci 1999;169(1-2):93-7.

82. Eisen A, Swash M. Clinical neurophysiology of ALS. Clin Neurophysiol 2001;112(12):2190-201.

83. Weber M, Eisen A. Peristimulus time histograms (PSTHs)--a marker for upper motor neuron involvement in ALS? Amyotroph Lateral Scler Other Motor Neuron Disord 2000;1 Suppl 2:S51-6.

84. Fisher RJ, Nakamura, Y., Bestmann, S., Rothwell, J.C. & Bostock, H. Two phrases of intracortical inhibition revealed by transcranial magnetic threshold tracking. Exp. Brain Research 2002;143:240-248.

85. Brooks BR. Functional scales: summary. Amyotroph Lateral Scler Other Motor Neuron Disord 2002;3 Suppl 1:S13-8.

86. Norris FH, Jr., Calanchini PR, Fallat RJ, Panchari S, Jewett B. The administration of guanidine in amyotrophic lateral sclerosis. Neurology 1974;24(8):721-8.

87. Mora G. Functional scales: pro. Amyotroph Lateral Scler Other Motor Neuron Disord 2002;3 Suppl 1:S9-10.

88. Guiloff RJ. Functional scales in ALS: cons. Amyotroph Lateral Scler Other Motor Neuron Disord 2002;3 Suppl 1:S11-2.

89. Appel V, Stewart SS, Smith G, Appel SH. A rating scale for amyotrophic lateral sclerosis: description and preliminary experience. Ann Neurol 1987;22(3):328-33.

90. Kimura F, Shinoda K, Fujiwara S, Fujimura C, Nakajima H, Furutama D, et al. [The changes of clinical characteristics in 100 Japanese amyotrophic lateral sclerosis patients between 1980 and 2000]. Rinsho Shinkeigaku 2003;43(7):385-91.

91. Cudkowicz ME, Shefner JM, Schoenfeld DA, Brown RH, Jr., Johnson H, Qureshi M, et al. A randomized, placebo-controlled trial of topiramate in amyotrophic lateral sclerosis. Neurology 2003;61(4):456-64.

92. Nozaki S, Kunitomi A, Saito T, Matsumura T, Shinno S. [Process of swallowing disturbance in amyotrophic lateral sclerosis--evaluation of videofluorography and respiratory function]. Rinsho Shinkeigaku 2003;43(3):77-83.

93. Cedarbaum JM, Stambler N, Malta E, Fuller C, Hilt D, Thurmond B, et al. The ALSFRS-R: a revised ALS functional rating scale that incorporates assessments of respiratory function. BDNF ALS Study Group (Phase III). J Neurol Sci 1999;169(1-2):13-21.

94. Ohashi Y, Tashiro K, Itoyama Y, Nakano I, Sobue G, Nakamura S, et al. [Study of functional rating scale for amyotrophic lateral sclerosis: revised ALSFRS(ALSFRS-R) Japanese version]. No To Shinkei 2001;53(4):346-55.

95. Bensimon G, Lacomblez L, Meininger V. A controlled trial of riluzole in amyotrophic lateral sclerosis. ALS/Riluzole Study Group. N Engl J Med 1994;330(9):585-91.

96. Lacomblez L, Bensimon G, Leigh PN, Guillet P, Powe L, Durrleman S, et al. A confirmatory dose-ranging study of riluzole in ALS. ALS/Riluzole Study Group-II. Neurology 1996;47(6 Suppl 4):S242-50.

97. Lai EC, Felice KJ, Festoff BW, Gawel MJ, Gelinas DF, Kratz R, et al. Effect of recombinant human insulin-like growth factor-I on progression of ALS. A placebo-controlled study. The North America ALS/IGF-I Study Group. Neurology 1997;49(6):1621-30.

98. Borasio GD, Robberecht W, Leigh PN, Emile J, Guiloff RJ, Jerusalem F, et al. A placebo-controlled trial of insulin-like growth factor-I in amyotrophic lateral sclerosis. European ALS/IGF-I Study Group. Neurology 1998;51(2):583-6.

99. A controlled trial of recombinant methionyl human BDNF in ALS: The BDNF Study Group (Phase III). Neurology 1999;52(7):1427-33.

100. A double-blind placebo-controlled clinical trial of subcutaneous recombinant human ciliary neurotrophic factor (rHCNTF) in amyotrophic lateral sclerosis. ALS CNTF Treatment Study Group. Neurology 1996;46(5):1244-9.

101. Miller RG, Bryan WW, Dietz MA, Munsat TL, Petajan JH, Smith SA, et al. Toxicity and tolerability of recombinant human ciliary neurotrophic factor in patients with amyotrophic lateral sclerosis. Neurology 1996;47(5):1329-31.

102. Miller RG, Moore DH, 2nd, Gelinas DF, Dronsky V, Mendoza M, Barohn RJ, et al. Phase III randomized trial of gabapentin in patients with amyotrophic lateral sclerosis. Neurology 2001;56(7):843-8.

103. Miller RG, Moore D, Young LA, Armon C, Barohn RJ, Bromberg MB, et al. Placebo-controlled trial of gabapentin in patients with amyotrophic lateral sclerosis.

WALS Study Group. Western Amyotrophic Lateral Sclerosis Study Group. Neurology 1996;47(6):1383-8.

104. Savas S, Delibas N, Savas C, Sutcu R, Cindas A. Pentoxifylline reduces biochemical markers of ischemia-reperfusion induced spinal cord injury in rabbits. Spinal Cord 2002;40(5):224-9.

105. Brooks BR, Miller RG, Swash M, Munsat TL. El Escorial revisited: revised criteria for the diagnosis of amyotrophic lateral sclerosis. Amyotroph Lateral Scler Other Motor Neuron Disord 2000;1(5):293-9.

106. Blain CR, Williams VC, Johnston C, Stanton BR, Ganesalingam J, Jarosz JM, et al. A longitudinal study of diffusion tensor MRI in ALS. Amyotroph Lateral Scler 2007:1-8.

107. Pioro EP, Majors AW, Mitsumoto H, Nelson DR, Ng TC. 1H-MRS evidence of neurodegeneration and excess glutamate + glutamine in ALS medulla. Neurology 1999;53(1):71-9.

108. Block W, Karitzky, J., Traber, F., Pohl, C., Keller, E., Mundegar, R.R., Lamerichs, R., Rink, H., Reis, F., Schild, H.H. & Jerusalem, F. Proton magnetic resonance spectroscopy of the primary motor cortex in patients with motor neuron disease. Arch Neurol. 1998;55:931-936.

109. Chan S, Shungu DC, Douglas-Akinwande A, Lange DJ, Rowland LP. Motor neuron diseases: comparison of single-voxel proton MR spectroscopy of the motor cortex with MR imaging of the brain. Radiology 1999;212(3):763-9.

110. Lloyd CM, Richardson MP, Brooks DJ, Al-Chalabi A, Leigh PN. Extramotor involvement in ALS: PET studies with the GABA(A) ligand [(11)C]flumazenil. Brain 2000;123 (Pt 11):2289-96.

111. Tanabe JL, Vermathen M, Miller R, Gelinas D, Weiner MW, Rooney WD. Reduced MTR in the corticospinal tract and normal T2 in amyotrophic lateral sclerosis. Magn Reson Imaging 1998;16(10):1163-9.

112. Kato Y, Matsumura K, Kinosada Y, Narita Y, Kuzuhara S, Nakagawa T. Detection of pyramidal tract lesions in amyotrophic lateral sclerosis with magnetization-transfer measurements. AJNR Am J Neuroradiol 1997;18(8):1541-7.

113. Abe O, Yamada H, Masutani Y, Aoki S, Kunimatsu A, Yamasue H, et al. Amyotrophic lateral sclerosis: diffusion tensor tractography and voxel-based analysis. NMR Biomed 2004;17(6):411-6.

114. Thorpe JW, Moseley IF, Hawkes CH, MacManus DG, McDonald WI, Miller DH. Brain and spinal cord MRI in motor neuron disease. J Neurol Neurosurg Psychiatry 1996;61(3):314-7.

115. Hofmann E, Ochs G, Pelzl A, Warmuth-Metz M. The corticospinal tract in amyotrophic lateral sclerosis: an MRI study. Neuroradiology 1998;40(2):71-5.

116. Cheung G, Gawel MJ, Cooper PW, Farb RI, Ang LC, Gawal MJ. Amyotrophic lateral sclerosis: correlation of clinical and MR imaging findings. Radiology 1995;194(1):263-70.

117. Hecht MJ, Fellner F, Fellner C, Hilz MJ, Heuss D, Neundorfer B. MRI-FLAIR images of the head show corticospinal tract alterations in ALS patients more frequently than T2-, T1- and proton-density-weighted images. J Neurol Sci 2001;186(1-2):37-44.

118. Oba H, Araki T, Ohtomo K, Monzawa S, Uchiyama G, Koizumi K, et al. Amyotrophic lateral sclerosis: T2 shortening in motor cortex at MR imaging. Radiology 1993;189(3):843-6.

119. da Rocha AJ, Oliveira AS, Fonseca RB, Maia AC, Jr., Buainain RP, Lederman HM. Detection of corticospinal tract compromise in amyotrophic lateral sclerosis with brain MR imaging: relevance of the T1-weighted spin-echo magnetization transfer contrast sequence. AJNR Am J Neuroradiol 2004;25(9):1509-15.

120. Waragai M, Shinotoh H, Hayashi M, Hattori T. High signal intensity on T1 weighted MRI of the anterolateral column of the spinal cord in amyotrophic lateral sclerosis. J Neurol Neurosurg Psychiatry 1997;62(1):88-91.

121. Ishikawa K, Nagura H, Yokota T, Yamanouchi H. Signal loss in the motor cortex on magnetic resonance images in amyotrophic lateral sclerosis. Ann Neurol 1993;33(2):218-22.

122. Comi G, Rovaris M, Leocani L. Review neuroimaging in amyotrophic lateral sclerosis. Eur J Neurol 1999;6(6):629-37.

123. Pioro EP, Antel JP, Cashman NR, Arnold DL. Detection of cortical neuron loss in motor neuron disease by proton magnetic resonance spectroscopic imaging in vivo. Neurology 1994;44(10):1933-8.

124. Rooney WD, Miller RG, Gelinas D, Schuff N, Maudsley AA, Weiner MW. Decreased N-acetylaspartate in motor cortex and corticospinal tract in ALS. Neurology 1998;50(6):1800-5.

125. Suhy J, Miller RG, Rule R, Schuff N, Licht J, Dronsky V, et al. Early detection and longitudinal changes in amyotrophic lateral sclerosis by (1)H MRSI. Neurology 2002;58(5):773-9.

126. Yagishita A, Nakano I, Oda M, Hirano A. Location of the corticospinal tract in the internal capsule at MR imaging. Radiology 1994;191(2):455-60.

127. Peretti-Viton P AJ, Trefouret S, Brunel H, Daniel C, Viton JM, Flori A, Salazard B, Pouget J, Serratrice G, Salamon G. MRI of the intracranial corticospinal tracts in amyotrophic and primary lateral sclerosis. Neuroradiology 1999;41:744-749.

128. Miaux Y M-DN, Cognard C, Weill A & Chiras J. Areas of high signal intensity in the posterior limbs of the internal capsules in amyotrophic lateral sclerosis: normal or pathologic MR finding? Radiology 1994;191:870-871.

129. Cosottini M, Giannelli M, Siciliano G, Lazzarotti G, Michelassi MC, Del Corona A, et al. Diffusion-tensor MR imaging of corticospinal tract in amyotrophic lateral sclerosis and progressive muscular atrophy. Radiology 2005;237(1):258-64.

130. Hajnal JV, Bryant DJ, Kasuboski L, Pattany PM, De Coene B, Lewis PD, et al. Use of fluid attenuated inversion recovery (FLAIR) pulse sequences in MRI of the brain. J Comput Assist Tomogr 1992;16(6):841-4.

131. Mirowitz S, Sartor K, Gado M, Torack R. Focal signal-intensity variations in the posterior internal capsule: normal MR findings and distinction from pathologic findings. Radiology 1989;172(2):535-9.

132. Yoshiura T HS, Rubio A, Shrier DA, Kwok WE, Iwanaga S & Numaguchi Y. Heschl and superior temporal gyri: low signal intensity of the cortex on T2-weighted MR images of the normal brain. Radiology 2000;214:217-221.

133. Goodin DS, Rowley HA, Olney RK. Magnetic resonance imaging in amyotrophic lateral sclerosis. Ann Neurol 1988;23(4):418-20.

134. Luis ML, Hormigo A, Mauricio C, Alves MM, Serrao R. Magnetic resonance imaging in motor neuron disease. J Neurol 1990;237(8):471-4.

135. Carella F, Grisoli M, Savoiardo M, Testa D. Magnetic resonance signal abnormalities along the pyramidal tracts in amyotrophic lateral sclerosis. Ital J Neurol Sci 1995;16(8):511-5.

136. Mascalchi M, Salvi F, Valzania F, Marcacci G, Bartolozzi C, Tassinari CA. Corticospinal tract degeneration in motor neuron disease. AJNR Am J Neuroradiol 1995;16(4 Suppl):878-80.

137. Terao S, Sobue G, Yasuda T, Kachi T, Takahashi M, Mitsuma T. Magnetic resonance imaging of the corticospinal tracts in amyotrophic lateral sclerosis. J Neurol Sci 1995;133(1-2):66-72.

138. Abe K, Fujimura H, Kobayashi Y, Fujita N, Yanagihara T. Degeneration of the pyramidal tracts in patients with amyotrophic lateral sclerosis. A premortem and postmortem magnetic resonance imaging study. J Neuroimaging 1997;7(4):208-12.

139. Waragai M. MRI and clinical features in amyotrophic lateral sclerosis. Neuroradiology 1997;39(12):847-51.

140. Jones AP, Gunawardena WJ, Coutinho CM, Gatt JA, Shaw IC, Mitchell JD. Preliminary results of proton magnetic resonance spectroscopy in motor neurone disease (amytrophic lateral sclerosis). J Neurol Sci 1995;129 Suppl:85-9.

141. Gredal O, Rosenbaum S, Topp S, Karlsborg M, Strange P, Werdelin L. Quantification of brain metabolites in amyotrophic lateral sclerosis by localized proton magnetic resonance spectroscopy. Neurology 1997;48(4):878-81.

142. Ellis CM, Suckling J, Amaro E, Jr., Bullmore ET, Simmons A, Williams SC, et al. Volumetric analysis reveals corticospinal tract degeneration and extramotor involvement in ALS. Neurology 2001;57(9):1571-8.

143. Pioro EP. MR spectroscopy in amyotrophic lateral sclerosis/motor neuron disease. J Neurol Sci 1997;152 Suppl 1:S49-53.

144. Cwik VA, Hanstock CC, Allen PS, Martin WR. Estimation of brainstem neuronal loss in amyotrophic lateral sclerosis with in vivo proton magnetic resonance spectroscopy. Neurology 1998;50(1):72-7.

145. Ellis CM, Simmons A, Andrews C, Dawson JM, Williams SC, Leigh PN. A proton magnetic resonance spectroscopic study in ALS: correlation with clinical findings. Neurology 1998;51(4):1104-9.

146. Bowen BC, Pattany PM, Bradley WG, Murdoch JB, Rotta F, Younis AA, et al. MR imaging and localized proton spectroscopy of the precentral gyrus in amyotrophic lateral sclerosis. AJNR Am J Neuroradiol 2000;21(4):647-58.

147. Pohl C, Block, W., Trber, F., Schmidt, S., Pels, H., Grothe, C., Schild, H.H. & Klockgether, T. Proton magnetic resonance spectroscopy and transcranial magnetic stimulation for the detection of upper motor neuron degeneration in ALS patients. Journal of the Neurological Sciences 2001;190:21-27.

148. Schuff N RW, Miller R, Gelinas DF, Amend DL, Maudsley AA & Weiner MW. Reanalysis of multislice (1) H MRSI in Amyotrophic Lateral Sclerosis. Magn Reson Imaging 2001;45:513-516.

149. Kalra SA, D.L. Imaging: MRS, MRI, PET/SECT: Con. ALS and other motor neuron disorders 2002;Suppl 1:S73-S74.

150. Gredal O, Pakkenberg H, Karlsborg M, Pakkenberg B. Unchanged total number of neurons in motor cortex and neocortex in amyotrophic lateral sclerosis: a stereological study. J Neurosci Methods 2000;95(2):171-6.

151. Basser PJ, Mattiello J, LeBihan D. Estimation of the effective self-diffusion tensor from the NMR spin echo. J Magn Reson B 1994;103(3):247-54.

152. Le Bihan D, Mangin JF, Poupon C, Clark CA, Pappata S, Molko N, et al. Diffusion tensor imaging: concepts and applications. J Magn Reson Imaging 2001;13(4):534-46.

153. Neil J, Miller J, Mukherjee P, Huppi PS. Diffusion tensor imaging of normal and injured developing human brain - a technical review. NMR Biomed 2002;15(7-8):543-52.

154. Chenevert TL, Brunberg JA, Pipe JG. Anisotropic diffusion in human white matter: demonstration with MR techniques in vivo. Radiology 1990;177(2):401-5.

155. Pierpaoli C, Jezzard P, Basser PJ, Barnett A, Di Chiro G. Diffusion tensor MR imaging of the human brain. Radiology 1996;201(3):637-48.

156. Hazlewood CF, Rorschach HE, Lin C. Diffusion of water in tissues and MRI. Magn Reson Med 1991;19(2):214-6.

157. Moseley ME, Cohen Y, Mintorovitch J, Chileuitt L, Shimizu H, Kucharczyk J, et al. Early detection of regional cerebral ischemia in cats: comparison of diffusion- and T2-weighted MRI and spectroscopy. Magn Reson Med 1990;14(2):330-46.

158. Doran M, Hajnal JV, Van Bruggen N, King MD, Young IR, Bydder GM. Normal and abnormal white matter tracts shown by MR imaging using directional diffusion weighted sequences. J Comput Assist Tomogr 1990;14(6):865-73.

159. Horsfield MA, Larsson HB, Jones DK, Gass A. Diffusion magnetic resonance imaging in multiple sclerosis. J Neurol Neurosurg Psychiatry 1998;64 Suppl 1:S80-4.

160. Mori S, van Zijl PC. Fiber tracking: principles and strategies - a technical review. NMR Biomed 2002;15(7-8):468-80.

161. Ellis CM, Simmonds, A., Jones, D., Bland, J., Dawson, J.M., Horsfield, M.A., Williams, S. & Leigh, P.N. Diffusion tensor MRI assesses corticospinal tract damage in ALS. Neurology 1999;53(5):1051-1058.

162. Toosy AT, Werring DJ, Orrell RW, Howard RS, King MD, Barker GJ, et al. Diffusion tensor imaging detects corticospinal tract involvement at multiple levels in amyotrophic lateral sclerosis. J Neurol Neurosurg Psychiatry 2003;74(9):1250-7.

163. Graham JM, Papadakis N, Evans J, Widjaja E, Romanowski CA, Paley MN, et al. Diffusion tensor imaging for the assessment of upper motor neuron integrity in ALS. Neurology 2004;63(11):2111-9.

164. Sach M, Winkler G, Glauche V, Liepert J, Heimbach B, Koch MA, et al. Diffusion tensor MRI of early upper motor neuron involvement in amyotrophic lateral sclerosis. Brain 2004;127(Pt 2):340-50.

165. Jacob S, Finsterbusch J, Weishaupt JH, Khorram-Sefat D, Frahm J, Ehrenreich H. Diffusion tensor imaging for long-term follow-up of corticospinal tract degeneration in amyotrophic lateral sclerosis. Neuroradiology 2003;45(9):598-600.

166. Ince PG, Lowe J, Shaw PJ. Amyotrophic lateral sclerosis: current issues in classification, pathogenesis and molecular pathology. Neuropathol Appl Neurobiol 1998;24(2):104-17.

167. Brownell B, Oppenheimer DR, Hughes JT. The central nervous system in motor neurone disease. J Neurol Neurosurg Psychiatry 1970;33(3):338-57.

168. Virta A, Barnett A, Pierpaoli C. Visualizing and characterizing white matter fiber structure and architecture in the human pyramidal tract using diffusion tensor MRI. Magn Reson Imaging 1999;17(8):1121-33.

169. Pierpaoli C, Barnett A, Pajevic S, Chen R, Penix LR, Virta A, et al. Water diffusion changes in Wallerian degeneration and their dependence on white matter architecture. Neuroimage 2001;13(6 Pt 1):1174-85.

170. Pierpaoli C, Basser PJ. Toward a quantitative assessment of diffusion anisotropy. Magn Reson Med 1996;36(6):893-906.

171. Oppenheimer EA. Treating respiratory failure in ALS; the details are becoming clearer. Journal of the Neurological Sciences 2003;209:1-4.

172. Velasco R, Salachas F, Munerati E, Le Forestier N, Pradat PF, Lacomblez L, et al. [Nocturnal oxymetry in patients with amyotrophic lateral sclerosis: role in predicting survival]. Rev Neurol (Paris) 2002;158(5 Pt 1):575-8.

173. Bourke SC, Shaw, P.J. & Gibson, G.J. Respiratory function vs sleep-disordered breathing as predictors of QOL in ALS. Lancet Neurology 2001;57(11):2040-2044.

174. Barthlen GML, D.J. Unexpectedly severe sleep and respiratory pathology in patients with ALS. European Journal of Neurology 2000;7:299-302.

175. Jackson CE, Rosenfeld, J., Moore, D.H., Bryan, W.W., Barohn, R.J., Wrench, M., Myers, D., Heberlin, L., King, R., Smith, J., Gelinas, D. & Miller, R.G. A preliminary evaluation of a prospective study of pulmonary function studies and symptoms of hypoventilation in ALS/MND patients. Journal of the Neurological Sciences 2001;191:75-78.

176. Bourke SC, Bullock RE, Williams TL, Shaw PJ, Gibson GJ. Noninvasive ventilation in ALS: Indications and effect on quality of life. Neurology 2003;61(2):171-177.

177. Newsom-Davis IC, Lyall, R.A., Leigh, P.N., Moxham, J. & Goldstein, L.H. The effect of non-invasive positive pressure ventilation (NIPPV) on cognitive function in ALS: a prospective study. J. Neurol. Neurosurg. Psychiatry 2001;71:482-487.

178. Takeawa H, Kubo, J., Miyamoto, T., Miyamoto, M . &Hirata, K. ALS associated with insomnia and the aggravation of sleep-disorded breathing. Psychiatry and Clinical Neurosciences 2001;55:263-264.

179. Kleopa AK, Sherman, M., Neal, B., Romano, G.J. & Heinman-Patterson, T. Bipap improves survival and rate of pulmonary function decline in patients with ALS. Journal of the Neurological Sciences 1999;164:82-88.

180. de Carvalho M, Matias T, Coelho F, Evangelista T, Pinto A, Luis ML. Motor neuron disease presenting with respiratory failure. J Neurol Sci 1996;139 Suppl:117-22.

181. Marti-Fabregas J, Dourado M, Sanchis J, Miralda R, Pradas J, Illa I. Respiratory function deterioration is not time-linked with upper-limb onset in amyotrophic lateral sclerosis. Acta Neurol Scand 1995;92(3):261-4.

182. Lechtzin N. Respiratory effects of amyotrophic lateral sclerosis: problems and solutions. Respir Care 2006;51(8):871-81; discussion 881-4.

183. Bourke SC, Gibson GJ. Non-invasive ventilation in ALS: current practice and future role. Amyotroph Lateral Scler Other Motor Neuron Disord 2004;5(2):67-71.

184. Polkey MI, Green M, Moxham J. Measurement of respiratory muscle strength. Thorax 1995;50(11):1131-5.

185. Fitting JW, Paillex R, Hirt L, Aebischer P, Schluep M. Sniff nasal pressure: a sensitive respiratory test to assess progression of amyotrophic lateral sclerosis. Ann Neurol 1999;46(6):887-93.

186. Morgan RK, McNally S, Alexander M, Conroy R, Hardiman O, Costello RW. Use of Sniff nasal-inspiratory force to predict survival in amyotrophic lateral sclerosis. Am J Respir Crit Care Med 2005;171(3):269-74.

187. Sleep-related breathing disorders in adults: recommendations for syndrome definition and measurement techniques in clinical research. The Report of an American Academy of Sleep Medicine Task Force. Sleep 1999;22(5):667-89.

188. Johns DP, Wilson J, Harding R, Walters EH. Airway distensibility in healthy and asthmatic subjects: effect of lung volume history. J Appl Physiol 2000;88(4):1413-20.

189. Salome CM, Thorpe CW, Diba C, Brown NJ, Berend N, King GG. Airway re-narrowing following deep inspiration in asthmatic and nonasthmatic subjects. Eur Respir J 2003;22(1):62-8.

190. Pasker HG, Schepers R, Clement J, Van de Woestijne KP. Total respiratory impedance measured by means of the forced oscillation technique in subjects with and without respiratory complaints. Eur Respir J 1996;9(1):131-9.

191. Marchal F, Loos N, Monin P, Peslin R. Methacholine-induced volume dependence of respiratory resistance in preschool children. Eur Respir J 1999;14(5):1167-74.

192. Briscoe WA, Dubois AB. The relationship between airway resistance, airway conductance and lung volume in subjects of different age and body size. J Clin Invest 1958;37(9):1279-85.

193. Huck S, Cormier W, Bounds W. t Tests, One-Way Analysis of Variance, and Multiple Comparison Procedures. In: Brown M, Hausdorff C, editors. Reading Statistics and Research. New York: Harper Collins; 1974. p. 49-73.

194. Bassetti C, Aldrich MS, Quint D. Sleep-disordered breathing in patients with acute supra- and infratentorial strokes. A prospective study of 39 patients. Stroke 1997;28(9):1765-72.

195. Czaplinski A, Yen AA, Appel SH. Forced vital capacity (FVC) as an indicator of survival and disease progression in an ALS clinic population. J Neurol Neurosurg Psychiatry 2006;77(3):390-2.

196. Ilzecka J, Stelmasiak Z, Balicka G. Respiratory function in amyotrophic lateral sclerosis. Neurol Sci 2003;24(4):288-9.

197. Miller RG, Rosenberg JA, Gelinas DF, Mitsumoto H, Newman D, Sufit R, et al. Practice parameter: the care of the patient with amyotrophic lateral sclerosis (an evidence-based review): report of the Quality Standards Subcommittee of the American Academy of Neurology: ALS Practice Parameters Task Force. Neurology 1999;52(7):1311-23.

198. Brinkmann JR, Andres P, Mendoza M, Sanjak M. Guidelines for the use and performance of quantitative outcome measures in ALS clinical trials. J Neurol Sci 1997;147(1):97-111.

199. Vincken W, Ghezzo H, Cosio MG. Maximal static respiratory pressures in adults: normal values and their relationship to determinants of respiratory function. Bull Eur Physiopathol Respir 1987;23(5):435-9.

200. Traynor BJ, Alexander M, Corr B, Frost E, Hardiman O. Effect of a multidisciplinary amyotrophic lateral sclerosis (ALS) clinic on ALS survival: a population based study, 1996-2000. J Neurol Neurosurg Psychiatry 2003;74(9):1258-61.

201. Butz M, Wollinsky KH, Wiedemuth-Catrinescu U, Sperfeld A, Winter S, Mehrkens HH, et al. Longitudinal effects of noninvasive positive-pressure ventilation in patients with amyotrophic lateral sclerosis. Am J Phys Med Rehabil 2003;82(8):597-604.

202. Similowski T, Fleury B, Launois S, Cathala HP, Bouche P, Derenne JP. Cervical magnetic stimulation: a new painless method for bilateral phrenic nerve stimulation in conscious humans. J Appl Physiol 1989;67(4):1311-8.

203. Lyall RA, Donaldson N, Polkey MI, Leigh PN, Moxham J. Respiratory muscle strength and ventilatory failure in amyotrophic lateral sclerosis. Brain 2001;124(Pt 10):2000-13.

204. Fitting JW. Sniff nasal inspiratory pressure: simple or too simple? Eur Respir J 2006;27(5):881-3.

205. Chaudhuri MB, Liu C, Watson L, Jefferson D, Kinnear WJ. Sniff nasal inspiratory pressure as a marker of respiratory function in motor neuron disease. Eur Respir J 2000;15(3):539-42.

206. Ince PG, Evans J, Knopp M, Forster G, Hamdalla HH, Wharton SB, et al. Corticospinal tract degeneration in the progressive muscular atrophy variant of ALS. Neurology 2003;60(8):1252-8.

207. Kaufmann PM, H. Amyotrophic lateral sclerosis: objective upper motor neuron markers. Curr. Neurol. Neurosci. Rep. 2002;2(1):55-60.

208. Chan S, Kaufmann P, Shungu DC, Mitsumoto H. Amyotrophic lateral sclerosis and primary lateral sclerosis: evidence-based diagnostic evaluation of the upper motor neuron. Neuroimaging Clin N Am 2003;13(2):307-26.

209. Rothstein JD. Excitotoxicity hypothesis. Neurology 1996;47(4 Suppl 2):S19-25; discussion S26.

210. Bruijn LI, Becher MW, Lee MK, Anderson KL, Jenkins NA, Copeland NG, et al. ALS-linked SOD1 mutant G85R mediates damage to astrocytes and promotes rapidly progressive disease with SOD1-containing inclusions. Neuron 1997;18(2):327-38.

211. Trotti D, Rolfs A, Danbolt NC, Brown RH, Jr., Hediger MA. SOD1 mutants linked to amyotrophic lateral sclerosis selectively inactivate a glial glutamate transporter. Nat Neurosci 1999;2(5):427-33.

212. Lacomblez L, Bensimon G, Leigh PN, Guillet P, Meininger V. Dose-ranging study of riluzole in amyotrophic lateral sclerosis. Amyotrophic Lateral Sclerosis/Riluzole Study Group II. Lancet 1996;347(9013):1425-31.

213. Miller RG, Mitchell JD, Lyon M, Moore DH. Riluzole for amyotrophic lateral sclerosis (ALS)/motor neuron disease (MND). Amyotroph Lateral Scler Other Motor Neuron Disord 2003;4(3):191-206.

214. Kiernan MC. Riluzole: a glimmer of hope in the treatment of motor neurone disease. Med J Aust 2005;182(7):319-20.

215. Eisen A, Kim S, Pant B. Amyotrophic lateral sclerosis (ALS): a phylogenetic disease of the corticomotoneuron? Muscle Nerve 1992;15(2):219-24.

216. Caramia MD, Cicinelli P, Paradiso C, Mariorenzi R, Zarola F, Bernardi G, et al. 'Excitability changes of muscular responses to magnetic brain stimulation in patients with central motor disorders. Electroencephalogr Clin Neurophysiol 1991;81(4):243-50.

217. Eisen A, Pant B, Stewart H. Cortical excitability in amyotrophic lateral sclerosis: a clue to pathogenesis. Can J Neurol Sci 1993;20(1):11-6.

218. Prout AJE, A.A. The cortical silent period and ALS. Muscle Nerve 1994;17(2):217-223.

219. Mills KR, Nithi KA. Corticomotor threshold is reduced in early sporadic amyotrophic lateral sclerosis. Muscle Nerve 1997;20(9):1137-41.

220. Desiato MT, Bernardi, G., Hagi, A.H., Boffa, L. & Caramia, M.D. Transcranial magnetic stimulation of motor pathways directed to muscles supplied by cranial nerves in ALS. Clinical Neurophysiology 2002;113:132-140.

221. Mills KR. The natural history of central motor abnormalities in amyotrophic lateral sclerosis. Brain 2003.

222. Vucic S, Kiernan MC. Novel threshold tracking techniques suggest that cortical hyperexcitability is an early feature of motor neuron disease. Brain 2006;129(Pt 9):2436-46.

223. Eisen A, Weber M. The motor cortex and amyotrophic lateral sclerosis. Muscle Nerve 2001;24(4):564-73.

224. Leigh PN SM. Cytoskeletal pathology in motor neuron diseases. In: Rowland LP, editor. Amyotrophic lateral sclerosis and other motor neuron diseases. New York: Raven Press; 1991. p. 115-24.

225. Nihei K, McKee AC, Kowall NW. Patterns of neuronal degeneration in the motor cortex of amyotrophic lateral sclerosis patients. Acta Neuropathol 1993;86(1):55-64.

226. Zanette G, Tamburin, S., Manganotti, P., Refatti, N., Forgione, A. & Rizzuto, N. Different mechanisms contribute to motor cortex hyperexcitability in ALS. Clinical Neurophysiology 2002;113:1688-1697.

227. Ziemann U, Winter M, Reimers CD, Reimers K, Tergau F, Paulus W. Impaired motor cortex inhibition in patients with amyotrophic lateral sclerosis. Evidence from paired transcranial magnetic stimulation. Neurology 1997;49(5):1292-8.

228. Kiernan JA, Hudson AJ. Changes in sizes of cortical and lower motor neurons in amyotrophic lateral sclerosis. Brain 1991;114 (Pt 2):843-53.

229. Pamphlett R, Kril J, Hng TM. Motor neuron disease: a primary disorder of corticomotoneurons? Muscle Nerve 1995;18(3):314-8.

230. Pamphlett R, Bayliss A. Lead uptake in motor axons. Muscle Nerve 1992;15(5):620-5.

231. Chou SM, Norris FH. Amyotrophic lateral sclerosis: lower motor neuron disease spreading to upper motor neurons. Muscle Nerve 1993;16(8):864-9.

232. Vucic S, Howells J, Trevillion L, Kiernan MC. Assessment of cortical excitability using threshold tracking techniques. Muscle Nerve 2006;33(4):477-86.

233. Basser PJ, Jones DK. Diffusion-tensor MRI: theory, experimental design and data analysis - a technical review. NMR Biomed 2002;15(7-8):456-67.

234. Warach S, Gaa J, Siewert B, Wielopolski P, Edelman RR. Acute human stroke studied by whole brain echo planar diffusion-weighted magnetic resonance imaging. Ann Neurol 1995;37(2):231-41.

235. Heide AC, Richards TL, Alvord EC, Jr., Peterson J, Rose LM. Diffusion imaging of experimental allergic encephalomyelitis. Magn Reson Med 1993;29(4):478-84.

236. Werring DJ TA, Clark CA, et al. Diffusion tensor imaging can detect and quantify corticospinal tract degeneration after stroke. Journal of Neurol Neurosurg Psychiatry 2000;69:269-72.

237. Wieshmann UC, Clark CA, Symms MR, Franconi F, Barker GJ, Shorvon SD. Reduced anisotropy of water diffusion in structural cerebral abnormalities demonstrated with diffusion tensor imaging. Magn Reson Imaging 1999;17(9):1269-74.

238. Werring DJ CC, Barker GJ, et al. The structural and functional mechanisms of motor recovery: complementary use of diffusion tensor and functional magnetic resonance imaging in traumatic injury of the internal capsule. Journal of Neurol Neurosurg Psychiatry 1998;65:863-9.

239. Wilson M, Tench CR, Morgan PS, Blumhardt LD. Pyramidal tract mapping by diffusion tensor magnetic resonance imaging in multiple sclerosis: improving correlations with disability. J Neurol Neurosurg Psychiatry 2003;74(2):203-7.

240. Guo AC, MacFall JR, Provenzale JM. Multiple sclerosis: diffusion tensor MR imaging for evaluation of normal-appearing white matter. Radiology 2002;222(3):729-36.

241. Abe O, Aoki S, Hayashi N, Yamada H, Kunimatsu A, Mori H, et al. Normal aging in the central nervous system: quantitative MR diffusion-tensor analysis. Neurobiol Aging 2002;23(3):433-41.

242. Sun Z, Wang F, Cui L, Breeze J, Du X, Wang X, et al. Abnormal anterior cingulum in patients with schizophrenia: a diffusion tensor imaging study. Neuroreport 2003;14(14):1833-6.

243. Papadakis NG, Xing D, Huang CL, Hall LD, Carpenter TA. A comparative study of acquisition schemes for diffusion tensor imaging using MRI. J Magn Reson 1999;137(1):67-82.

244. Hong YH, Lee KW, Sung JJ, Chang KH, Song IC. Diffusion tensor MRI as a diagnostic tool of upper motor neuron involvement in amyotrophic lateral sclerosis. J Neurol Sci 2004;227(1):73-8.

245. Karlsborg M, Rosenbaum S, Wiegell M, Simonsen H, Larsson H, Werdelin L, et al. Corticospinal tract degeneration and possible pathogenesis in ALS evaluated by MR diffusion tensor imaging. Amyotroph Lateral Scler Other Motor Neuron Disord 2004;5(3):136-40.

246. Le Bihan D, van Zijl P. From the diffusion coefficient to the diffusion tensor. NMR Biomed 2002;15(7-8):431-4.

247. Wiegell MR, Larsson HB, Wedeen VJ. Fiber crossing in human brain depicted with diffusion tensor MR imaging. Radiology 2000;217(3):897-903.

248. Aoki S, Iwata NK, Masutani Y, Yoshida M, Abe O, Ugawa Y, et al. Quantitative evaluation of the pyramidal tract segmented by diffusion tensor tractography: feasibility study in patients with amyotrophic lateral sclerosis. Radiat Med 2005;23(3):195-9.

249. Mori S, Zhang J. Principles of diffusion tensor imaging and its applications to basic neuroscience research. Neuron 2006;51(5):527-39.

250. Behrens TE, Johansen-Berg H, Woolrich MW, Smith SM, Wheeler-Kingshott CA, Boulby PA, et al. Non-invasive mapping of connections between human thalamus and cortex using diffusion imaging. Nat Neurosci 2003;6(7):750-7.

251. Eduardo E, Burke D. The optimal recording electrode configuration for compound sensory action potentials. J Neurol Neurosurg Psychiatry 1988;51(5):684-7.

252. Irnich W. Georges Weiss' fundamental law of electrostimulation is 100 years old. Pacing Clin Electrophysiol 2002;25(2):245-8.

253. de Carvalho M, Swash M. Nerve conduction studies in amyotrophic lateral sclerosis. Muscle Nerve 2000;23(3):344-52.

254. de Carvalho M, Lopes A, Scotto M, Swash M. Reproducibility of neurophysiological and myometric measurement in the ulnar nerve-abductor digiti minimi system. Muscle Nerve 2001;24(10):1391-5.

255. Mills KR, Murray NM. Electrical stimulation over the human vertebral column: which neural elements are excited? Electroencephalogr Clin Neurophysiol 1986;63(6):582-9.

256. Claus D. Central motor conduction: method and normal results. Muscle Nerve 1990;13(12):1125-32.

257. Cros D, Chiappa KH, Gominak S, Fang J, Santamaria J, King PJ, et al. Cervical magnetic stimulation. Neurology 1990;40(11):1751-6.

258. Kujirai T, Caramia MD, Rothwell JC, Day BL, Thompson PD, Ferbert A, et al. Corticocortical inhibition in human motor cortex. J Physiol 1993;471:501-19.

259. Nakamura H, Kitagawa H, Kawaguchi Y, Tsuji H. Intracortical facilitation and inhibition after transcranial magnetic stimulation in conscious humans. J Physiol 1997;498 (Pt 3):817-23.

260. Di Lazzaro V, Oliviero A, Meglio M, Cioni B, Tamburrini G, Tonali P, et al. Direct demonstration of the effect of lorazepam on the excitability of the human motor cortex. Clin Neurophysiol 2000;111(5):794-9.

261. Hanajima R, Ugawa Y, Terao Y, Sakai K, Furubayashi T, Machii K, et al. Cortico-cortical inhibition of the motor cortical area projecting to sternocleidomastoid muscle in normals and patients with spasmodic torticollis or essential tremor. Electroencephalogr Clin Neurophysiol 1998;109(5):391-6.

262. Cantello R, Gianelli M, Civardi C, Mutani R. Magnetic brain stimulation: the silent period after the motor evoked potential. Neurology 1992;42(10):1951-9.

263. Jiang H, van Zijl PC, Kim J, Pearlson GD, Mori S. DtiStudio: resource program for diffusion tensor computation and fiber bundle tracking. Comput Methods Programs Biomed 2006;81(2):106-16.

264. Sage CA, Peeters RR, Gorner A, Robberecht W, Sunaert S. Quantitative diffusion tensor imaging in amyotrophic lateral sclerosis. Neuroimage 2006.

265. Peioglou-Harmoussi S, Fawcett PR, Howel D, Barwick DD. F-response frequency in motor neuron disease and cervical spondylosis. J Neurol Neurosurg Psychiatry 1987;50(5):593-9.

266. Vucic S, Kiernan MC. Axonal excitability properties in amyotrophic lateral sclerosis. Clin Neurophysiol 2006;117(7):1458-66.

267. de Carvalho M, Scotto M, Lopes A, Swash M. Clinical and neurophysiological evaluation of progression in amyotrophic lateral sclerosis. Muscle Nerve 2003;28(5):630-3.

268. Yokota T, Yoshino A, Inaba A, Saito Y. Double cortical stimulation in amyotrophic lateral sclerosis. J Neurol Neurosurg Psychiatry 1996;61(6):596-600.

269. Sommer M, Tergau F, Wischer S, Reimers CD, Beuche W, Paulus W. Riluzole does not have an acute effect on motor thresholds and the intracortical excitability in amyotrophic lateral sclerosis. J Neurol 1999;246 Suppl 3:III22-6.

270. Stefan K, Kunesch E, Benecke R, Classen J. Effects of riluzole on cortical excitability in patients with amyotrophic lateral sclerosis. Ann Neurol 2001;49(4):536-9.

271. Roshan L, Paradiso GO, Chen R. Two phases of short-interval intracortical inhibition. Exp Brain Res 2003;151(3):330-7.

272. Ziemann U. TMS and drugs. Clin Neurophysiol 2004;115(8):1717-29.

273. Liepert J, Schwenkreis P, Tegenthoff M, Malin JP. The glutamate antagonist riluzole suppresses intracortical facilitation. J Neural Transm 1997;104(11-12):1207-14.

274. Kuo JJ, Siddique T, Fu R, Heckman CJ. Increased persistent Na(+) current and its effect on excitability in motoneurones cultured from mutant SOD1 mice. J Physiol 2005;563(Pt 3):843-54.

275. Inghilleri M, Berardelli A, Cruccu G, Manfredi M. Silent period evoked by transcranial stimulation of the human cortex and cervicomedullary junction. J Physiol 1993;466:521-34.

276. Chen R, Lozano AM, Ashby P. Mechanism of the silent period following transcranial magnetic stimulation. Evidence from epidural recordings. Exp Brain Res 1999;128(4):539-42.

277. Ziemann U, Eisen A. TMS for ALS: why and why not. Clin Neurophysiol 2004;115(6):1237-8.

278. Connors BW, Malenka RC, Silva LR. Two inhibitory postsynaptic potentials, and GABAA and GABAB receptor-mediated responses in neocortex of rat and cat. J Physiol 1988;406:443-68.

279. Avoli M, Hwa G, Louvel J, Kurcewicz I, Pumain R, Lacaille JC. Functional and pharmacological properties of GABA-mediated inhibition in the human neocortex. Can J Physiol Pharmacol 1997;75(5):526-34.

280. Werhahn KJ, Kunesch E, Noachtar S, Benecke R, Classen J. Differential effects on motorcortical inhibition induced by blockade of GABA uptake in humans. J Physiol 1999;517 (Pt 2):591-7.

281. Raynor EM, Shefner JM. Recurrent inhibition is decreased in patients with amyotrophic lateral sclerosis. Neurology 1994;44(11):2148-53.

282. Drory VE, Kovach I, Groozman GB. Electrophysiologic evaluation of upper motor neuron involvement in amyotrophic lateral sclerosis. Amyotroph Lateral Scler Other Motor Neuron Disord 2001;2(3):147-52.

283. Mori S, Crain BJ, Chacko VP, van Zijl PC. Three-dimensional tracking of axonal projections in the brain by magnetic resonance imaging. Ann Neurol 1999;45(2):265-9.

284. Mori S, Kaufmann WE, Davatzikos C, Stieltjes B, Amodei L, Fredericksen K, et al. Imaging cortical association tracts in the human brain using diffusion-tensor-based axonal tracking. Magn Reson Med 2002;47(2):215-23.

285. Xue R, van Zijl PC, Crain BJ, Solaiyappan M, Mori S. In vivo three-dimensional reconstruction of rat brain axonal projections by diffusion tensor imaging. Magn Reson Med 1999;42(6):1123-7.

286. Yin H, Lim CC, Ma L, Gao Y, Cai Y, Li D, et al. Combined MR spectroscopic imaging and diffusion tensor MRI visualizes corticospinal tract degeneration in amyotrophic lateral sclerosis. J Neurol 2004;251(10):1249-54.

287. Thivard L, Pradat PF, Lehericy S, Lacomblez L, Dormont D, Chiras J, et al. Diffusion tensor imaging and voxel based morphometry study in amyotrophic lateral sclerosis: relationships with motor disability. J Neurol Neurosurg Psychiatry 2007;78(8):889-92.

288. Wong JC, Concha L, Beaulieu C, Johnston W, Allen PS, Kalra S. Spatial profiling of the corticospinal tract in amyotrophic lateral sclerosis using diffusion tensor imaging. J Neuroimaging 2007;17(3):234-40.

289. Beaulieu C. The basis of anisotropic water diffusion in the nervous system - a technical review. NMR Biomed 2002;15(7-8):435-55.

290. Winhammar JM, Rowe DB, Henderson RD, Kiernan MC. Assessment of disease progression in motor neuron disease. Lancet Neurol 2005;4(4):229-38.

291. Mitchell JD, Borasio GD. Amyotrophic lateral sclerosis. Lancet 2007;369(9578):2031-41.

292. Leigh PN, Simmons, A., Williams, S., Williams, V., Turner, M. & Brooks, D. Imaging: MRS/MRI/PET/SPECT: Summary. ALS and other motor neuron disorders 2002;Suppl 1:S75-S80.

293. Pioro EP. Imaging: MRS/MRI/PET/SPECT: Pro. ALS and other motor neuron disorders 2002;suppl 1:S71.

294. Ziemann U. Cortical threshold and excitability measurements. In: Eisen A, editor. Clinical neurophysiology of motor neuron diseases. Handbook of clinical neurophysiology. Amsterdam: Elsevier; 2004. p. 317-35.

295. Hanajima R, Ugawa Y, Terao Y, Ogata K, Kanazawa I. Ipsilateral cortico-cortical inhibition of the motor cortex in various neurological disorders. J Neurol Sci 1996;140(1-2):109-16.

Appendix A - Analysis of Upper Motor Neuron Abnormalities with Diffusion Tensor Imaging and Transcranial Magnetic Stimulation in the Parry-Romberg Syndrome.

Introduction

Parry-Romberg (PR) syndrome is a clinically heterogenous disorder characterised by hemifacial atrophy, and variable associated intracerebral abnormalities that produce contralateral neurological manifestations, including hemiparesis, hemianopia and focal seizures[1]. The syndrome usually begins in adolescence and is often associated with linear scleroderma, with a typical facial appearance of 'coup de sabre'. The aetiology of PR syndrome is unknown, but there are a few reported associations with scleroderma[2]. PR syndrome allows a unique interrogation of upper motor neuron (UMN) abnormalities, because of the unilateral involvement of the cerebral hemisphere and corticospinal tract. We describe a subject with PR syndrome who had assessment of the UMN with diffusion tensor imaging (DTI) and transcranial magnetic stimulation (TMS) to identify abnormalities and in the motor cortex and in the corticospinal tract. While previous authors have used either DTI[3, 4] or TMS[5] to identify motor cortex and corticospinal tract abnormalities in PR syndrome, this is the first description of the use of both of these methods in the assessment UMN pathology in the PR syndrome. Data from a patient with PR syndrome is compared with normal subjects and subjects with UMN abnormalities as a part of Amyotrophic Lateral Sclerosis (ALS).

Case History

A 26-year-old right handed woman presented with a seven year history of right facial weakness and more recent gait disturbance due to left hemiparesis. There was no contributory family history. With no medication allergies, the patient took no regular medication. There was no significant intercurrent medical or past surgical history.

The patient was first noted to have right facial weakness of a mild degree seven years prior to first review. Two years prior to presentation, the onset of minor unsteadiness when ascending and descending stairs was noted, but with the advent of difficulty riding a bicycle, and completing exercise tasks, clinical assessment one year prior to initial review noted weakness in a pyramidal pattern in the left leg. Investigations at that time demonstrated evidence of denervation in all muscles innervated by the right facial nerve with reduced facial compound muscle action potential of 0.2 mV. An MRI scan of the brain identified a one cm area of abnormality near the right caudate head, with heterogenous signal change, thought to represent a venous vascular abnormality. There was no enhancement with contrast, and minor calcification on CT scan.

Subjectively at the time of initial review, she had weakness in the right side of her face and her left leg, and difficulty with regaining her balance on uneven ground. There was no functional disturbance in her left arm or right limbs. She had gait disturbance, needing to circumduct her left leg, with difficulty lifting her left leg. There was no disturbance of her bladder or bowel, or no systemic features of a connective tissue disorder.

Physical examination revealed normal cognition, speech and language. Her skin, joints and general examination were normal. Visual acuity, fields and fundi were normal. Eye movements and pupillary responses were normal. Masseter and temporalis muscles were normal. Facial sensation was normal. There was a moderately severe right pattern facial nerve weakness with a lower motor neuron, with atrophy of the facial muscles. The soft palate, tongue and neck muscles were normal. Tone was normal in all limbs without clonus. There was minor pyramidal weakness in the left arm, with a moderate degree of pyramidal weakness in the left leg. Deep tendon reflexes were asymmetrically increased with propagation on the left. The plantar response was extensor on the left and flexor on the right. Coordination was appropriate for the degree of weakness, consistent with an upper motor neuron pattern of disturbance. There was no sensory abnormality.

Investigations

No abnormalities were identified on haematological, biochemical and immunological testing, apart from a polyclonal elevation of IgG to 15.8g/L (range 6.72-14.4g/L). Specifically antinuclear antibodies and extractable nuclear antibodies were negative.

Transcranial magnetic stimulation (TMS) was applied to the motor cortex by a 90mm circular coil oriented to induce a current flow in a posterior-anterior direction, according to previously published method[6]. Initially, the coil was centred over the vertex and then moved in the antero-posterior and medial-lateral direction to find the optimal position to evoke maximal amplitude from the right APB muscle. Induction currents were generated by two high-power magnetic stimulators connected via a Magstim Bistim system (Magstim, Whitland, South West Wales,

UK). This ensured that the conditioning and test stimuli could be independently set and delivered through one coil[6]. Compound Muscle Action Potential (CMAP) and Motor Evoked Potential (MEP) recordings were amplified and filtered (3HZ-3kHZ) using a Grass ICP511 A.C. amplifier (Grass-Telefactor, Astro-Med, West Warwick, Rhode Island) and sampled at 10 kHZ using a 16-bit data acquisition card (National Instruments, Austin, Texas; PCI-MIO-16E-4). Data acquisition and stimulation delivery were controlled by QTRAC software (Prof. Hugh Bostock, Institute of Neurology, Queen Square, London, UK).

Threshold tracking was performed using a paired-pulse paradigm with a conditioning stimulus delivered at intervals before a suprathreshold test stimulus, according to previously published methods[6-8]. The conditioning and test stimuli were kept at constant intensities in conventional paired-pulse technique and the changes in the MEP amplitude were measured. The MEP response was fixed at 0.2mV (+/- 20%) and the test stimulus intensity varied to generate this target response[6]. The intensity was then varied from 60, 70, 80, 90, 100, 110, 120, 130, 140 and 150% of the Resting Motor Threshold (RMT), to determine the stimulus response curve for cortical stimulation of the subject. At each level of intensity three stimuli were delivered. Maximum MEP amplitude (mV) and MEP onset latency (ms) were recorded for each stimulus. Subjects were asked to perform a weak voluntary contraction, estimated to represent 10%-30% of maximum voluntary contraction, during single pulse TMS to record the cortical silent period (CSP), which was measured from the beginning of MEP to the return of EMG activity[9]. Short-Interval Intracortical Inhibition (SICI) was investigated using two different paired pulse paradigms, according to previously published methods[6].

MRI studies were performed using a 3 Tesla Philips Intera system (Philips Medical Systems, Best, The Netherlands) with an eight channel, phased array head coil and gradient coils (0-33mT/m). Head motion was restricted by placing pads on both sides of the subject's head. A single shot spin echo- EPI (echo planar imaging) diffusion weighted sequence was performed for DTI acquisition. Fifteen-directional scans were used with an isotropic voxel resolution of 2.5mm (field of view 240mm, matrix of 96 x 96, slice thickness of 2.5mm, no gap). Fifty five slices were collected with an echo time of 110ms; repetition time of 8404ms and a b value of 1000 (s/mm^2). Additionally one set of images with no diffusion weighting (b=0 s/mm^2) was acquired. The identical sequence was acquired six times and averaged after reconstruction to improve signal to noise, with a total scan time of 30 minutes. To exclude other pathologies, a whole brain T2-weighted inversion recovery (FLAIR: TR=11000ms, TE=110ms, TI=2800ms) and a T1-weighted fast spin echo (TR=5.6ms, TE=2.6ms) whole brain sequences were acquired.

DTIStudio was used to post-process the DTI sequences (www.mristudio.org). Quantitative diffusion parameter maps were generated including; Fractional Anisotropy (FA), trace Apparent Diffusion Coefficient (ADC), and colour vector maps. In addition parallel diffusivity (ParaD, Ev1), and perpendicular diffusion (PerpD: [Ev2+Ev3]/2) coefficients were calculated for each region of interest. Fiber assignment by the continuous tracking algorithm and brute-force reconstruction enabled generation of three dimensional fiber tracts and identification of the corticospinal tract for further measurement of DTI parameters within the tract (Fiber tracking – FT). In addition, region of interest analysis of the corticospinal tract was performed using normalisation of DTI acquisition data via the Stereotactic White

Matter Atlas of Talairaich method, or SWAT. Using this method, identical regions of interest were measured simultaneously in subject brains normalised to a reference atlas, so that regions of interest were interrogated simultaneously from each subject using the ROI editor function. Four regions of interest were analysed along each corticospinal tract, starting from the cerebral peduncle (Point 1) up to the internal capsule at the level of the AC/PC line (Point 4), with two further measures equidistant between these points (Points 2 and 3).

Results

MRI examination of the brain identified a 1cm x 2cm x 1cm cavernous haemangioma in the right subcortical white matter adjacent to the head of the right caudate (Figures 1). There was generalised atrophy of the right cerebral and cerebellar hemispheres compared with the left, with no evidence of impingement of the cavernous haemangioma on the right corticospinal tract. There was no abnormal signal of the subcortical white matter on FLAIR sequences.

Diffusion tensor image data was processed with DTIStudio using both the FT and SWAT methods prior to region of interest analysis. The corticospinal tract in the right cerebral hemisphere demonstrated abnormalities compared to the left (Figure 2). The mean number of fibres in the right corticospinal tract as measured by FT analysis was significantly fewer than on the left (right CST=209, left CST=303 fibres, $p<0.05$). In addition, the DTI findings identified higher perpendicular diffusivity (PerpD in Figure 3) and lower fractional anisotropy (FA in Figure 4) in the right cerebral peduncle and along the right CST compared to the left. These findings were consistent using both the FT and SWAT methods. The DTI measurements of the right CST were similar to measurements of the CST from ten subjects with ALS, and the measurements of the left CST were similar to measurements of the CST from ten normal subjects.

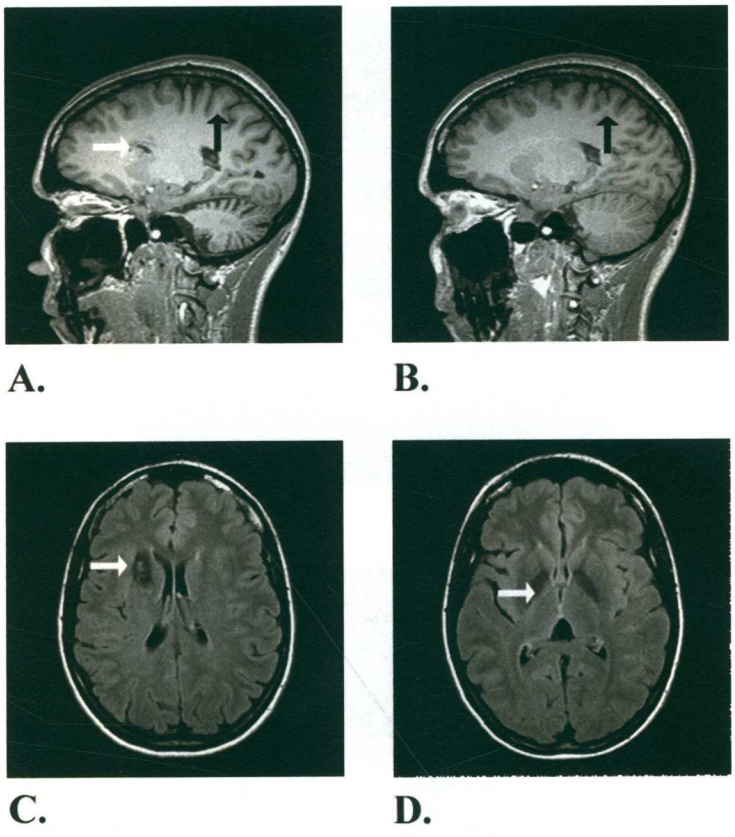

Figure 1

Images from the routine MRI sequences of the brain are shown. Figures 1A and 1B are from the T1-weighted sagittal whole brain sequence, 2cm to either side of the midline. A 1cm x 2cm x 1cm cavernous haemangioma is demonstrated to the right of the midline (Fig. 1A, white arrow), together with evidence of atrophy of the cerebral (black arrows) and cerebellar hemispheres on the right and not on the left. Figures 1C and 1D are from a T2-weighted FLAIR axial sequence, which further confirms the location of the cavernous haemangioma as anterior to the corticospinal tract in the right hemisphere (Fig. 1C, white arrow), which lies more dorsally in the posterior limb of the internal capsule (Fig. 1D, white arrow). Atrophy of the right cerebral hemisphere is also evident on the axial sequences, with a more prominent Sylvian fissure and sulci on the right compared with the left (Figures 1C and 1D).

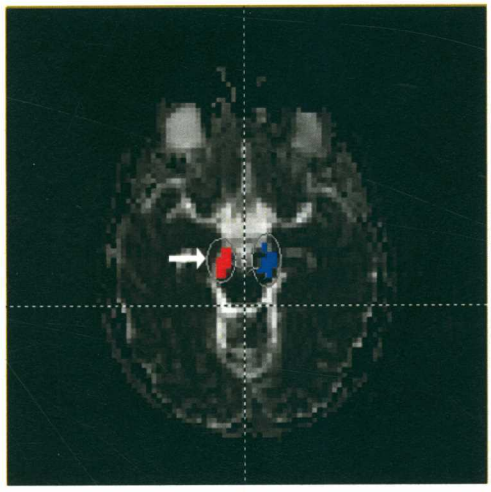

A.

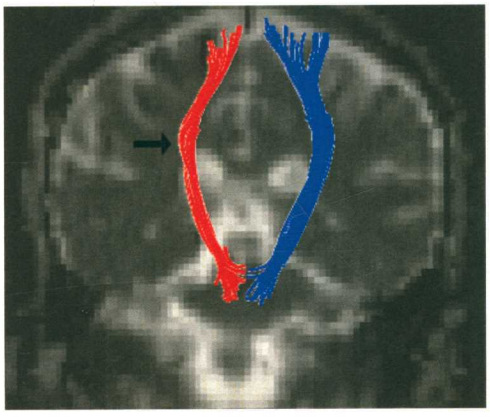

B.

Figure 2

Analysis images from DTISudio, which demonstrate fibres from the right (red) and left (blue) corticospinal tracts, as they pass through the cerebral peduncle (Point 1) at the level of the midbrain (Figure 2A). The right corticospinal tract (red – arrow) is shown inside the region of interest selection tool used to select the tract as it passes from the cerebral peduncle through the internal capsule to the motor cortex. Figure 2B shows both corticospinal tracts superimposed on a coronal image. Analysis of the number of fibres identified by FT confirms the visual impression that the right corticospinal tract (red - arrow), has fewer fibres than the left corticospinal tract (blue) ($p<0.05$).

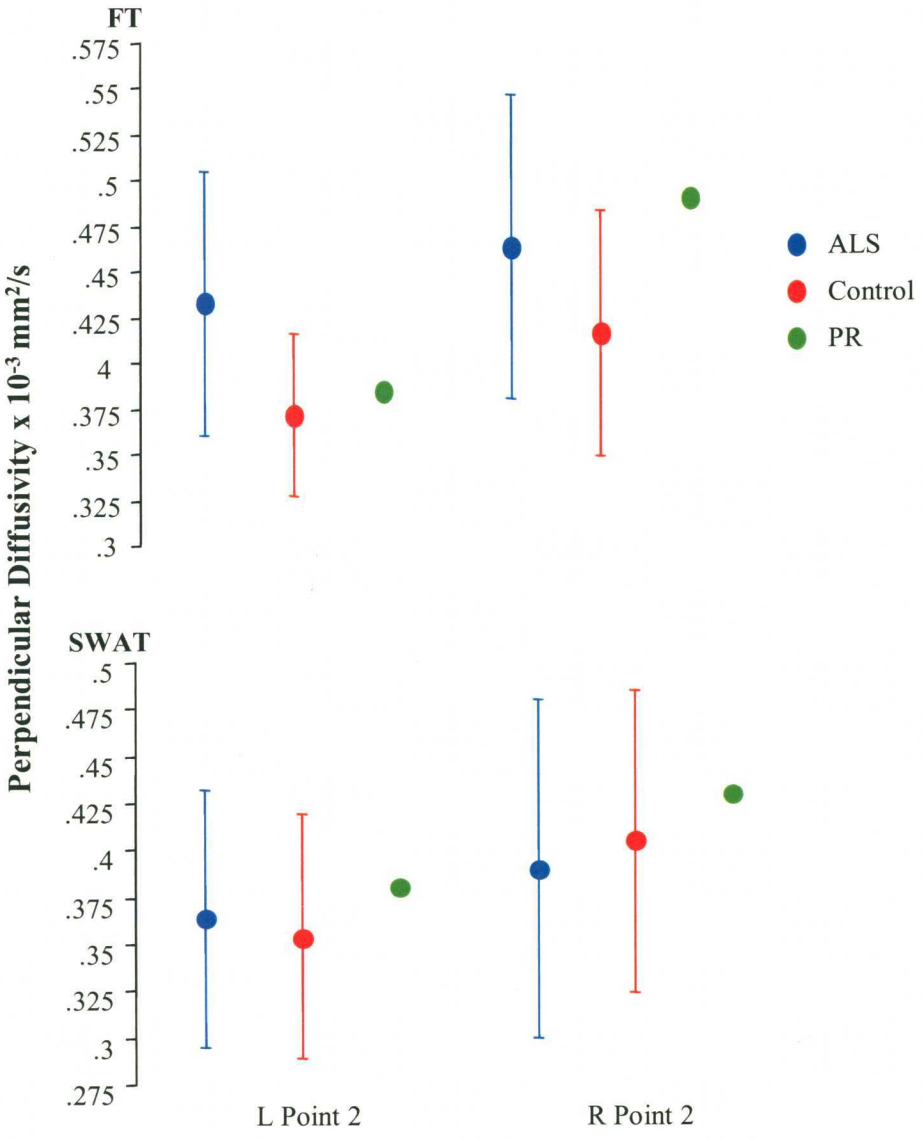

Figure 3

Representative data of the PR subject (green) which demonstrates a higher Perpendicular Diffusivity (PerpD) value in the right CST at Point 2 in the CST compared with the left using both the FT and SWAT methods. The PR subject values are graphed relative to the mean values (± 1SD) of ten ALS (blue) and ten control (red) subjects.

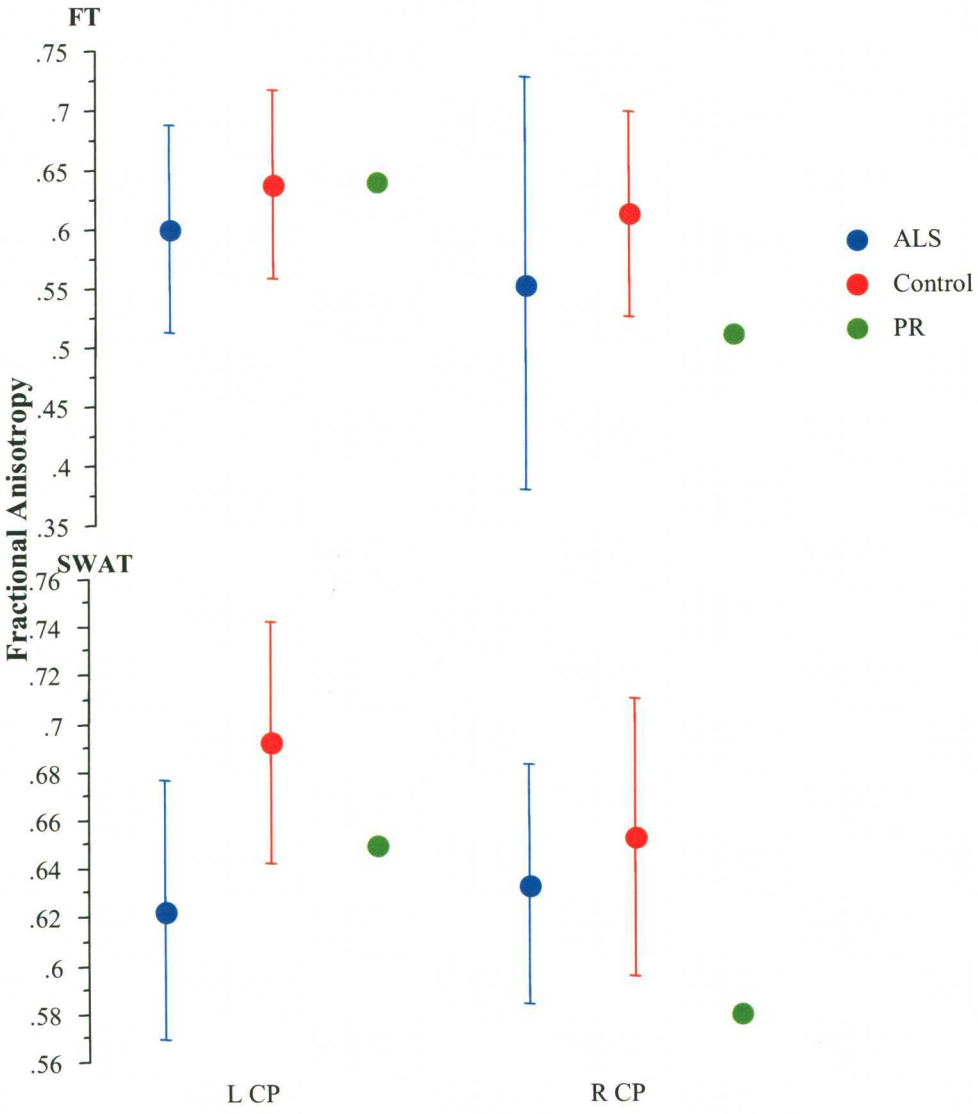

Figure 4.

The PR subject (green) had a lower Fractional Anisotropy (FA) value in the right CST at the cerebral peduncle (R CP) compared with the left (L CP) using both FT and SWAT methods of analysis. The PR subject values are graphed relative to the mean values (± 1SD) of ten ALS (blue) and ten control (red) subjects.

There were differences between the PR patient's right and left cerebral cortex and CST as measured by TMS, shown in Table 1. The Resting Motor Threshold (RMT) was higher in the right hemisphere as was the Central Motor Conduction Time (CMCT) and Neurophysiological Index (NPI), confirming the asymmetry of the hemispheres. This was consistent with the trend demonstrated in TMS studies from ten ALS patients and ten control subjects when the PR subject's values were compared with the mean values of each parameter (please see patient cohorts described in Chapter 3). It is important to note that the Motor Evoked Potential amplitude (MEPamp) was markedly reduced in the right hemisphere, with a relatively preserved Compound Muscle Action Potential (CMAPamp), consistent with a marked reduction of the UMN pool, with preservation of the output of the LMN pool in the spinal cord. The Motor Evoked Potential amplitude (MEPamp) and Short-Interval Intracortical Inhibition (SICI) were lower in the right hemisphere, also identical to the findings in ALS patients. This suggests a disturbance of cortical inhibition in PR, concordant with that found in ALS but isolated to the right hemisphere. Most TMS values from the left hemisphere in the PR subject were within the mean ± 1SD of the control subjects.

	RMT (MSO%)	MEP amp (mV)	CMAP amp (mV)	F wave latency (ms)	CMCT (ms)	NPI	SICI
ALS	55.7±6.7	1.8±1.6	4.7±4.4	32.5±2.5	4.7±1.8	0.8±1	-1.7±7
Control	58.7±8.9	2.8±2	8.7±2.5	28.5±1.6	5.3±1.5	2.1±0.5	7.2±6
P value	ns	ns	**<0.01**	**<0.01**	ns	**<0.01**	**0.013**
PR Right Hemisphere	90	1.2	8	27.3	7.95	2	-5.58
PR Left Hemisphere	74	4.4	7.5	28.7	3.7	1.4	4.25

Table 1. Table of Clinical Neurophysiological Data

The table shows the mean (±1 SD) TMS data for ten ALS patients and ten control subjects from the left hemisphere. PR Right Hemisphere indicates the TMS values from the right cerebral hemisphere of the PR patient, and in the last row are the TMS values from the left cerebral hemisphere. There is reduction of the Motor Evoked Potential amplitude (MEPamp) in the presence of a preserved Compound Muscle Action Potential (CMAPamp) from the PR right hemisphere. The Central Motor Conduction Time (CMCT) is markedly prolonged on the right, and both CMCT and Short-Interval Intracortical Inhibition (SICI) values from the right are in the ALS range. Most of the values from the PR left cerebral hemisphere are with the control ranges.

RMT – Resting Motor Threshold, NPI – Neurophysiological Index

The TMS and DTI findings were then combined in a novel ratio derived from studies on ALS and control subjects. In this ratio, an UMN index was developed using the TMS parameter, SICI, and various DTI measurements to quantify UMN damage. As demonstrated in Chapter 3, with SICI as numerator, and various DTI measurements as denominator, a powerful ratio able to measure abnormality in the UMN was developed. This same concept was applied to the TMS and DTI results from the PR subject to interrogate the concept of an UMN index further. DTI and TMS data were applied to the formula:

$$\text{UMN Index} = \frac{\text{SICI}}{\text{DTI parameter}}$$

As shown in Figure 5, there is a marked difference between the UMN Index derived from the right hemisphere compared that derived from the left, using FA as the DTI parameter. This difference was regardless of whether data from the whole corticospinal tract was used, or whether the FA from any of four regions of interest along the CST were used. Only the FA values derived from FT analysis of the DTI data are shown, as the results are identical to the UMN index derived from the SWAT data (data not shown).

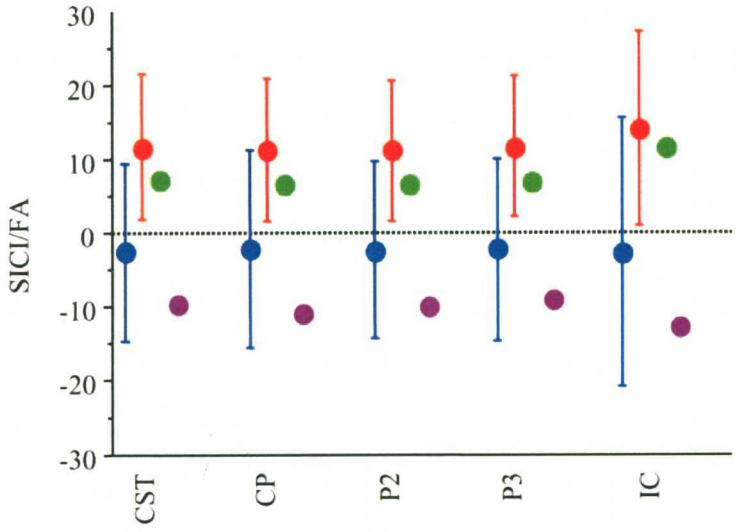

Figure 5. UMN Index derived from SICI/FA of the left (green) and right (mauve) cerebral hemispheres of the PR patient, compared with mean UMN Index data from ten ALS (blue) and ten normal (red) subjects (± 1SD). The index derived from FA data generated by the FT method is shown from the whole corticospinal tract (CST), and from each of four points along the CST, namely the cerebral peduncle (CP), internal capsule (IC) and two points equidistant along the tract (P2 and P3). The UMN index generated from the right cerebral hemisphere of the PR patient is in the range of the ALS patients at all points along the CST, whereas the UMN index generated from the left hemisphere is within the range of normal subjects.

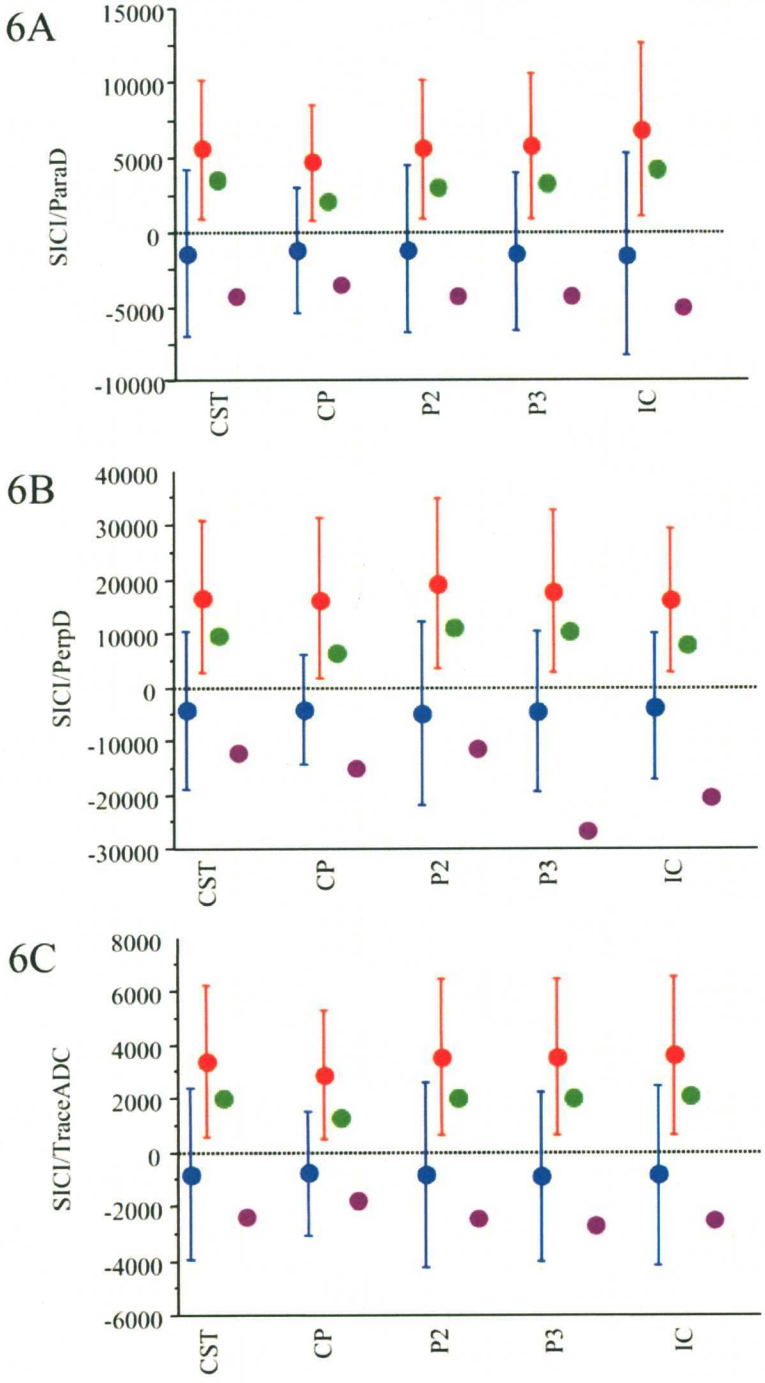
6A
SICI/ParaD
15000
10000
5000
0
-5000
-10000
CST
CP
P2
P3
IC
6B
SICI/PerpD
40000
30000
20000
10000
0
-10000
-20000
-30000
CST
CP
P2
P3
IC
6C
SICI/TraceADC
8000
6000
4000
2000
0
-2000
-4000
-6000
CST
CP
P2
P3
IC

Figure 6. UMN Indices derived from SICI/DTI parameters from the left (green) and right (mauve) cerebral hemispheres of the PR patient, compared with UMN Index data derived from ten ALS (blue) and ten normal (red) subjects (± 1SD). All DTI data is derived from the FT method. Figure 6A is the UMN Index derived from SICI/ParaD, Figure 6B derived from SICI/PerpD, Figure 6C from SICI/traceADC ratio. Irrespective of the DTI parameter, the UMN Index shows a marked difference between the left and right corticospinal tract, with the values from the left CST in the range of normal values, and the right CST in the range of ALS values. These are consistent regardless of whether the whole CST is measured (CST), or whether four regions of interest in the CST, the cerebral peduncle (CP), internal capsule (IC) or two points equidistant along the tract (P2 and P3) are used in the index.

Discussion

DTI and TMS were examined in a subject with Parry Romberg syndrome to quantify abnormalities of the UMN in the affected cerebral hemisphere. PR syndrome allows the interrogation of a normal motor cortex and corticospinal tract in one hemisphere, and an abnormal motor cortex and corticospinal tract in the other hemisphere. Although a small cavernous haemangioma was identified in the right subcortical white matter, it was placed anteriorly to the path of the corticospinal tract. TMS studies demonstrated that the right hemisphere was abnormal on neurophysiological testing, with a reduced pool of UMN in the motor cortex, hyper-excitability of the cortex, and prolonged central motor conduction time, consistent with an abnormal corticospinal tract. Furthermore, using two different methods of analysis of DTI sequences, Fibretracking and SWAT, similar data were obtained from the tracts regardless of the method. Fractional anisotropy and perpendicular diffusion in the right CST was abnormal, in the range of values obtained from the CST of patients with ALS, whereas analysis of the left CST revealed values in the range of normal subjects. Lastly, the data obtained from the PR syndrome patient was applied to a novel index of UMN damage, again with all indices obtained from the right hemisphere similar to those obtained from ALS patients, and all indices from the left hemisphere in the range of normal subjects. This illustrative case confirms the validity of the concept of the UMN index derived from TMS and DTI data.

There is only one prior case report of TMS in PR syndrome[5], demonstrating a reduction of resting motor threshold, enhanced cortical excitability, and a

prolonged cortical silent period in the abnormal cerebral hemisphere in a single patient, identical to our findings. While there are several case reports and small series of MRI abnormalities in PR syndrome, only two papers report diffusion tensor imaging and tractogaphy[3, 4]. A reduction in fractional anisotropy was reported in the affected hemisphere (with white matter abnormalities demonstrated on FLAIR sequences), without quantification[4]. The corticospinal tract in the affected hemisphere was identified using fibre tracking, but there was no conclusion regarding the integrity of the tract itself. More recently, tractography was used to demonstrate abnormalities in the white matter of the affected hemisphere, especially in the sensory fibres[3]. We did not perform analysis of the sensory fibre pathways in our PR subject, but rather used tractography to identify the CST with a high degree of accuracy.

This case report illustrates the ability to quantify abnormalities of the UMN from the abnormal cerebral hemisphere of a patient with PR syndrome. While the pathogenesis of PR syndrome is not known, study of this subject has enabled validation of a method to quantify the UMN abnormality using TMS and DTI.

References

1. Barker RA, Scolding NJ, Rowe D, Larner AJ. The A-Z of Neurological Practice. Cambridge: Cambridge University Press; 2005.

2. Larner AJ, Bennison DP. Some observations on the aetiology of progressive hemifacial atrophy ("Parry-Romberg syndrome"). J Neurol Neurosurg Psychiatry 1993;56(9):1035-6.

3. Moon WJ, Kim HJ, Roh HG, Oh J, Han SH. Diffusion Tensor Imaging and Fiber Tractography in Parry-Romberg Syndrome. AJNR Am J Neuroradiol 2008.

4. Okumura A, Ikuta T, Tsuji T, Kato T, Fukatsu H, Naganawa S, et al. Parry-Romberg syndrome with a clinically silent white matter lesion. AJNR Am J Neuroradiol 2006;27(8):1729-31.

5. Aktekin B, Oguz Y, Aydin H, Senol U. Cortical silent period in a patient with focal epilepsy and Parry-Romberg syndrome. Epilepsy Behav 2005;6(2):270-3.

6. Vucic S, Kiernan MC. Novel threshold tracking techniques suggest that cortical hyperexcitability is an early feature of motor neuron disease. Brain 2006;129(Pt 9):2436-46.

7. Kujirai T, Caramia MD, Rothwell JC, Day BL, Thompson PD, Ferbert A, et al. Corticocortical inhibition in human motor cortex. J Physiol 1993;471:501-19.

8. Nakamura H, Kitagawa H, Kawaguchi Y, Tsuji H. Intracortical facilitation and inhibition after transcranial magnetic stimulation in conscious humans. J Physiol 1997;498 (Pt 3):817-23.

9. Cantello R, Gianelli M, Civardi C, Mutani R. Magnetic brain stimulation: the silent period after the motor evoked potential. Neurology 1992;42(10):1951-9.

Appendix B – DTI Manual

This is a manual written by me for Dr. S. Mori to accompany the DTIStudio software. This manual is referred to on page 89.

DTI requires involved post-processing (tensor calculation) to produce images, unlike conventional MRI. DTI calculation can produce various types of images including: Apparent Diffusion Constant (ADC) maps, anisotropy maps, principal eigenvalue maps, eigenvector images, colour maps and 3-D tract reconstruction. DtiStudio is a versatile resource program for Diffusion Tensor Image (DTI) computation and fiber tracking. An over-determined linear equation system is solved by using a tensor calculation. Tensor elements, eigenvalues, eigenvectors, diffusion anisotropy, diffusion constants and colour-coded orientations can be calculated. Interactive results are then able to be viewed interactively in orthogonal and three dimensional views. Fiber Assignment by Continuous Tracking (FACT) algorithm and brute-force reconstruction approach is how 3-D tracts are reconstructed[263]. In the tracking algorithm, voxels with FA-values lower than 0.25 were excluded to avoid inclusion of grey matter and CSF[264]. The reconstruction angle for the tract is set at 70% (default setting for DTIStudio).

Using DtiStudio in colour, FA and Trace maps (all derived from diffusion tensor and therefore in the same space), three types of ROI drawing tools exist (polygon, oval and rectangle). As soon as a ROI is drawn, fibers that penetrate it are retrieved from memory and shown by a colour defined by the user. These fibers are shown in three 2D orthogonal views and a 3D tri-planar view. For multiple ROI approaches there are three types of operations including: OR, NOT and AND which are used to obtain the desired fibers. For example, to select the Corticospinal Tract

(CST) fibers a single ROI can be drawn manually applied bilaterally just below the cerebral peduncle using the OR function. Then a second ROI can be placed just above the internal capsule (in the same hemisphere) using the AND function to only select the tracts that passed through these two areas of the brain.

The whole CST FA and trace values in both the left and right hemisphere can then be recorded using the statistics button. A manual circular ROI can then be placed between your two ROI regions used to obtain the CST fibers to obtain more values along the desired tract.

DTI Studio Step 1 – OR Function

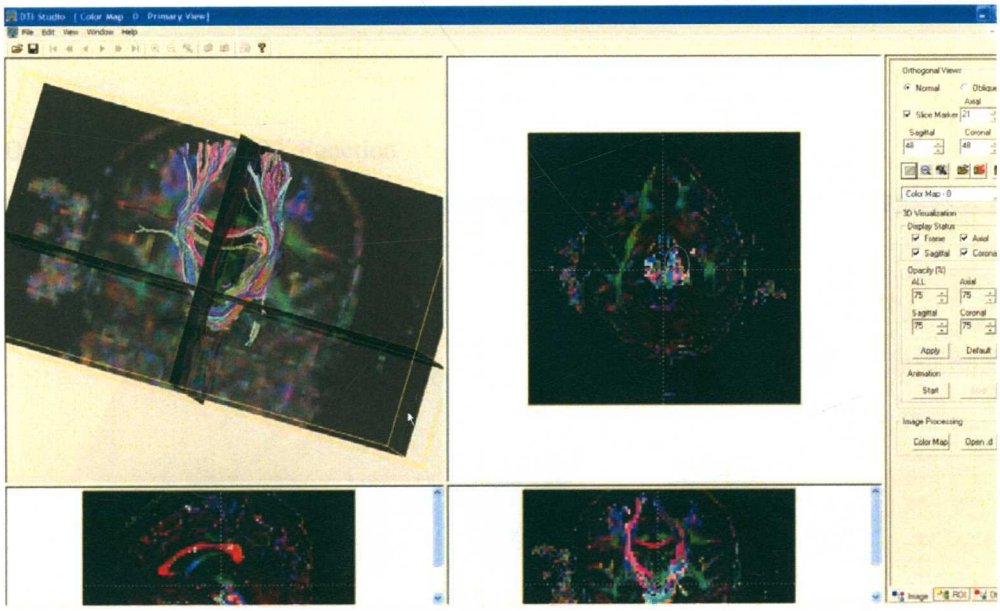

DTI Studio Step 2 – AND Function

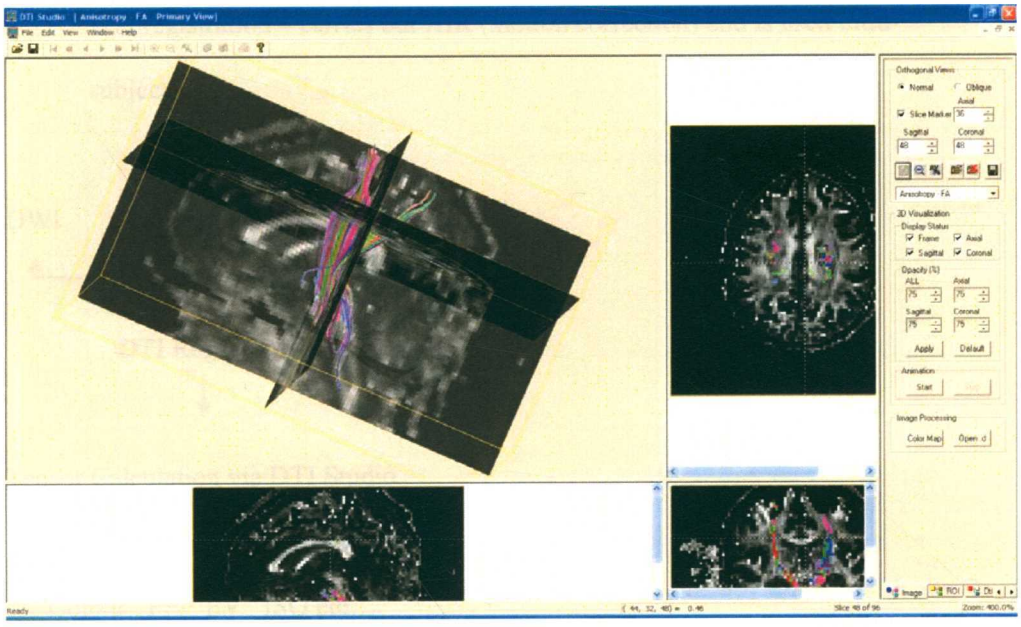

DTI Studio Step 3 - NOT Function

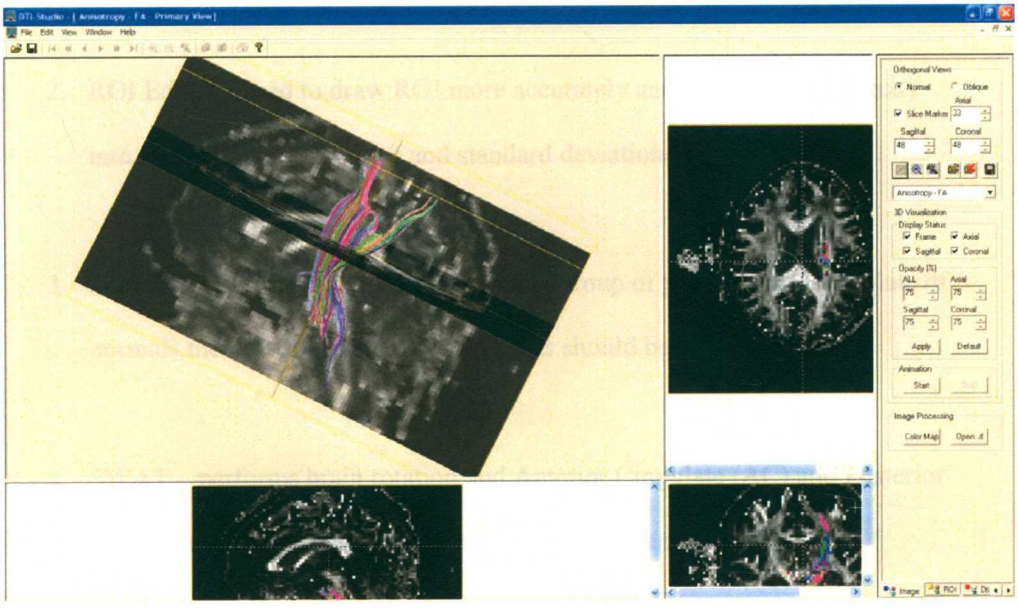

There are four programs:

1. DTI registration – carries out AIR (motion correction) and is used intra-subjects:

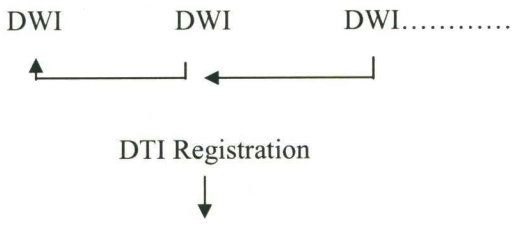

Tensor Calculation via DTI Studio

This data can then be studied by ROI Editor.

2. ROI Editor – used to draw ROI more accurately and can be saved directly into excel with mean values and standard deviations.

3. HOWEVER, if there is a need to create a group of people with a template of normals then the following two programs should be used:

4. SWAT – performs brain rotation and Anterior Cingulate (AC) and Posterior Cingulated (PC) orientation. Then Landmarker can be used:

5. Landmarker – Uses a template of 100 healthy controls to make the experimental group geographically the same via landmarks (either your own or 150 predetermined ones). ROI Editor can then be used on all of the images as long as they are all loaded at the same time.

DTI Registration

1. First of all you need to open a gradient file in a notepad format. This contains the image parameters and the matrix file.
2. All of the parameters need to be checked as does the matrix (remember to change for 15 and 6 directions) make sure that there are no commas or spaces in both files.
3. Import all the Rec files (only three at a time otherwise file becomes too big) into :C:\DTIsoftware
4. Copy these files into the gradient file in notepad and save.
5. Open DTI registration: click on alline, find your gradient file via "select" and click on "start registration".
6. The output will be saved as an AIR_file in the directory the you specified in notepad.
7. Change the dpf file to and AIR_file.
8. Open DTI studio and click on "open file" then "DTI Mapping" and then on "DTI parameter file (.dpf).
9. Perform the tensor, colour map (consider the B value) and Mean (DWI and B0s).
10. View the original ADC-Mean-STD and deselect and bad images.

ROI Editor

1. Open a processed file i.e. FA, DWI or colour etc NOT a raw data file.
2. Load as many images as you want to analyze.
3. Draw ROI and view the data via the "MSD" button. The data can be saved as a word file and be opened in excel.

SWAT

1. Load the data via "file open", then "raw image", then load FA, DWI or colour etc.
2. Go to tools and image registration.
3. To straighten the brain:

   Click on the image then press "shift" and use the mouse to drag the brain into an upright position in line with the grid. Put the sagital line in the middle then go through the axial view to make sure it is still in the middle of the brain.
4. To line the brain up in the sagital view:

   Use the colour image (adjust the image colour to make it easier to see the AC and PC). Find the AC on the sagital view and then check the axial view. Roughly the sagital coordinates are 36,35,57. Then click on the second point PC (this should be the faint red area above the brainstem) roughly coordinates 49,36,30.
5. Select the images to be registered.

6. Click on "Re-slice" (this will rotate the brain and change it from your parameters to 1x1x1).
7. New images are saved as <**name*. Resave as raw data.
8. The image has now been transformed.

LANDMARKER

1. Load the template first via warp companion (atlas root path)

   C:/DTIsoftware

   Adam

   AverageISO28.img

2. Load your data and check the parameters all the DWI, colour, FA and trace etc. Select DWI.
3. Select AIR and check the noise value and make the noise threshold above the noise level but below the brain eg 50, 50. Then click on "Affine".
4. Give this file a new name.
5. Save the images individually and close them and then open e.g. JW_FA_Tupdated etc.
6. Load the images back (so the computer doesn't work on the original, unchanged image).
7. Draw the landmarks of your own.

   OR

   Load Adams landmarks found in the file c:/DTISoftware/Adamlandmarks.

8. To adjust the landmarks on the subject brain click on the corresponding number in the landmarks box and adjust the landmark using the arrows.
9. Click on "save landmarks" button. It will save it as a text file and to reopen you need to open the updated file first and then the landmark file.
10. To transform the image click on the transformation tools in the program header, whereby you can choose:
    a. Translation
    b. Rigid
    c. Affine
    d. LDDMM

SWAT program used for CST

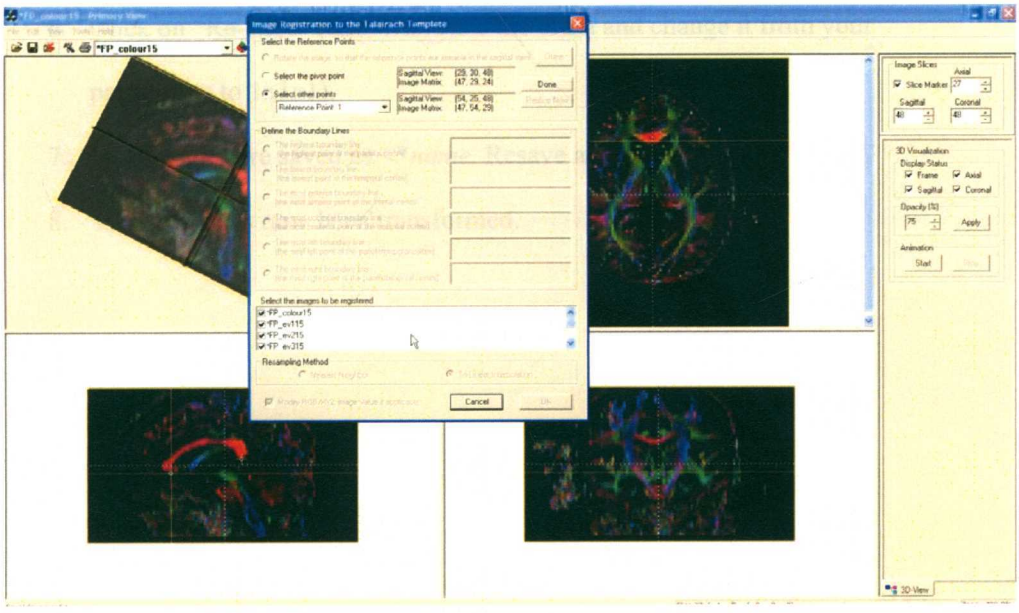

1. Load the data via "file open", then "raw image", then load FA, DWI or colour etc.
2. Go to tools and image registration

3. To straighten the brain:

   Click on the image then press "shift" and use the mouse to drag the brain into an upright position in line with the grid. Put the sagital line in the middle then go through the axial view to make sure it is still in the middle of the brain.

4. To line the brain up in the sagital view:

   Use the colour image (adjust the image colour to make it easier to see the AC and PC). Find the AC on the sagital view and then check the axial view. Roughly the sagital coordinates are 36,35,57. Then click on the second point PC (this should be the faint red area above the brainstem) roughly coordinates 49,36,30.

5. Select the images to be registered.
6. Click on "Re-slice" (this will rotate the brain and change it from your parameters to 1x1x1).
7. New images are saved as <**name*. Resave as raw data.
8. The image has now been transformed.

Landmarker program used for CST

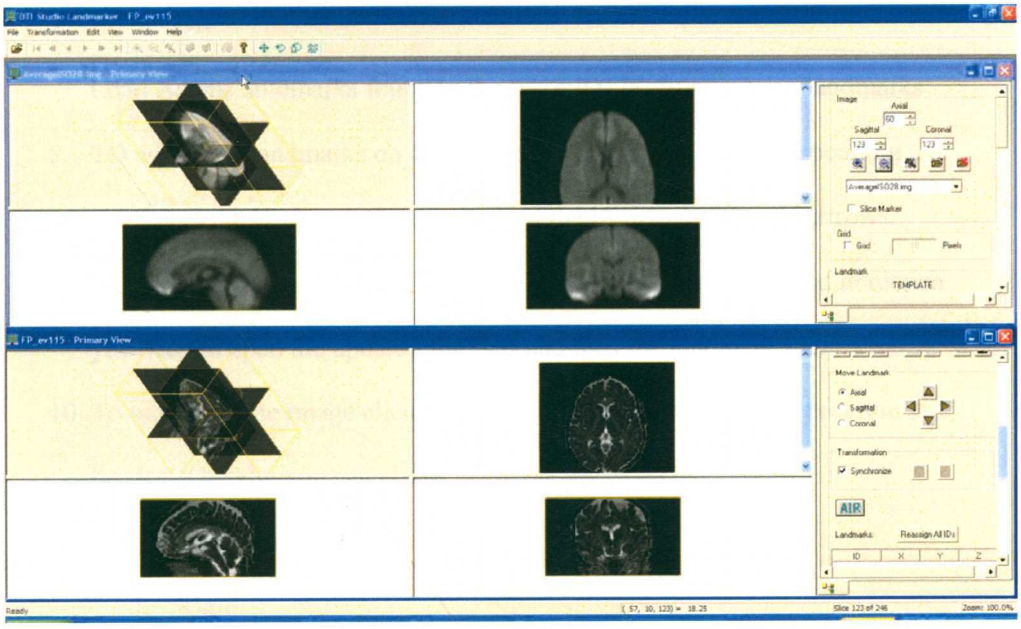

1. Load the template first via warp companion (atlas root path)

   C:/DTIsoftware

   Adam

   AverageISO28.img

2. Load your data and check the parameters all the DWI, colour, FA and trace etc. Select DWI
3. Select AIR and check the noise value and make the noise threshold above the noise level but below the brain eg 50, 50. Then click on "Affine"
4. Give this file a new name.
5. Save the images individually and close them and then open e.g. JW_FA_Tupdated etc
6. Load the images back (so the computer doesn't work on the original, unchanged image).

7. Draw the landmarks of your own

   OR

   Load Adams landmarks found in the file c:/DTISoftware/Adamlandmarks

8. TO adjust the landmarks on the subject brain click on the corresponding number in the landmarks box and adjust the landmark using the arrows.
9. Click on "save landmarks" button. It will save it as a text file and to reopen you need to open the updated file first and then the landmark file.
10. To transform the image click on the transformation tools in the program header, whereby you can chose:
    e. Translation
    f. Rigid
    g. Affine
    h. LDDMM

ROI Editor program used for CST

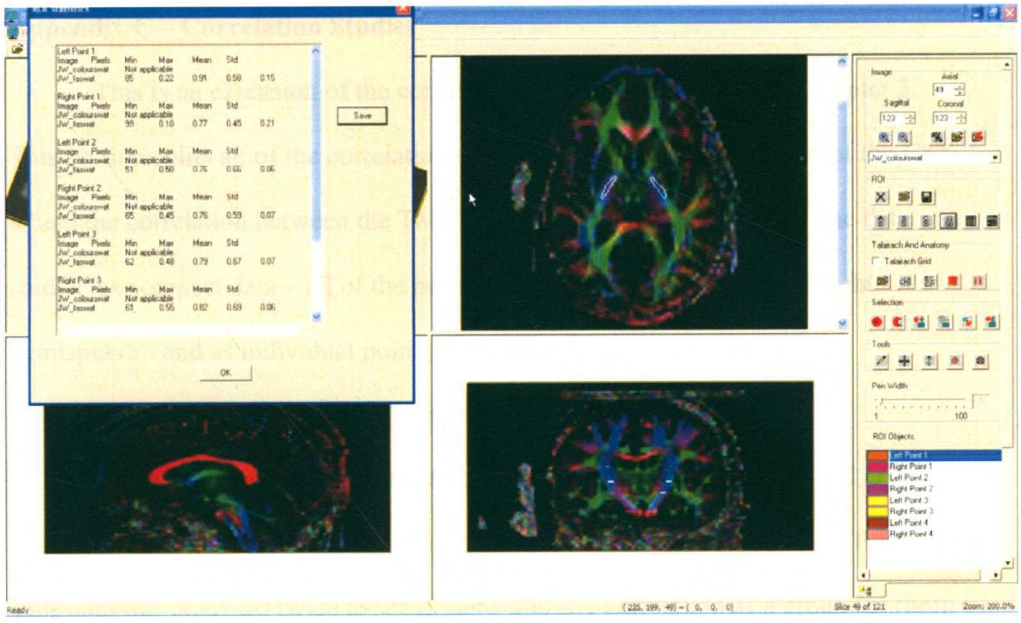

1. Open a processed file i.e. FA, DWI or colour etc., NOT a raw data file.
2. Load as many images as you want to analyze.
3. Draw ROI by selecting the pencil from the "tools" box, draw first ROI click on the "F" in the "selection" box and then the third option in the "selection" box to assign this data to the first ROI.
4. To add another ROI in the "ROI objects" box right click with the mouse in this box and select the option to add as many ROI objects as desired (this is also how you change the name of your object).
5. Draw another ROI and click on the subsequent ROI object you want the value to go to and repeat point 3.
6. You can view the dat3a via the "MSD" button. The data can be saved as a word file and be opened in excel.

Appendix C – Correlation Studies

This is an extension of the correlation studies carried out from Chapter 3. This section splits all of the correlation studies up so that the exact point of the CST where the correlation between the TMS and DTI parameter is located. The data was studied as compact data – all of the points along the CST in the left and right hemisphere - and as individual points along the left and right CST.

Correlations using Fiber tracking (compact data)

There was a significant correlation between the following TMS and DTI parameters in FT when looking at the compact data at the points shown in Table A. This data was analysed twice to see if there was any correlation as a group (g) (both ALS and control) or when split up into ALS (a) and control (c) categories.

Significance was found in six instances for the group category and eight instances in the ALS category but none for the control category. Most of these correlations occurred in the perpendicular diffusion and trace ADC for the DTI parameters. The TMS parameter MEP/latency correlated the most with DTI parameters.

Compact Fiber Tracking	Parallel Diffusion	Perpendicular Diffusion	Trace ADC	FA
MEP/LAT	g&a		g&a	
CMAPlat		g	g	
F Wave latency		g	g	
MEP/CMAP		a		a
NPI		a		
MEPAMP		a		a
CMAPamp			a	

Table A. Correlations between compact DTI (fiber tracking) parameters and TMS parameters. Correlations were studied including all of the participants (g – black text), and split into ALS (a – blue text) and controls no correlations found in this instance. Six correlations existed for the group category and eight correlations existed for the ALS category.

Correlations using fiber tracking (Individual points along the CST)

After the compact data analysis, the individual points along the CST were investigated for correlations with the TMS parameters. A significant correlation existed between some of the TMS and DTI parameters (Table B).

Again, the data was analysed twice to see if there was any correlation as a group (ALS and controls), or when split up into ALS and control categories. Each CST point was observed in this analysis (CP-left cerebral peduncle, IC-left internal capsule, 2-left point 2, 3-left point 3). Significance was found in 18 instances for the group analysis, 11 instances for the ALS group and 5 instances for the control group.

The DTI parameter giving the most correlation with TMS was perpendicular diffusion, but all of the other DTI parameters correlated too. The TMS parameter giving the most correlation was F Wave latency, followed by MEP/AMP, followed by MEP/latency.

Individual pts Fiber Tracking	Parallel Diffusion	Perpendicular Diffusion	Trace ADC	FA
MEP/LAT	3(g&a)	Whole(g)	Whole(g)&3(g)	
CMAPlat	IC(c)	Whole(g)		Whole(g)
F Wave latency		Whole(g) 2&3(g) 3(c)	Whole(g&a)&3(g)	3(g)
MEP/CMAP		3(g&a) CP(c)		Whole(a)
NPI			Whole(a)	
RT		CP(g&a)	CP(a)	
MEPAMP	Whole(a)	3(g&c) CP(c)	Whole(g)	Whole(a) & 3(g)
CMAPamp			Whole(a)	
CMT	3(g&a)			

Table B. Each CST point was observed in this analysis (Whole-Whole left tract, CP-left cerebral peduncle, IC-left internal capsule, 2-left point 2, 3-left point 3). Correlations were studied including all of the participants (g – black text), and split into ALS (a – blue text) and controls (c – red text). Significance was found in 18 instances for the group analysis, 11 instances for the ALS group and five instances for the control group. The DTI parameter with the most correlation with TMS was perpendicular diffusion, but all of the other DTI parameters also correlated. The TMS parameter giving the most correlation was F Wave latency and MEP AMP.

Correlations using SWAT (compact data)

There was a significant correlation between the TMS and DTI parameters in SWAT when looking at compact data (i.e. values as a group for the whole CST in the left hemisphere) seen in Table C. This data was analysed to determine correlations as a whole (irrespective of disease state), or when split up into ALS and control categories. Significance was found in eight instances for the group category and five instances in the ALS category but none for the control category. Most of these correlations occurred in the perpendicular diffusion and trace ADC for the DTI parameters.

Compact SWAT	Parallel Diffusion	Perpendicular Diffusion	Trace ADC	FA
SICI	g		g	
MEP/LAT			g	
CMAPlat		g	g	
F Wave latency		g	g	
MEP/CMAP	a	a		g&a
MEP AMP		a		a

Table C. Correlations between DTI (SWAT) parameters and TMS parameters. Correlations were studied including all of the participants (g – black text) and ALS (a – blue text). Eight correlations existed for the group category and five correlations existed for the ALS category.

Correlations using SWAT (on individual points along the CST)

After the compact data analysis the individual points along the CST were investigated for correlations with TMS parameters. A significant correlation existed between some of the TMS and DTI parameters (Table D).

Again, the data was analysed to see if there was any correlation as a group (ALS and controls), or when split up into ALS and control categories. Each CST point was observed in this analysis (CP-left cerebral peduncle, IC-left internal capsule, 2-left point 2, 3-left point 3). Significance was found in 13 instances for the group analysis, 14 instances for the ALS group and 2 instances for the control group.

The DTI parameter giving the most correlation with TMS was perpendicular diffusion, but all of the other DTI parameters correlated. The TMS parameter giving the most correlation was MEP/CMAP, followed by RT, followed by SICI.

Individual pts SWAT	Parallel Diffusion	Perpendicular Diffusion	Trace ADC	FA
SICI	CP(g)	CP (g)	CP (g) IC (c)	CP (g)
MEP/LAT	IC(g&a)		IC(g)	
CMAPlat			3(g)	
F Wave latency	CP(g)		CP(g) 3(g)	
MEP/CMAP	3(a)	2(a) 3(a) IC(g)	3 (a)	2(a) 3(a)
RT		2(g&a) 3(a)		2(g&a) 3(a)
MEPAMP		3(a)	3(a)	
CMAPamp	IC(a)	CP(c)		

Table D. Correlations between the TMS parameters and DTI SWAT parameters when investigating individual points along the CST. Correlations were studied including all of the participants (g – black text), and split into ALS (a – blue text) and controls (c – red text). Twenty nine statistically significant correlations were observed.

Appendix D – Publications

Assessment of disease progression in motor neuron disease

Jennica M C Winhammar, Dominic B Rowe, Robert D Henderson, Matthew C Kiernan

Lancet Neurol 2005; 4: 229–38

Department of Neurology and Multidisciplinary Motor Neurone Disease Clinic, Royal North Shore Hospital (J M C Winhammar MSc, D B Rowe FRACP), Multidisciplinary Motor Neurone Disease Service, Prince of Wales Hospital and Prince of Wales Medical Research Institute and Prince of Wales Clinical School, University of New South Wales (M C Kiernan FRACP), NSW, Australia; Department of Neurology, Royal Brisbane Hospital and Department of Medicine, University of Queensland, QLD, Australia (R D Henderson FRACP)

Correspondence to:
Dr Matthew C Kiernan, Prince of Wales Medical Research Institute, Barker St, Randwick, Sydney, NSW 2031, Australia
M.kiernan@unsw.edu.au

Motor neuron disease (MND) is characterised by progressive deterioration of the corticospinal tract, brainstem, and anterior horn cells of the spinal cord. There is no pathognomonic test for the diagnosis of MND, and physicians rely on clinical criteria—upper and lower motor neuron signs—for diagnosis. The presentations, clinical phenotypes, and outcomes of MND are diverse and have not been combined into a marker of disease progression. No single algorithm combines the findings of functional assessments and rating scales, such as those that assess quality of life, with biological markers of disease activity and findings from imaging and neurophysiological assessments. Here, we critically appraise developments in each of these areas and discuss the potential of such measures to be included in the future assessment of disease progression in patients with MND.

Without a clear understanding of the cause of motor neuron disease (MND), the task of effectively managing patients with this relentlessly progressive disorder is difficult.[1] Charcot's[2] original description was clear but there is no universally recognised rating scale to categorise the severity and progression of symptoms. Little progress was made in the understanding of MND pathophysiology until the discovery of a mutation on chromosome 21q22.1 in the gene for copper/zinc superoxide dismutase 1 (SOD1).[3] This leap in understanding, although related to the rarer familial type of MND, has provided an impetus for research into MND and suggested new therapeutic strategies. Elucidation of the role of copper/zinc SOD1 in the detoxification of superoxide radicals led to the first pharmaceutical treatment—riluzole, an inhibitor of glutamate release—that increased survival of patients with MND.[4–7] In some countries, including Australia, the manufacturer of riluzole had difficulty in gaining government subsidy through listing the drug on the pharmaceutical benefits scheme, in part owing to issues related to quality of life, despite data that showed improvement in longevity.[1] Given the difficulties in interpreting MND progression and outcomes, we review the effectiveness of current methods of monitoring disease progression in MND, with emphasis on clinical assessment and rating scales, and developments in biological, neurophysiological, and clinical-imaging assessment.

Clinical presentations of MND

Classification of MND is difficult because of its heterogeneous nature and clinical features. The diverse presentations of MND, familiar to clinicians who have diagnosed and managed patients with the disorder,[8,9] are also crucial to understanding and development of measures of disease progression.[10] Briefly, the presentations include: amyotrophic lateral sclerosis, which presents with a combination of upper motor neuron and lower motor neuron signs in the limbs; bulbar-onset MND, which presents with speech and swallowing difficulties, and later in the course of the disease with limb and occasionally cognitive features; primary lateral sclerosis, which is less common than the other presentations, with only upper motor neuron involvement; and progressive muscular atrophy, with only lower motor neuron signs. Although MND is typically relentless in progression, with 50% of patients surviving for less than 3 years after diagnosis, about 20% of patients can survive for 5–10 years.[11] More recent subclassifications include flail limb variant (figure 1), characterised by predominant lower motor neuron involvement and a long disease progression.[11–13] In this review, MND is synonymous with amyotrophic lateral sclerosis.

Some diagnostic certainty in patients with combinations of upper motor neuron signs (spasticity, weakness, and hyper-reflexia) and lower motor neuron signs (fasciculation, wasting, weakness, and hypo-reflexia) is possible by use of the El Escorial criteria,[14] revised in 1997.[15] The universality of El Escorial criteria is shown by their use in clinical trials to enrol patients with either probable or definite MND, although some have argued that use of these diagnostic features as enrolment criteria is restrictive.[1,16] Furthermore, these criteria might lack sensitivity, particularly in the early stages of MND when patients could benefit most from therapeutic intervention.[16] The criteria have been modified according to these criticisms, to facilitate early diagnosis,[17] and to optimise diagnostic certainty, which is essential in the clinical-trial setting.[18] Whereas some studies have found that the diagnosis of "definite" MND could have a prognostic effect,[19] this finding has not been confirmed in other studies,[16] which suggests that other quantitative methods of assessment are needed in clinical trials.

Methods for diagnosis and assessment of disease progression

Although there is no single test to diagnose MND, diagnosis can be made from a combination of clinical and neurophysiological assessments. Nerve conduction studies and electromyography can also identify other potentially treatable lower motor neuron disorders confined to motor fibres, particularly immune-mediated demyelinating neuropathies[20–23] and multifocal motor neuropathy,[24–30] in addition to disorders with features that resemble MND.[31,32]

Because the motor unit has few responses to different disease processes (figure 2), the problems associated

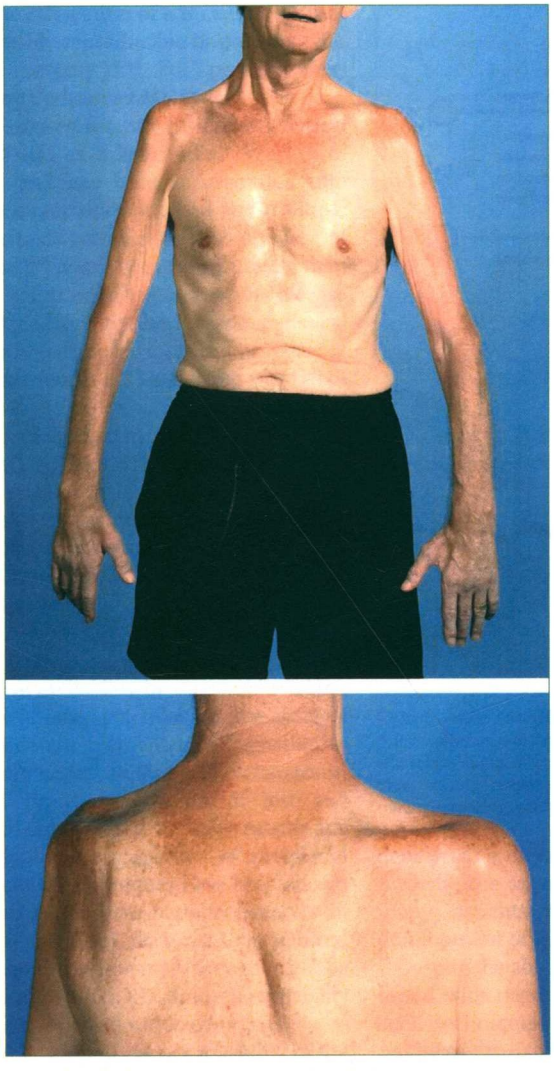

Figure 1: **Flail-limb variant of MND**
Top: Wasting is symmetrical and predominantly proximal, with weakness of both arms. This patient was unable to abduct his arms against gravity ("man-in-the-barrel" presentation). Leg function tends to be preserved for an extended period. Bottom: Shoulders were slumped with prominent wasting, especially involving the supraspinatus muscles.

with standard neurophysiological methods quickly become exposed; such problems are notable when attempting to assess MND progression.[33,34] Reliable methods for serial quantification of the loss of motor units (particularly motor-unit number estimation [MUNE]) and techniques to assess the pathophysiology of MND at axons (eg, nerve excitability) have been researched.

MUNE

The anterior horn cell in the spinal cord and its corresponding motor axon, neuromuscular junctions, and muscle fibres are grouped as the motor unit. The progressive loss of motor units in MND leads to weakness that can be quantified with strength testing.[35] Weakness however, is typically apparent only when there has been a moderate to severe loss of motor units, partly owing to re-innervation of muscle fibres for which the motor axon has been lost, by sprouting of the surrounding "normal" motor units (figure 2). The inability to biopsy nerves to count motor axons, and the need for a marker of MND progression, has led to the development of surrogate markers of loss of motor units.[36] Several methods of MUNE have been described, but there is no gold standard.

The aim of all MUNE methods is to find the number of motor nerves supplying a muscle. Because of active denervation in MND, assessment via MUNE methods is more difficult for this disease than for inactive or slowly progressing diseases, such as poliomyelitis. The absence of a gold standard for MUNE is a central problem for the development of reliable clinical methods.[37] Even histological studies of the number of motor nerves need an approximation,[38] and analysis by means of retrograde transport needs further physiological manipulation.[39]

The first method of MUNE developed by McComas,[40,41] and automation of this method, made use of the gradual increments in the compound muscle action potential that happen with small, initial increases in stimulus intensity. However, this method was soon recognised to be poor when motor-unit firing is variable (also known as alternation or probabilistic firing)[42] and its use stopped. Similarly, another early MUNE method that has not been widely applied in MND made use of the F-wave, which represents the volley from an anterior horn cell after retrograde travel of the stimulus.[43] The number of motor units can be estimated through calculation of the mean size of reproducible F-waves and division into the total compound muscle action potential. Although this technique is simple, it is now rarely used to assess patients with MND because of variable results.

Subsequent MUNE methods involved calculation of mean motor-unit size and sampling of the motor units along different parts of the nerve (multiple point stimulation) or the use of surface EMG to show single motor units (spike-triggered averaging).[44–46] The latter method had the advantage of including different nerve-muscle combinations, whereas other MUNE methods have generally examined the median, ulnar, or peroneal nerves. Multiple point stimulation seems to be the most widely used MUNE technique, correlating with histological methods[47] and finding normal estimates of about 170 motor units in hand muscles.

The variable activation of motor units after stimulation has led to the development of statistical MUNE techniques. The Poisson statistical method is the most widely used;[48] this method seems faster and more reproducible than the multiple point stimulation method.[49] Poisson statistical methods have been

modified to enable the calculation of a mean motor-unit size; MUNE is reasonably reproducible in patients with MND of moderate severity[37,48–50] but probably less accurate in patients with advanced MND.[51,52]

MUNE has now been used for over a decade in clinical assessment of MND and as a longitudinal marker of disease progression, and has been incorporated into treatment trials. The incremental method and multiple point stimulation methods are able to follow the loss of motor units over time,[46,53] possibly more accurately than other clinical and respiratory measures of disease progression in MND.[53,54] Recently the Poisson statistical method was incorporated in a multicentre trial of creatine for MND, and found a 23% decline in MUNE over 6 months.[52]

Bayesian statistics, widely used in biological situations, might be applied to MUNE in the future.[55] For MUNE to be useful in clinical trials of MND treatment, a method must be widely available in electromyography machines, reliable yet easily understood, and applicable to the different stages of MND. After 30 years of research, this target is close but still elusive.

Axonal excitability

Measurements of nerve excitability by threshold tracking are sensitive to membrane potential at the site of stimulation and provide complementary information to conventional nerve conduction studies.[56] The changes in excitability produced by a combination of test and conditioning currents can be used to infer membrane potential and the biophysical properties of peripheral axons. Although excitability techniques have been shown to be suitable for studying human peripheral nerves in vivo and have been useful in documenting induced changes in resting membrane potential, they may not be suitable for use in patients with MND. Study of excitability techniques in patients has yielded variable findings.

The first clinical application of nerve excitability in the assessment of patients with MND was done with threshold electrotonus by Bostock and colleagues.[57] These studies suggested that, despite normal conduction velocities, peripheral motor axons had abnormal membrane properties. Excitability increased when the axonal membrane was depolarised (type 1 response); this feature was attributed to low activity of potassium ion channels. Support for a selective abnormality of potassium ion channels was derived from experiments on rat spinal roots in vitro, in which similar abnormalities in threshold electrotonus could be induced by blocking potassium ion channels with a combination of 4-aminopyridine and tetraethylammonium.[57] Further studies have confirmed that threshold electrotonus is commonly abnormal in MND,[58,59] with the additional finding of high persistent sodium ion conductances.[60,61] The low potassium ion activity would tend to produce low hyperpolarisation and the high sodium ion conductance would lead to a high depolarising drive; together these changes are likely to underlie the axonal hyperexcitability that is present in many patients with MND and contribute to the development of fasciculation.[62,63]

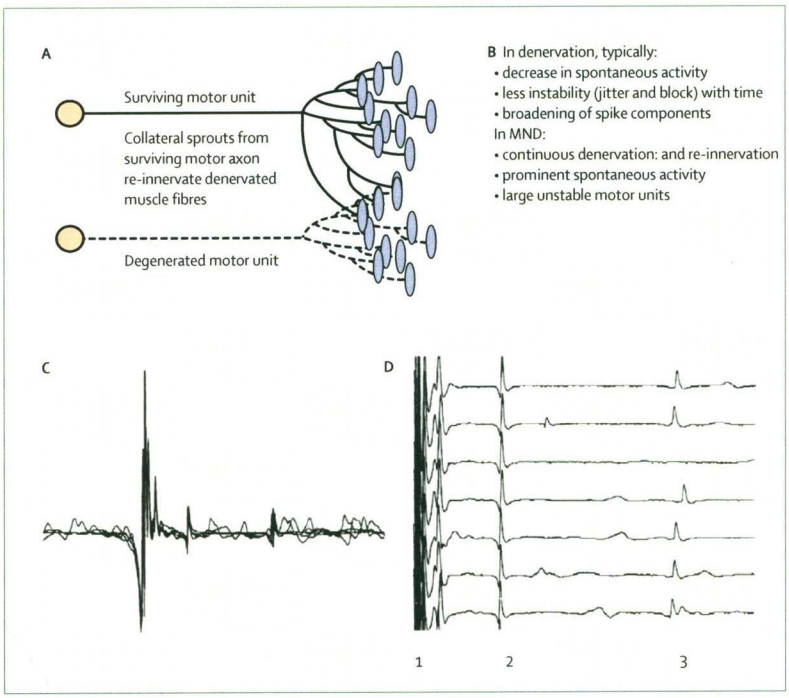

Figure 2: **Motor-unit responses to disease processes**
A: Pathophysiology of motor-unit degeneration and re-innervation. B: Differences in the clinical neurophysiological effects of MND and other processes associated with denervation. C: Superimposition of individual motor unit traces. D: Complex motor-unit changes in MND (sweep duration 50 ms), with (1,2) stable, myelinated late components, and (3) unstable components showing increased jitter and block.

Despite the abnormalities in axonal properties in MND found with nerve excitability techniques, application of such techniques to the serial assessment of patients produces variable results. Can excitability studies therefore be of clinical use in monitoring of disease progression in MND? This variability arises partly because studies of axonal excitability provide information about only the surviving axons.[64] Such studies provide no information about axons that no longer exist and probably provide little information about the "sickest" axons. In some longitudinal studies in MND, abnormal waveforms have become more normal despite clear progression of the disease, probably because the most abnormally responding axons died. Although nerve excitability can give insight into disease mechanisms, it is an unreliable measure of disease severity in an individual. One way to reduce this variability could be to study the behaviour of a single motor unit. However, in patients with MND, a single unit might not be available in serial studies and, if it were, it might be too healthy to be representative of the overall disease process. Part of the difficulty in interpreting the variability might yet be overcome with the use of combinations of nerve

excitability techniques.[65–67] Through such a process, measures of nerve excitability might become useful as a tool in the diagnosis and monitoring of disease progression in MND.

Transcranial magnetic stimulation

The only method for objective, clinical, neurophysiological assessment of upper motor neuron function and cortical abnormalities in MND is transcranial magnetic stimulation (TMS). This method gives insight into the discharge characteristics of single motor units or compound motor responses. Many studies of cortical changes have been done with TMS, with somewhat varied findings (panel).[68–72] Although TMS is non-invasive and generally well tolerated by patients, universal criteria must be established before it can provide a useful surrogate assessment of upper motor neuron dysfunction in MND.[73]

Clinical assessment

The best balance of function, impairment, and disability is yet to be found in a single functional scale for assessment of patients with MND. Ideally, functional scales should reliably and independently measure these different aspects in MND. Most functional scales rely on self-reporting by patients, typically in conjunction with scales ranked by clinicians on the function of different anatomical domains. Because clinical scales are commonly used in a multidisciplinary clinical setting, several factors are important in the selection of a scale, including: training needed; administration method and time; equipment; ease of completion; fatigue of the patient; and psychological effects.[74] The study sample used to standardise the test is equally crucial; if the SDs of a clinometric scale score are small, the study may not represent the range of patients with MND.[74] The scale chosen must have high inter-rater reliability, to ensure consistency by different assessors, and also be sensitive to change.[74]

The Norris scale was the first of many attempts to quantify the deficit in patients with MND.[75] This scale seemed to be reliable because it integrated clinical and functional data with linear decline, and it was used in many clinical trials.[76] The Norris scale has 22 functional indices, including bulbar, respiratory, trunk, arm, leg, and general domains, with additional ratings for clinical signs, such as reflexes, fasciculations, and muscle atrophy. Although this scale could measure impairment and disability in a single patient, the main disadvantages were that disparate measures were equally weighted (eg, breathing and the ability to empty the bladder were equal), and that it could be insensitive to change, attributable to a ceiling effect from a rating scale of 0–3.[77]

The Appel scale gives compound quantitative estimates of clinical status linked to MND progression. Strength of bulbar and respiratory muscles and function of arms and legs are assessed. The scale yielded reproducible data for each group of functions tested, leading to a total MND score.[78] Several team members are needed to acquire the data, and although this scale is the most sensitive of all of the scales for detecting change, it is time consuming in the busy clinic setting.

The amyotrophic lateral sclerosis functional rating scale (ALSFRS) was developed from the amyotrophic lateral sclerosis severity scale,[79] to measure mortality, muscle strength, and pulmonary function in clinical trials, with a focus on disease-related disability. The ALSFRS measures activities of daily living and global function, but it was perceived as novel because it assesses function independently of strength testing. Although generally regarded as being internally consistent and reliable, this scale requires that all parts are done by the same assessor at each visit.[74,76] The total score from use of the ALSFRS at the time of diagnosis is closely related to the progression of symptoms and MND outcome,[80] prompting incorporation of this scale into many pharmacological trials.[81]

In a large clinical trial of ciliary neurotrophic factor, ALSFRS had high internal consistency, reliability, validity, and responsiveness to change.[82] Not only did the patients who had a low score on the ALSFRS die earlier than those with a high score, but also the change in the scale closely paralleled other measures,[79] such as isometric muscle strength,[82,83] muscle mass,[84] and brainstem abnormalities.[85] However, there are problems with the scale; assessment of the patient's swallowing with the bulbar subscore, which is measured by observation of the

***Panel:* Typical TMS measurements in patients with MND**

Cortical motor threshold
The current needed to stimulate the motor cortex is normal or low early in the course of MND, possibly owing to reduced inhibition, and increases with disease progression.[68]

Cortical silent period
The pause in electromyographic activity after motor-cortex stimulation is reduced in MND,[69–71] possibly owing to loss of GABAergic neurons and motor-cortex reorganisation.

Peristimulus time histograms
TMS changes the firing of the motor unit such that there is higher resynchronisation over time,[69,71] reflecting dysfunction of corticomotorneuron pathways.[72]

Central conduction time
The latency from cortex to selected limb muscle is normal or slightly prolonged in MND owing to preferential degeneration of the fastest axons, derived from larger anterior horn cells.

Motor evoked potentials
Activation of motor units by TMS suggests upper motorneuron dysfunction and seems to relate to functional deficit.

patient's ability to manage solids and liquids of various consistency, has poor association with the results of videofluorography.[86] The other main weakness of the scale is the disproportionate weighting of limb and bulbar measurements relative to respiratory dysfunction.[77]

A revised version (ALSFRS-R) included additional assessments of dyspnoea, orthopnoea, and the need for ventilation,[87] and was found to be more sensitive to change than the original ALSFRS.[83] Scores on the revised scale relate to those on the global clinical impression of change (GCIC), when they are given by neurologists,[88] and to the sickness impact profile.[87] In a 9-month phase III trial of gabapentin,[89] the ALSFRS-R was a good predictor of survival; this result led to use of the scale in the clinical trials of minocycline[79] and other novel treatments (table 1).[76,82,89–98]

In addition to functional assessments, manual muscle-strength testing has been included as a measure of weakness in many of the MND clinical trials. Most muscle-strength testing has used grading systems developed from the Medical Research Council scale, but another method is to test muscle strength against a load—maximum voluntary isometric contraction. A multicentre assessment of the two measures of strength assessment found reasonable equivalence between these methods but suggested that manual muscle-strength testing is more sensitive in detecting change over time, because more muscles are studied overall.[99] Maximum voluntary isometric contraction has been used as a primary outcome measure in studies of the efficacy of topiramate, gabapentin, and creatine in MND.[81,89,100]

Quality of life is a nebulous measure, and the findings of clinical trials with this endpoint in patients with MND have been inconsistent to date,[90] probably because the determinants of quality of life are yet to be established for MND. Increasing limb weakness, problems with breathing, and bulbar impairment inevitably lead to changes in lifestyle, and in the nature of relationships with family and friends.[78,93,101–103] Illness progression, dependency issues, and problems with speech and muscle weakness seem to be important factors in determining quality of life in MND,[104] and somewhat surprisingly, physical status does not. Rather, the quality of life of patients with MND could depend to a large extent on psychosocial, supportive, and spiritual factors, highlighting the importance of the psychological needs of both patients and their carers.[105–107] Although quality of life is not a measure of disease progression in MND, it could be useful as a measure of adverse consequences in trials of future therapies.

Pulmonary function

Patients with MND invariably develop respiratory weakness, and most die from pulmonary complications. Increasingly, pulmonary function is being used to predict function and estimate survival in patients with MND (table 2).[108–122] Of the many measures available to assess respiratory status in MND, forced vital capacity has generally been the method used in the larger clinical trials.[81,89,92]

Although respiratory failure in patients with MND is a direct consequence of muscle weakness during endstage disease,[123] some patients develop early and severe respiratory difficulties during sleep. These early difficulties, called nocturnal hypoventilation, may become a predictor of survival independent of respiratory muscle weakness. Mean nocturnal arterial oxygen saturation of less than 93% has been associated with a very short mean survival, typically less than 6 months.[124]

Imaging techniques

The longer the patient's disease duration, the greater the atrophy of the precentral gyrus and the associated corticospinal tract; microscopy shows loss of pyramidal cells in the motor cortex and degeneration of the corticospinal tract.[125] Neuroimaging techniques can be used to assess CNS involvement in vivo, which might not be clinically detectable. The substantial variation in phenotype of any patient with MND can lead to great

Year	Scale	Measure	Advantages	Disadvantages
1979	Norris	Integrated clinical and functional data	Reliable, linear decline, easy to administer[76] Used in riluzole clinical trials[91,92]	Bulbar and respiratory function assigned only 21% of total-score weighting Assesses bowel and bladder function (typically not affected) Self-reported symptoms, functions, and clinical signs are combined (mixes impairments and disabilities)
1989	ALSSS (Hilliel)	Pure disability, four domains (two bulbar, spinal, and forced vital capacity)	Valid, sensitive, reliable, easy and quick[76]	Excludes respiratory assessment Poor prognostic information
1987	Appel	Clinical and functional data, five domains: bulbar, respiration, strength, upper motor neuron, and lower motor neuron	Five ratings per domain Simple, validated, reliable, easy to administer Used in IGF-I clinical trials[93,94]	No learning effects Reproducibility not widely accepted Difficult to use in patients who are severely affected Unclear relation to function Mixes impairments and disabilities
1996	ALSFRS	ten domains, including three bulbar, two upper motor neuron, two lower motor neuron, one respiratory	Easy to administer and sensitive to change Widely used in clinical trials (BDNF,[95] CNTF,[82,96] gabapentin,[89,97] xaliproden, and topiramate[98])	Reliability of statistical methods questioned Assessment grades are arbitrarily assigned

ALSSS=amyotrophic lateral sclerosis severity scale; IGF-I=insulin-like growth factor I; BDNF=brain-derived neurotrophic factor; CNTF=ciliary neurotrophic factor.

Table 1: **Functional scales for the assessment of patients with MND**

Feature	Measures	Advantages	Disadvantages
Spirometry	Forced vital capacity and forced expiratory volume	Can be used as a prognostic measure Forced vital capacity relates to survival[108,109]	Needs tight mouth seal (difficult with bulbar involvement) May not detect diaphragmatic weakness
Strength of inspiratory and expiratory muscles	Diaphragmatic function	Investigates the cause of hypercapnic respiratory failure Can detect when assisted cough is needed	Patients can have isolated weakness in inspiratory or expiratory phase[110,111]
Mouth pressures	Muscle strength	Provides additional information about strength	Less accurate than invasive tests and newer, non-invasive tests Needs tight mouth seal[112] May underestimate true strength[113-115]
Invasive measures	Gastric and oesophageal pressures	Gold-standard measure of diaphragmatic strength[112,116,117]	Invasive and not the most popular choice for patients unwilling to have serial tests
Nasal pressure	Respiratory sufficiency	Accurately reflects intrathoracic pressures[118,119]	Relatively insensitive to change over time
Respiratory mechanics	Breathing patterns	Tidal volume and lung compliance predictive of survival[116]	Not in widespread clinical use
Gas exchange and sleep studies	Hypercapnia (uncommon) and nocturnal desaturation (common[120])	Maximum inspiratory respiration is associated with nocturnal desaturation[114,115,121]	Pulse oximetry should not be relied on because arterial hypoxaemia is a late occurrence in hypoventilation[122]

Table 2: **Tests of respiratory function for patients with MND**

difficulty in the clinical assessment of corticospinal-tract involvement. Even in the "pure" clinical motor neuron phenotype, the corticospinal tract shows abnormalities in most patients at post mortem, especially in a subgroup with rapid progression.[126] Therefore, imaging techniques that can detect early involvement of the corticospinal tract are crucial in the assessment of disease progression in MND.

Many MRI, magnetic resonance spectroscopy, PET, and single-photon-emission CT studies have shown central abnormalities in patients with MND. The ideal technique for assessment of MND should be sensitive and specific in early diagnosis, enabling the identification of disorders that mimic MND. The technique should also be sensitive to disease progression and reflect the efficacy of treatment.[127,128] There is no gold standard to detect abnormalities within the corticospinal tract in vivo, and therefore, as with central neurophysiological techniques, the potential of imaging to detect early changes within the corticospinal tract is unknown.

Initial attempts to use MRI to assess the prognosis of patients with MND focused on measuring atrophy, especially in the motor cortex.[129-132] Early changes within affected motor neurons and the projection in the corticospinal tract have also been studied.[133] Focal hyperintensity of normal white matter from the primary motor cortex to the centrum semiovale, posterior limb of the internal capsule, and cerebral peduncle into the pons has been shown by many researchers with various MRI techniques, including fast spin echo (T1, T2, and proton-density), inversion-recovery, magnetisation-transfer,[134,135] and diffusion-weighted imaging (figure 3).[136,137] These techniques provide a measure of cellular changes that accompany axonal degeneration of the corticospinal tract, but there are problems with sensitivity and specificity attributable to measurement variability.[127] In addition, because of the issues with sensitivity and specificity, no clear associations between MRI abnormalities in the corticospinal tract and disease stages or rates of progression have been found.[127]

Diffusion-tensor imaging has identified higher than normal mean diffusivity and lower than normal fractional anisotropy along the corticospinal tract between the internal capsule and midbrain in patients with MND, and most strikingly in those with bulbar onset. Disease severity is associated with a reduction in fractional anisotropy, and disease duration is associated with an increase in mean diffusivity.[128] This technique has also been used to image the spinal cord.[138] Axonal-fibre tracking, an extension of diffusion tensor imaging, successfully imaged the human brainstem[139] and might well be used to map corticospinal tract damage in patients with MND. There is much interest in diffusion tensor imaging for quantification of abnormalities in the corticospinal tract, particularly in the identification of early involvement,[140] among many other areas.[141]

Cerebral blood flow and neuronal metabolism in the sensorimotor regions of the brain have been assessed with nuclear medicine techniques such as PET and single-photon-emission CT.[142] Proton magnetic resonance spectroscopy studies have assessed the integrity of the motor cortex. Many studies suggest that concentrations of N-acetyl aspartate are lower than normal in patients with MND.[143-146] Follow-up studies have found a substantial decrease in the ratio of N-acetyl aspartate to choline with the development of upper motor neuron signs.[143,147] Whereas the severity of clinical findings is associated with the amount of cortical

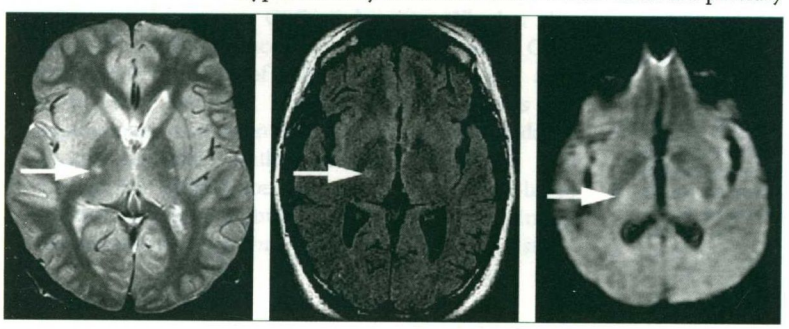

Figure 3: **Imaging techniques for the identification of corticospinal-tract abnormalities in MND**
Axial proton-density-weighted image (left), fluid-attenuated inversion-recovery image (middle), and diffusion-weighted image (right) of patients with upper motor neuron features in MND. The arrows show areas of axonal degeneration in the corticospinal tracts.

Search strategy and selection criteria

The MEDLINE and EMBASE databases were searched from 1966 and 1980, respectively, until October, 2004, with the terms: "motor neurone disease", "amyotrophic lateral sclerosis", "MUNE", "axonal excitability", "disease progression", and "functional scales". Further articles were included from reference lists, review articles, and major textbook chapters on motor neuron disease.

neuronal abnormality,[143] staging (by use of clinical rating scales) is not associated.[146] The ratio of N-acetyl aspartate to choline in patients with progressive spinal atrophy and multifocal motor neuropathy does not differ substantially from that in controls,[143,145,147] and therefore may help to distinguish these diseases from MND. Magnetic resonance spectroscopy has also been used to monitor the effect of treatment.[148] Researchers have used several imaging techniques, combined with neurophysiological measurements, such as TMS, to help in the refinement and identification of upper motor neuron involvement in MND;[149,150] however, no prospective data are available. A combination of techniques will probably improve objective measurement of progression in MND.

Other biological markers

An ideal peripheral biological marker of MND would be sensitive and specific to the disease process. It would correspond to disease progression and respond to interventions that change the outcome of the disease. Such a marker would be intricately involved in the pathogenesis of the disease, either in the underlying mechanism or as a direct result of the disease process. The search for a reliable peripheral marker that is sensitive and specific for MND has so far been unsuccessful. Although researchers have reported disease sensitivity and specificity in assays of peripheral blood,[151] CSF,[152] and muscle,[153] their findings have yet to be replicated. Sophisticated biological methods are now being applied in the search for disease specific signatures in serum, CSF, and urine. Whether this approach will be successful is not known. Gene expression profiling of spinal-cord tissue taken after death (and therefore, end-stage, heterogeneous cell populations) has identified inflammation, oxidative stress, neuronal death, abnormal signalling, and cytoskeletal dysfunction in MND.[154] Peripheral-blood genomic profiling might be applied to MND in a similar way to other diseases for a specific and sensitive test.[155]

Conclusion

There are many challenges in the diagnosis and reliable monitoring of MND. Survival in MND is likely to be determined by many factors, including phenotype, rate of disease progression, the early presence of respiratory failure, and nutritional status. Improved survival of patients with MND will depend on elucidation of the pathogenesis of MND, early specific diagnostic methods, and the development of therapies that not only slow the progression of the disorder, but also address the consequences of respiratory failure and malnutrition.

Acknowledgments

We thank Pam Dawes and the Medical Illustrations Unit, Prince of Wales Hospital, NSW, Australia. Research support from the Motor Neurone Disease Research Institute of Australia is gratefully acknowledged.

Authors' contributions

We all contributed equally to the preparation of this review.

Conflicts of interest

We have no conflicts of interest.

Role of the funding source

No funding source was involved in the preparation of this paper or in the decision to submit it for publication.

References

1 Kiernan MC. Motor neuron disease: a Pandora's box. *Med J Aust* 2003; **178**: 311–12.
2 Charcot J JA. Deux cas d'astrophie musculaire progressive avec lesions de la substance grise et des faisceaux antero lateraux de la moelle epiniere. *Arch Physiol Neurol Pathol* 1869; **2**: 744–54.
3 Rosen DR, Siddique T, Patterson D, et al. Mutations in Cu/Zn superoxide dismutase gene are associated with familial amyotrophic lateral sclerosis. *Nature* 1993; **362**: 59–62.
4 Lacomblez L, Bensimon G, Leigh PN, Guillet P, Meininger V. Dose-ranging study of riluzole in amyotrophic lateral sclerosis. *Lancet* 1996; **347**: 1425–31.
5 Bradley WG, Anderson F, Bromberg M, et al. Current management of ALS: comparison of the ALS CARE Database and the AAN Practice Parameter. *Neurology* 2001; **57**: 500–04.
6 Iwasaki Y, Ikeda K, Kinoshita M. Molecular and cellular mechanism of glutamate receptors in relation to amyotrophic lateral sclerosis. *Curr Drug Target CNS Neurol Disord* 2002; **1**: 511–18.
7 Miller RG, Mitchell JD, Lyon M, Moore DH. Riluzole for amyotrophic lateral sclerosis (ALS)/motor neuron disease (MND). *Amyotroph Lateral Scler Other Motor Neuron Disord* 2003; **4**: 191–206.
8 Davenport RJ, Swingler RJ, Chancellor AM, Warlow CP. Avoiding false positive diagnoses of motor neuron disease: lessons from the Scottish Motor Neuron Disease Register. *J Neurol Neurosurg Psychiatry* 1996; **60**: 147–51.
9 Mitsumoto H, Chad DA, Pioro EP. Terminology and classification of ALS. In: Amyotrophic lateral sclerosis. Philadelphia: FA Davis Company, 1998: 3–15.
10 Ringel SP, Murphy JR, Alderson MK, et al. The natural history of amyotrophic lateral sclerosis. *Neurology* 1993; **43**: 1316–22.
11 Talman P, Mathers S, Mostert E, Forbes A. Evaluation of clinical patterns and rate of progression of motor neuron disease. *Amyotroph Lateral Scler Other Motor Neuron Disord* 2002; **3**: 93.
12 Czaplinski A, Steck AJ, Andersen PM, Weber M. Flail arm syndrome: a clinical variant of amyotrophic lateral sclerosis. *Eur J Neurol* 2004; **11**: 567–68.
13 Hu MT, Ellis CM, Al-Chalabi A, Leigh PN, Shaw CE. Flail arm syndrome: a distinctive variant of amyotrophic lateral sclerosis. *J Neurol Neurosurg Psychiatry* 1998; **65**: 950–51.
14 Brooks BR. El Escorial World Federation of Neurology criteria for the diagnosis of amyotrophic lateral sclerosis. *J Neurol Sci* 1994; **124**: 96–107.
15 Miller RG, Munsat TL, Swash M, Brooks BR. Consensus guidelines for the design and implementation of clinical trials in ALS. *J Neurol Sci* 1999; **169**: 2–12.
16 Traynor BJ, Codd MB, Corr B, Forde C, Frost E, Hardiman M. Clinical features of amyotrophic lateral sclerosis according to the El Escorial and Airlie House Diagnostic Criteria. *Arch Neurol* 2000; **57**: 1171–76.
17 Ross MA, Miller RG, Berchert L, et al. Toward earlier diagnosis of

amyotrophic lateral sclerosis: revised criteria. *Neurology* 1998; **50**: 768–72.

18 Beghi E, Balzarini C, Bogliun G, et al. Reliability of the El Escorial diagnostic criteria for amyotrophic lateral sclerosis. *Neuroepidemiology* 2002; **21**: 265–70.

19 Chio A, Mora G, Leone M, et al. Early symptom progression rate is related to ALS outcome: a prospective population-based study. *Neurology* 2002; **59**: 99–103.

20 Bouchard C, Lacroix C, Plante V, et al. Clinicopathologic findings and prognosis of chronic inflammatory demyelinating polyneuropathy. *Neurology* 1999; **52**: 498–503.

21 Barohn RJ, Kissel JT, Warmolts JR, Mendell JR. Chronic inflammatory demyelinating polyradiculoneuropathy: clinical characteristics, course, and recommendations for diagnostic criteria. *Arch Neurol* 1989; **46**: 878–84.

22 Rotta FT, Sussman AT, Bradley WG, Ram Ayyar D, Sharma KR, Shebert RT. The spectrum of chronic inflammatory demyelinating polyneuropathy. *J Neurol Sci* 2000; **173**: 129–39.

23 Latov N. Diagnosis of CIDP. *Neurology* 2002; **59**: S2–6.

24 Roth G, Rohr J, Magistris MR, Ochsner F. Motor neuropathy with proximal multifocal persistent conduction block, fasciculations, and myokymia: evolution to tetraplegia. *Eur Neurol* 1986; **25**: 416–23.

25 Parry GJ, Clarke S. Multifocal acquired demyelinating neuropathy masquerading as motor neuron disease. *Muscle Nerve* 1988; **11**: 103–07.

26 Pestronk A, Cornblath DR, Ilyas AA, et al. A treatable multifocal motor neuropathy with antibodies to GM1 ganglioside. *Ann Neurol* 1988; **24**: 73–78.

27 Pestronk A, Chaudhry V, Feldman EL, et al. Lower motor neuron syndromes defined by patterns of weakness, nerve conduction abnormalities, and high titers of antiglycolipid antibodies. *Ann Neurol* 1990; **27**: 316–26.

28 Bouche P, Moulonguet A, Younes-Chennoufi AB, et al. Multifocal motor neuropathy with conduction block: a study of 24 patients. *J Neurol Neurosurg Psychiatry* 1995; **59**: 38–44.

29 Taylor BV, Wright RA, Harper CM, Dyck PJ. Natural history of 46 patients with multifocal motor neuropathy with conduction block. *Muscle Nerve* 2000; **23**: 900–08.

30 Kiernan MC, Guglielmi JM, Kaji R, Murray NM, Bostock H. Evidence for axonal membrane hyperpolarization in multifocal motor neuropathy with conduction block. *Brain* 2002; **125**: 664–75.

31 Hirayama K, Tsubaki T, Toyokura Y, Okinaka S. Juvenile muscular atrophy of unilateral upper extremity. *Neurology* 1963; **13**: 373–80.

32 Krishnan AV, Pamphlett R, Burke D, Kiernan MC. Cytoplasmic-body myopathy masquerading as motor neurone disease. *Muscle Nerve* 2004; **30**: 667–72.

33 Swash M, de Carvalho M. The neurophysiological index in ALS. *Amyotroph Lateral Scler Other Motor Neuron Disord* 2004; **5**: 108–10.

34 de Carvalho M, Scotto M, Lopes A, Swash M. Clinical and neurophysiological evaluation of progression in amyotrophic lateral sclerosis. *Muscle Nerve* 2003; **28**: 630–33.

35 Colombo R, Mazzini L, Mora G, et al. Measurement of isometric muscle strength: a reproducibility study of maximal voluntary contraction in normal subjects and amyotrophic lateral sclerosis patients. *Med Eng Phys* 2000; **22**: 167–74.

36 Shefner JM. Motor unit number estimation in human neurological diseases and animal models. *Clin Neurophysiol* 2001; **112**: 955–64.

37 Lomen-Hoerth C, Slawnych MP. Statistical motor unit number estimation: from theory to practice. *Muscle Nerve* 2003; **28**: 263–72.

38 Santo Neto H, de Carvalho VC, Marques MJ. Estimation of the number and size of human flexor digiti minimi muscle motor units using histological methods. *Muscle Nerve* 1998; **21**: 112–14.

39 Arasaki K, Tamaki M, Hosoya Y, Kudo N. Validity of electromyograms and tension as a means of motor unit number estimation. *Muscle Nerve* 1997; **20**: 552–60.

40 McComas AJ, Fawcett PR, Campbell MJ, Sica RE. Electrophysiological estimation of the number of motor units within a human muscle. *J Neurol Neurosurg Psychiatry* 1971; **34**: 121–31.

41 Galea V, de Bruin H, Cavasin R, McComas AJ. The numbers and relative sizes of motor units estimated by computer. *Muscle Nerve* 1991; **14**: 1123–30.

42 Stein RB, Yang JF. Methods for estimating the number of motor units in human muscles. *Ann Neurol* 1990; **28**: 487–95.

43 Stashuk DW, Doherty TJ, Kassam A, Brown WF. Motor unit number estimates based on the automated analysis of F-responses. *Muscle Nerve* 1994; **17**: 881–90.

44 Bromberg MB. Motor unit estimation: reproducibility of the spike-triggered averaging technique in normal and ALS subjects. *Muscle Nerve* 1993; **16**: 466–71.

45 Felice KJ. Thenar motor unit number estimates using the multiple point stimulation technique: reproducibility studies in ALS patients and normal subjects. *Muscle Nerve* 1995; **18**: 1412–16.

46 Wang FC, Delwaide PJ. Number and relative size of thenar motor units in ALS patients: application of the adapted multiple point stimulation method. *Electroencephalogr Clin Neurophysiol* 1998; **109**: 36–43.

47 Neto HS, Filho JM, Passini R Jr, Marques MJ. Number and size of motor units in thenar muscles. *Clin Anat* 2004; **17**: 308–11.

48 Daube JR. Estimating the number of motor units in a muscle. *J Clin Neurophysiol* 1995; **12**: 585–94.

49 Lomen-Hoerth C, Olney RK. Comparison of multiple point and statistical motor unit number estimation. *Muscle Nerve* 2000; **23**: 1525–33.

50 Shefner JM, Jillapalli D, Bradshaw DY. Reducing intersubject variability in motor unit number estimation. *Muscle Nerve* 1999; **22**: 1457–60.

51 Henderson RD, McClelland R, Daube JR. Effect of changing data collection parameters on statistical motor unit number estimates. *Muscle Nerve* 2003; **27**: 320–31.

52 Shefner JM, Cudkowicz ME, Zhang H, Schoenfeld D, Jillapalli D. The use of statistical MUNE in a multicenter clinical trial. *Muscle Nerve* 2004; **30**: 463–69.

53 Armon C, Brandstater ME. Motor unit number estimate-based rates of progression of ALS predict patient survival. *Muscle Nerve* 1999; **22**: 1571–75.

54 Felice KJ. A longitudinal study comparing thenar motor unit number estimates to other quantitative tests in patients with amyotrophic lateral sclerosis. *Muscle Nerve* 1997; **20**: 179–85.

55 Henderson RD, McCombe PA, Ridall GR, Pettitt AN. Bayesian statistics for estimating motor unit numbers. *Neurology* 2004; **62**: 455.

56 Burke D, Kiernan MC, Bostock H. Excitability of human axons. *Clin Neurophysiol* 2001; **112**: 1575–85.

57 Bostock H, Sharief MK, Reid G, Murray NM. Axonal ion channel dysfunction in amyotrophic lateral sclerosis. *Brain* 1995; **118**: 217–25.

58 Kodawa M KR, Kojima Y. Threshold electronus in patients with amyotrophic lateral sclerosis: further experience with Japanese subjects. *Electroenceph Clin Neurophysiol* 1995; **97**: S172.

59 Horn S, Quasthoff S, Grafe P, Bostock H, Renner R, Schrank B. Abnormal axonal inward rectification in diabetic neuropathy. *Muscle Nerve* 1996; **19**: 1268–75.

60 Burke D, Kiernan MC, Mogyoros I, Bostock H. Differences in the properties of human sensory and motor axons. In: Kimura J, Kaji R, eds. Physiology of ALS and related diseases. Amsterdam: Elsevier, 1997: 41–51.

61 Mogyoros I, Kiernan MC, Burke D, Bostock H. Strength-duration properties of sensory and motor axons in amyotrophic lateral sclerosis. *Brain* 1998; **121**: 851–59.

62 Burke D, Mogyoros I, Kiernan MC, Bostock H. Excitability of cutaneous afferents in amyotrophic lateral sclerosis. In: Kimura J, Kaji R, eds. Physiology of ALS and related diseases. Amsterdam: Elsevier, 1997: 145–54.

63 Kiernan MC. Impulse conduction. In: Aminoff MJ, Daroff RB, ed. Encyclopedia of the neurological sciences. San Diego, USA: Academic Press, 2003: 639–42.

64 Kiernan MC, Burke D. Threshold electronus in the assessment of motor neuron disease. In: Eisen A, ed. Handbook of clinical neurophysiology: clinical neurophysiology of motor neuron diseases. Amsterdam: Elsevier, 2004: 359–66.

65 Kiernan MC, Burke D, Andersen KV, Bostock H. Multiple measures of axonal excitability: a new approach in clinical testing. *Muscle Nerve* 2000; **23**: 399–409.

66 Kiernan MC, Hart IK, Bostock H. Excitability properties of motor

axons in patients with spontaneous motor unit activity. *J Neurol Neurosurg Psychiatry* 2001; **70**: 56–64.

67 Krishnan AV, Lin CS, Kiernan MC. Nerve excitability properties in lower-limb motor axons: evidence for a length-dependent gradient. *Muscle Nerve* 2004; **29**: 645–55.

68 de Carvalho M, Evangelista T, Sales-Luis ML. The corticomotor threshold is not dependent on disease duration in amyotrophic lateral sclerosis. *Amyotroph Lateral Scler Other Motor Neuron Disord* 2002; **3**: 39–42.

69 Olney RK. Transcranial magnetic stimulation: pro. *Amyotroph Lateral Scler Other Motor Neuron Disord* 2002; **3**: S111.

70 Siciliano G, Manca ML, Sagliocco L, et al. Cortical silent period in patients with amyotrophic lateral sclerosis. *J Neurol Sci* 1999; **169**: 93–97.

71 Eisen A, Swash M. Clinical neurophysiology of ALS. *Clin Neurophysiol* 2001; **112**: 2190–201.

72 Weber M, Eisen A. Peristimulus time histograms (PSTHs)—a marker for upper motor neuron involvement in ALS? *Amyotroph Lateral Scler Other Motor Neuron Disord* 2000; **1**: S51–56.

73 Winhammar JMC, Kiernan MC, Rowe DB. Transcranial magnetic stimulation in motor neuron disease. *Clin Neurophysiol* 2004; **115**: 990–93.

74 Brooks BR. Functional scales: summary. *Amyotroph Lateral Scler Other Motor Neuron Disord* 2002; **3**: S13–18.

75 Norris FH Jr, Calanchini PR, Fallat RJ, Panchari S, Jewett B. The administration of guanidine in amyotrophic lateral sclerosis. *Neurology* 1974; **24**: 721–28.

76 Mora G. Functional scales: pro. *Amyotroph Lateral Scler Other Motor Neuron Disord* 2002; **3**: S9–10.

77 Guiloff RJ. Functional scales in ALS: cons. *Amyotroph Lateral Scler Other Motor Neuron Disord* 2002; **3**: S11–12.

78 Appel V, Stewart SS, Smith G, Appel SH. A rating scale for amyotrophic lateral sclerosis: description and preliminary experience. *Ann Neurol* 1987; **22**: 328–33.

79 Gordon PH, Miller RG, Moore DH. ALSFRS-R. *Amyotroph Lateral Scler Other Motor Neuron Disord* 2004; **5**: 90–93.

80 Kimura F, Shinoda K, Fujiwara S, et al. [The changes of clinical characteristics in 100 Japanese amyotrophic lateral sclerosis patients between 1980 and 2000]. *Rinsho Shinkeigaku* 2003; **43**: 385–91.

81 Cudkowicz ME, Shefner JM, Schoenfeld DA, et al. A randomized, placebo-controlled trial of topiramate in amyotrophic lateral sclerosis. *Neurology* 2003; **61**: 456–64.

82 ALS CNTF Treatment Study Group. A double-blind placebo-controlled clinical trial of subcutaneous recombinant human ciliary neurotrophic factor (rHCNTF) in amyotrophic lateral sclerosis. *Neurology* 1996; **46**: 1244–49.

83 Cedarbaum JM, Stambler N. Performance of the amyotrophic lateral sclerosis functional rating scale (ALSFRS) in multicenter clinical trials. *J Neurol Sci* 1997; **152**: S1–9.

84 Kasarskis EJ. Anthropmetrics in the assessment of muscle atrophy in amyotrophic lateral sclerosis. *Neurology* 1998; **50**: A429.

85 Pioro EP. MR spectroscopy in amyotrophic lateral sclerosis/motor neuron disease. *J Neurol Sci* 1997; **152**: S49–53.

86 Nozaki S, Kunitomi A, Saito T, Matsumura T, Shinno S. [Process of swallowing disturbance in amyotrophic lateral sclerosis—evaluation of videofluorography and respiratory function]. *Rinsho Shinkeigaku* 2003; **43**: 77–83.

87 Cedarbaum JM, Stambler N, Malta E, et al. The ALSFRS-R: a revised ALS functional rating scale that incorporates assessments of respiratory function. *J Neurol Sci* 1999; **169**: 13–21.

88 Ohashi Y, Tashiro K, Itoyama Y, et al. [Study of functional rating scale for amyotrophic lateral sclerosis: revised ALSFRS(ALSFRS-R). *No To Shinkei* 2001; **53**: 346–55.

89 Miller RG, Moore DH 2nd, Gelinas DF, et al. Phase III randomized trial of gabapentin in patients with amyotrophic lateral sclerosis. *Neurology* 2001; **56**: 843–48.

90 Leigh PN, Swash M, Iwasaki Y, et al. Amyotrophic lateral sclerosis: a consensus viewpoint on designing and implementing a clinical trial. *Amyotroph Lateral Scler Other Motor Neuron Disord* 2004; **5**: 84–98.

91 Bensimon G, Lacomblez L, Meininger V. A controlled trial of riluzole in amyotrophic lateral sclerosis. *N Engl J Med* 1994; **330**: 585–91.

92 Lacomblez L, Bensimon G, Leigh PN, et al. A confirmatory dose-ranging study of riluzole in ALS. *Neurology* 1996; **47**: S242–50.

93 Lai EC, Felice KJ, Festoff BW, et al. Effect of recombinant human insulin-like growth factor-I on progression of ALS: a placebo-controlled study. *Neurology* 1997; **49**: 1621–30.

94 Borasio GD, Robberecht W, Leigh PN, et al. A placebo-controlled trial of insulin-like growth factor-I in amyotrophic lateral sclerosis. *Neurology* 1998; **51**: 583–86.

95 A controlled trial of recombinant methionyl human BDNF in ALS. *Neurology* 1999; **52**: 1427–33.

96 Miller RG, Bryan WW, Dietz MA, et al. Toxicity and tolerability of recombinant human ciliary neurotrophic factor in patients with amyotrophic lateral sclerosis. *Neurology* 1996; **47**: 1329–31.

97 Miller RG, Moore D, Young LA, et al. Placebo-controlled trial of gabapentin in patients with amyotrophic lateral sclerosis. *Neurology* 1996; **47**: 1383–88.

98 Savas S, Delibas N, Savas C, Sutcu R, Cindas A. Pentoxifylline reduces biochemical markers of ischemia-reperfusion induced spinal cord injury in rabbits. *Spinal Cord* 2002; **40**: 224–29.

99 Great Lakes ALS Study Group. A comparison of muscle strength testing techniques in amyotrophic lateral sclerosis. *Neurology* 2003; **61**: 1503–07.

100 Mazzini L, Balzarini C, Colombo R, et al. Effects of creatine supplementation on exercise performance and muscular strength in amyotrophic lateral sclerosis: preliminary results. *J Neurol Sci* 2001; **191**: 139–44.

101 Lai EC. Therapeutic developments in amyotrophic lateral sclerosis. *Exp Opin Invest Drugs* 1999; **8**: 347–61.

102 Haverkamp LJ, Appel V, Appel SH. Natural history of amyotrophic lateral sclerosis in a database population: validation of a scoring system and a model for survival prediction. *Brain* 1995; **118**: 707–19.

103 Ganzini L, Johnston WS, Hoffman WF. Correlates of suffering in amyotrophic lateral sclerosis. *Neurology* 1999; **52**: 1434–40.

104 Trail M, Nelson N, Van JN, Appel SH, Lai EC. Major stressors facing patients with amyotrophic lateral sclerosis (ALS): a survey to identify their concerns and to compare with those of their caregivers. *Amyotroph Lateral Scler Other Motor Neuron Disord* 2004; **5**: 40–45.

105 Chio A, Gauthier A, Montuschi A, et al. A cross sectional study on determinants of quality of life in ALS. *J Neurol Neurosurg Psychiatry* 2004; **75**: 1597–601.

106 Bremer BA, Simone AL, Walsh S, Simmons Z, Felgoise SH. Factors supporting quality of life over time for individuals with amyotrophic lateral sclerosis: the role of positive self-perception and religiosity. *Ann Behav Med* 2004; **28**: 119–25.

107 Neudert C, Wasner M, Borasio GD. Individual quality of life is not correlated with health-related quality of life or physical function in patients with amyotrophic lateral sclerosis. *J Palliat Med* 2004; **7**: 551–57.

108 Fallat RJ, Jewitt B, Bass M, Kamm B, Norris FH Jr. Spirometry in amyotrophic lateral sclerosis. *Arch Neurol* 1979; **36**: 74–80.

109 Schiffman PL, Belsh JM. Pulmonary function at diagnosis of amyotrophic lateral sclerosis: rate of deterioration. *Chest* 1993; **103**: 508–13.

110 Polkey MI, Lyall RA, Green M, Nigel Leigh P, Moxham J. Expiratory muscle function in amyotrophic lateral sclerosis. *Am J Respir Crit Care Med* 1998; **158**: 734–41.

111 Kreitzer SM, Saunders NA, Tyler HR, Ingram RH, Jr. Respiratory muscle function in amyotrophic lateral sclerosis. *Am Rev Respir Dis* 1978; **117**: 437–47.

112 Polkey MI, Green M, Moxham J. Measurement of respiratory muscle strength. *Thorax* 1995; **50**: 1131–35.

113 Fitting JW, Paillex R, Hirt L, Aebischer P, Schluep M. Sniff nasal pressure: a sensitive respiratory test to assess progression of amyotrophic lateral sclerosis. *Ann Neurol* 1999; **46**: 887–93.

114 Gay PC, Westbrook PR, Daube JR, Litchy WJ, Windebank AJ, Iverson R. Effects of alterations in pulmonary function and sleep variables on survival in patients with amyotrophic lateral sclerosis. *Mayo Clin Proc* 1991; **66**: 686–94.

115 David WS, Bundlie SR, Mahdavi Z. Polysomnographic studies in amyotrophic lateral sclerosis. *J Neurol Sci* 1997; **152**: S29–35.

116 Vitacca M, Clini E, Facchetti D, et al. Breathing pattern and

respiratory mechanics in patients with amyotrophic lateral sclerosis. *Eur Respir J* 1997; **10**: 1614–21.

117 Lyall RA, Donaldson N, Polkey MI, Leigh PN, Moxham J. Respiratory muscle strength and ventilatory failure in amyotrophic lateral sclerosis. *Brain* 2001; **124**: 2000–13.

118 Heritier F, Rahm F, Pasche P, Fitting JW. Sniff nasal inspiratory pressure: a noninvasive assessment of inspiratory muscle strength. *Am J Respir Crit Care Med* 1994; **150**: 1678–83.

119 Chaudhuri MB, Liu C, Watson L, Jefferson D, Kinnear WJ. Sniff nasal inspiratory pressure as a marker of respiratory function in motor neuron disease. *Eur Respir J* 2000; **15**: 539–42.

120 Arnulf I, Similowski T, Salachas F, et al. Sleep disorders and diaphragmatic function in patients with amyotrophic lateral sclerosis. *Am J Respir Crit Care Med* 2000; **161**: 849–56.

121 Pinto AC, Evangelista T, Carvalho M, Paiva T, Sales-Luis M. Respiratory disorders in ALS: sleep and exercise studies. *J Neurol Sci* 1999; **169**: 61–68.

122 Rochester DF, Esau SA. Assessment of ventilatory function in patients with neuromuscular disease. *Clin Chest Med* 1994; **15**: 751–63.

123 Oppenheimer EA. Treating respiratory failure in ALS; the details are becoming clearer. *J Neurol Sci* 2003; **209**: 1–4.

124 Velasco R, Salachas F, Munerati E, et al. Oxymetrie nocturne chez les patients atteints de sclerosie laterale amyotrophique: analyse de son role predictif sur la survie. *Rev Neurol (Paris)* 2002; **158**: 575–78.

125 Brownell B, Oppenheimer DR, Hughes JT. The central nervous system in motor neurone disease. *J Neurol Neurosurg Psychiatry* 1970; **33**: 338–57.

126 Ince PG, Evans J, Knopp M, et al. Corticospinal tract degeneration in the progressive muscular atrophy variant of ALS. *Neurology* 2003; **60**: 1252–58.

127 Comi G, Rovaris M, Leocani L. Review neuroimaging in amyotrophic lateral sclerosis. *Eur J Neurol* 1999; **6**: 629–37.

128 Ellis CM, Simmonds A, Jones D, et al. Diffusion tensor MRI assesses corticospinal tract damage in ALS. *Neurology* 1999; **53**: 1051–58.

129 Cheung G, Gawel MJ, Cooper PW, Farb RI, Ang LC, Gawal MJ. Amyotrophic lateral sclerosis: correlation of clinical and MR imaging findings. *Radiology* 1995; **194**: 263–70.

130 Thorpe JW, Moseley IF, Hawkes CH, MacManus DG, McDonald WI, Miller DH. Brain and spinal cord MRI in motor neuron disease. *J Neurol Neurosurg Psychiatry* 1996; **61**: 314–17.

131 Waragai M, Shinotoh H, Hayashi M, Hattori T. High signal intensity on T1 weighted MRI of the anterolateral column of the spinal cord in amyotrophic lateral sclerosis. *J Neurol Neurosurg Psychiatry* 1997; **62**: 88–91.

132 Imon Y, Yamaguchi S, Katayama S, et al. A decrease in cerebral cortex intensity on T2-weighted with ageing images of normal subjects. *Neuroradiology* 1998; **40**: 76–80.

133 Goodin DS, Rowley HA, Olney RK. Magnetic resonance imaging in amyotrophic lateral sclerosis. *Ann Neurol* 1988; **23**: 418–20.

134 Segawa F KM, Kishibayashi J, Sunohara M, Shimizu Z. MRI of ALS and Wallerian degeneration: analysis of diffusion coefficient and magnetic transfer. Proceedings of Third Scientific Meeting of the International Society for Magnetic Resonance in Medicine, 1995: 1299.

135 Kato Y, Matsumura K, Kinosada Y, Narita Y, Kuzuhara S, Nakagawa T. Detection of pyramidal tract lesions in amyotrophic lateral sclerosis with magnetization-transfer measurements. *AJNR Am J Neuroradiol* 1997; **18**: 1541–47.

136 Toft PB, Leth H, Peitersen B, Lou HC, Thomsen C. The apparent diffusion coefficient of water in gray and white matter of the infant brain. *J Comput Assist Tomogr* 1996; **20**: 1006–11.

137 Wu RH BR, Berchtenbreiter C, Borrasio T, Heuck A, Reiser M. Evaluation of diffusion weighted MR-imaging in patients with ALS. Proceedings of Sixth Scientific Meeting of the International Society for Magnetic Resonance in Medicine, 1998: 1249.

138 Leigh PN, Simmons A, Williams S, Williams V, Turner M, Brooks D. Imaging: MRS/MRI/PET/SPECT summary. *Amyotroph Lateral Scler Other Motor Neuron Disord* 2002; **3**: S75–80.

139 Stieltjes B, Kaufmann WE, van Zijl PC, et al. Diffusion tensor imaging and axonal tracking in the human brainstem. *Neuroimage* 2001; **14**: 723–35.

140 Sach M, Winkler G, Glauche V, et al. Diffusion tensor MRI of early upper motor neuron involvement in amyotrophic lateral sclerosis. *Brain* 2003; **127**: 340–50.

141 Toosy AT, Werring DJ, Orrell RW, et al. Diffusion tensor imaging detects corticospinal tract involvement at multiple levels in amyotrophic lateral sclerosis. *J Neurol Neurosurg Psychiatry* 2003; **74**: 1250–57.

142 Kew JJ, Brooks DJ, Passingham RE, Rothwell JC, Frackowiak RS, Leigh PN. Cortical function in progressive lower motor neuron disorders and amyotrophic lateral sclerosis: a comparative PET study. *Neurology* 1994; **44**: 1101–10.

143 Pioro EP, Antel JP, Cashman NR, Arnold DL. Detection of cortical neuron loss in motor neuron disease by proton magnetic resonance spectroscopic imaging in vivo. *Neurology* 1994; **44**: 1933–38.

144 Jones AP, Gunawardena WJ, Coutinho CM, Gatt JA, Shaw IC, Mitchell JD. Preliminary results of proton magnetic resonance spectroscopy in motor neurone disease (amyotrophic lateral sclerosis). *J Neurol Sci* 1995; **129**: 85–89.

145 Gredal O, Rosenbaum S, Topp S, Karlsborg M, Strange P, Werdelin L. Quantification of brain metabolites in amyotrophic lateral sclerosis by localized proton magnetic resonance spectroscopy. *Neurology* 1997; **48**: 878–81.

146 Ellis CM, Simmons A, Andrews C, Dawson JM, Williams SC, Leigh PN. A proton magnetic resonance spectroscopic study in ALS: correlation with clinical findings. *Neurology* 1998; **51**: 1104–09.

147 Block W, Karitzky J, Traber F, et al. Proton magnetic resonance spectroscopy of the primary motor cortex in patients with motor neuron disease. *Arch Neurol* 1998; **55**: 931–36.

148 Weiner MF. Alzheimer's disease: diagnosis and treatment. *Harv Rev Psychiatry* 1997; **4**: 306–16.

149 Kaufmann P, Mitsumoto H. Amyotrophic lateral sclerosis: objective upper motor neuron markers. *Curr Neurol Neurosci Rep* 2002; **2**: 55–60.

150 Kaufmann P, Pullman SL, Shungu DC, et al. Objective tests for upper motor neuron involvement in amyotrophic lateral sclerosis (ALS). *Neurology* 2004; **62**: 1753–57.

151 Simpson EP, Henry YK, Henkel JS, Smith RG, Appel SH. Increased lipid peroxidation in sera of ALS patients: a potential biomarker of disease burden. *Neurology* 2004; **62**: 1758–65.

152 Henkel JS, Engelhardt JI, Siklos L, et al. Presence of dendritic cells, MCP-1, and activated microglia/macrophages in amyotrophic lateral sclerosis spinal cord tissue. *Ann Neurol* 2004; **55**: 221-35.

153 Dupuis L, Gonzalez de Aguilar JL, di Scala F, et al. Nogo provides a molecular marker for diagnosis of amyotrophic lateral sclerosis. *Neurobiol Dis* 2002; **10**: 358–65.

154 Dangond F, Hwang D, Camelo S, et al. Molecular signature of late-stage human ALS revealed by expression profiling of postmortem spinal cord gray matter. *Physiol Genomics* 2004; **16**: 229–39.

155 Tang Y, Lu A, Aronow BJ, Sharp FR. Blood genomic responses differ after stroke, seizures, hypoglycemia, and hypoxia: blood genomic fingerprints of disease. *Ann Neurol* 2001; **50**: 699–707.

Internal Medicine Journal **36** (2006) 419–422

ORIGINAL ARTICLE

Nocturnal hypoxia in motor neuron disease is not predicted by standard respiratory function tests

J. M. C. Winhammar,[1,2] D. Joffe,[2,3] R. Simmul,[3] R. Schoeffel,[3] M. C. Kiernan[4] and D. B. Rowe[1,2]

Departments of [1]Neurology and [3]Thoracic Medicine, Royal North Shore Hospital and [4]Multidisciplinary Motor Neuron Disease Service, Prince of Wales Hospital and Prince of Wales Medical Research Institute and Prince of Wales Clinical School, University of New South Wales, and [2]Northern Clinical School, University of Sydney, Sydney, New South Wales, Australia

Key words
motor neuron disease (MND), nocturnal hypoxia (NH), respiratory function test, nocturnal oximetry, rapid eye movement (REM).

Correspondence
Dominic Rowe, Department of Neurology, Royal North Shore Hospital, Reserve Road, St Leonards, Sydney, NSW 2065, Australia.
Email: drowe@med.usyd.edu.au

Received 29 June 2005; accepted 23 December 2005.

doi:10.1111/j.1445-5994.2006.01102.x

Abstract

Background: With increasing awareness of motor neuron disease (MND) in Australia, the approach to respiratory management of patients with this disease will more commonly face the respiratory physician.
Aim: The aim of this study was to determine if standard respiratory function tests could determine the presence of nocturnal hypoxia (NH) in patients with MND.
Methods: Respiratory function tests were used to examine daytime respiratory function, and sleep studies were used to detect NH in 16 consecutive patients with MND and in 9 healthy control subjects. Demographic data, clinical parameters, respiratory function tests and sleep studies were obtained. Statistical analyses were carried out using *t*-tests and ANOVA, where appropriate.
Results: NH was detected in 50% of patients with MND, with no hypoxic events detected in the control group. Standard respiratory function tests were not able to predict the presence of NH.
Conclusion: There was no correlation between respiratory function tests and NH. This study emphasizes the inability of standard respiratory function tests to predict NH that may arise early in the course of MND.

Introduction

Motor neuron disease (MND) is a progressive neurodegenerative disease that produces weakness and ultimately death from respiratory failure. MND results in the death of nearly 400 Australians per year, with a median survival of only 2–3 years from diagnosis.[1]

Although respiratory failure in patients with MND is a direct consequence of muscle weakness during disease end-stage, a proportion of patients develop early and severe respiratory difficulties during sleep.[2] Notably, there is no direct relationship between clinical weakness, its distribution or the site of first onset and the onset of respiratory muscle involvement in the early stages of the disease. Nocturnal hypoxia (NH) is increasingly recognized as a predictor of survival, independent of respiratory muscle weakness.[3,4] Velasco *et al.* showed that a mean nocturnal arterial oxygen saturation of less than 93% is predictive of a dramatically shortened mean survival time of less than 6 months.[4]

The mechanisms involved in NH in MND are largely unexplained.[5] It is observed that rapid eye movement related desaturation often precedes the development of daytime symptoms of respiratory failure. This suggests that simple measures of lung physiology, even when taken into account with daytime symptoms, do not increase the sensitivity of current techniques to predict respiratory failure in sleep and therefore survival in patients with MND.

Consequently, the aim of this study was to investigate the relationship between multiple common respiratory

Funding: J. M. C. W. is the recipient of a scholarship from the Australian Rotary Health Research Fund and is also supported by Nicks Foundation
Potential conflicts of interest: None

function tests and nocturnal oxygen saturation levels in patients with early limb-onset MND. None of the patients had bulbar dysfunction, orthopnoea, symptomatic hypercapnia or excessive daytime sleepiness. We recorded demographic data, respiratory function tests and sleep studies to determine whether there was a measure of lung function that may correlate to the presence of NH.

Methods

Data were collected during the course of standard MND assessment from 16 consecutive patients with early limb-onset MND, none of whom had bulbar dysfunction, orthopnoea, symptomatic hypercapnia or excessive daytime sleepiness.[6] All the patients were diagnosed with MND by El Escorial criteria and referred to the Multidisciplinary MND Clinic at Royal North Shore Hospital.[7] In addition, nine healthy controls underwent similar assessment, with the study approved by the Human Ethics Committee at Royal North Shore Hospital.

All patients and controls underwent one night of continuous nocturnal oximetry (Invivo 4500; Invivo Research Inc., Broken Arrow, OK, USA, and Stardust Respironics, Philadelphia, PA, USA). NH was determined when there was a clear evidence of desaturation to a level of 90% or less for a period of more than 2 min. The pattern of desaturation was deemed consistent with hypoventilation on the basis of poor resaturation, with a fall from the baseline saturation of $\geq$4%. The absence of obesity or the demonstrable underlying cardiorespiratory disease was therefore, by exclusion, consistent with respiratory failure of an alternative cause. The lack of resaturation to baseline was considered sufficient to exclude obstructive sleep apnoea in the absence of coexistent obesity. Furthermore, in those in whom a Stardust study was available, analysis of the respitrace signal was consistent with hypoventilation as opposed to obstruction. All patients with MND were taking riluzole as part of their therapy.

All patients underwent standard respiratory function testing, including the measurement of spirometry (forced expiratory volume in 1 s (FEV_1) and vital capacity (VC)), lung volumes by whole-body plethysmography and diffusion for carbon monoxide as well as measurement of maximal expiratory pressure (MEP) and maximal inspiratory pressure (MIP). The same experienced respiratory scientists carried out all the tests.

Statistics

Statistical analyses were carried out using paired *t*-tests where appropriate. Otherwise, ANOVA methods were used, with Scheffe's *F*-test for measures of lung function.[8] This test was chosen as the variances of the cells were unequal and the *n* value for each class was different. Significance was determined at a level of $P < 0.05$. All statistics were carried out using Statview V5 (SAS Institute, Cary, NC, USA).

Results

The demographic details of the subjects at the time of entry into the study are given in Table 1. Sixteen patients with MND and nine controls were studied. NH was detected in 8 of 16 patients and in none of the controls. For analytical purposes, the patients with MND were split up into two groups: those who suffer from NH (MNDNH+) and those who do not suffer from NH (MNDNH−).

NH is illustrated in a patient with MND in Figure 1. This figure shows ongoing diminished effort of the chest wall (measured by chest wall expansion), followed by a lack of return to the baseline for saturation. As there is still a flow, it is believed that this is not caused by an obstruction.

The respiratory function results are shown in Figure 2. The results have been split up into three groups: MNDNH+, MNDNH− and the control group. Seven parameters were studied including FEV_1, forced VC (FVC), peak expiratory flow, VC, residual volume, MIP and MEP.

After analysis, there were no statistically significant differences for any of the respiratory function tests between the MNDNH+ and the MNDNH− groups or between the MNDNH− and the control group.

There was a borderline significant difference ($P = 0.049$) between the MNDNH+ and the control group only in the MEP measurement, with a mean MEP value in the MNDNH+ group of 61 ± 24% of the predicted and in the control group 96 ± 26%. It is important to note that in threshold analysis, no arbitrary MEP value was able to discriminate between MNDNH+ and MNDNH−.

Discussion

To assess the sensitivity of standard respiratory investigation in determining the presence of NH in MND, an array of respiratory function tests was carried out in 16 patients with MND and 9 healthy controls in addition to a formal sleep assessment. Fifty per cent of patients with MND were identified with NH and none in the control group.

Table 1 Demographic data for the three groups; MNDNH+, MNDNH− and controls

	MNDNH+	MNDNH−	Controls
Subjects	8	8	9
Sex, M/F	7 M, 1 F	4 M, 4 F	6 M, 3 F
Age (years)	58.9 ± 15.1	58.8 ± 11.8	55.2 ± 10.2
Body mass index (kg/m^2)	24.8 ± 5.42	25.4 ± 5.06	27.4 ± 7.8

F, female; M, male.

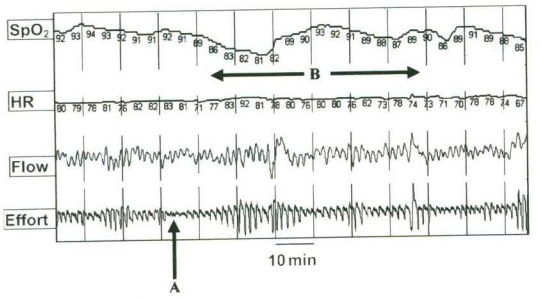

Figure 1 Sleep study recording of a patient with MND showing nocturnal hypoxia in the setting of ongoing diminished effort. The trace represents hypoventilation at (A), in the setting of diminished effort. This is followed by a lack of return to the baseline (B), which shows poor resaturation. There is still a flow, so the hypoxia is not caused by an obstruction. HR, heart rate; MND, motor neuron disease; SpO_2, oxygen saturation.

Although there was a borderline significance in only one respiratory parameter, MEP between the MNDNH+ patients and controls, the MEP value in isolation was not able to predict the presence of NH. These results suggest that standard clinical respiratory function tests cannot reliably predict the presence of NH.

This study emphasizes the need to measure overnight oximetry in patients with MND for the presence of NH, which occurs independently of voluntary maximal respiratory effort measured in routine respiratory tests. Furthermore, the absence of change in standard respiratory function tests suggests involvement of additional mechanisms, perhaps by central involvement of the respiratory centres, in the genesis of NH. This possibility may be addressed by correlating the findings of dynamic sleep studies with

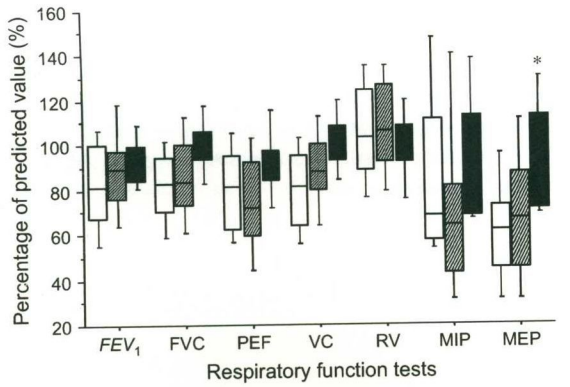

Figure 2 Respiratory function test results in MNDNH+, MNDNH− and the control groups. The only significant difference found was between the MNDNH+ and the control group for MEP (*). FEV_1, forced expiratory volume in 1 s; FVC, forced vital capacity; MEP, maximal expiratory pressure; MIP, maximal inspiratory pressure; PEF, peak expiratory flow; RV, residual volume; VC, vital capacity. (□), MNDNH+; (▨), MNDNH−; (■), Control.

investigation of upper motor neuron function, including clinical neurophysiological methods such as transcranial magnetic stimulation and structural assessment of the corticospinal tract using diffusion tensor imaging.[9]

The routine respiratory function tests used in this study were unable to identify the presence of NH and are therefore unlikely to be intimately involved in the mechanism of NH. It is becoming increasingly apparent that there is a number of problems in using FVC and other standard respiratory function measures to monitor disease progression and survival in MND. For instance, FVC has been used as an important indicator of survival in MND.[10,11] However, Velasco *et al.* recently showed that FVC does not correlate to either NH or survival in MND and that there was a high mortality in MND patients with NH.[4] In addition, FEV_1 has previously been found to be highly variable and does not correlate well with disease progression.[12] MIP and MEP have a large range of normal values, with many technical variables.[13]

Recently, sniff nasal inspiratory force (SNIF) has shown a predictive measure of survival, with improved sensitivity and specificity over conventional lung function tests and significant positive correlation between SNIF values and levels of nocturnal desaturation.[11] Our unit is currently undertaking a prospective study of SNIF to determine whether these results can be replicated.

The presence of NH is a potent predictor of survival in MND. Unfortunately, the mechanisms that produce NH in patients with MND remain unknown. Studies in patients with stroke show the complexity of the anatomy and physiology of central breathing control, particularly during sleep.[14]

If patients with MND are found to suffer from NH, they can be offered non-invasive positive-pressure ventilation (NIPPV) as part of a multidisciplinary care approach,[15] with resultant significant improvement in sleep quality, less daytime sleepiness, physical fatigue and depression.[16] Not only can NIPPV assist lung function and exert therapeutic effect on symptoms and quality of life, and have an effect on cognitive function,[17] but it can also delay the need for tracheostomy and prolongs survival.[18] In a recently published randomized controlled trial, non-invasive ventilation improves both survival and quality of life in MND.[19]

Optimizing care and delivering NIPPV for patients with MND require accurate predictive tests for disease progression including the ability to detect NH and to determine the best time to institute NIPPV. Clearly, the goal in this area is the development of a non-invasive reproducible tool that can accurately predict when desaturation is beginning to occur and what factors (including those outside the diaphragm) are important in its genesis. Although SNIF is promising, routine respiratory function tests do not

necessarily help the clinician with this decision. Routine surveillance oximetry to detect NH is suggested in the management of patients with MND.

Acknowledgements

We would like to thank all the participants involved in this study.

References

1 Kiernan MC. Motor neurone disease: a Pandora's box. *Med J Aust* 2003; **178**: 311–2.
2 Oppenheimer EA. Treating respiratory failure in ALS; the details are becoming clearer. *J Neurol Sci* 2003; **209**: 1–4.
3 Winhammar JMC, Rowe DB, Henderson RD, Kiernan MC. Assessment of disease progression in motor neuron disease. *Lancet Neurol* 2005; **4**: 229–38.
4 Velasco R, Salachas F, Munerati E, Le Forestier N, Pradat PF, Lacomblez L *et al.* Nocturnal oxymetry in patients with amyotrophic lateral sclerosis: role in predicting survival. *Rev Neurol (Paris)* 2002; **158**: 575–8.
5 Winhammar JMC, Kiernan MK, Rowe DB. Transcranial magnetic stimulation in motor neuron disease. *Clin Neurophysiol* 2004; **115**: 990–3.
6 Appel V, Stewart SS, Smith G, Appel SH. A rating scale for amyotrophic lateral sclerosis: description and preliminary experience. *Ann Neurol* 1987; **22**: 328–33.
7 Brooks BR, Miller RG, Swash M, Munsat TL. El Escorial revisited: revised criteria for the diagnosis of amyotrophic lateral sclerosis. *Amyotroph Lateral Scler Other Motor Neuron Disord* 2000; **1**: 293–9.
8 Huck S, Cormier W, Bounds W. T tests, one-way analysis of variance, and multiple comparison procedures. In: Brown M, Hausdorff C, eds. *Reading Statistics and Research*. New York: Harper Collins; 1974; 49–73.
9 Winhammar JMC, Trevillion L, Howells JT, Rowe DB, Joffe D, Kiernan MC. Mechanisms of nocturnal hypoventilation in motor neuron disease. *Clin Neurophysiol* 2005; **116**: e20.
10 Miller RG, Rosenberg JA, Gelinas DF, Mitsumoto H, Newman D, Sufit R *et al.* Practice parameter: the care of the patient with amyotrophic lateral sclerosis (an evidence-based review): report of the Quality Standards Subcommittee of the American Academy of Neurology: ALS Practice Parameters Task Force. *Neurology* 1999; **52**: 1311–23.
11 Morgan RK, McNally S, Alexander M, Conroy R, Hardiman O, Costello RW. Use of Sniff nasal-inspiratory force to predict survival in amyotrophic lateral sclerosis. *Am J Respir Crit Care Med* 2005; **171**: 269–74.
12 Brinkmann JR, Andres P, Mendoza M, Sanjak M. Guidelines for the use and performance of quantitative outcome measures in ALS clinical trials. *J Neurol Sci* 1997; **147**: 97–111.
13 Vincken W, Ghezzo H, Cosio MG. Maximal static respiratory pressures in adults: normal values and their relationship to determinants of respiratory function. *Bull Eur Physiopathol Respir* 1987; **23**: 435–9.
14 Bassetti C, Aldrich MS, Quint D. Sleep-disordered breathing in patients with acute supra- and infratentorial strokes. A prospective study of 39 patients. *Stroke* 1997; **28**: 1765–72.
15 Traynor BJ, Alexander M, Corr B, Frost E, Hardiman O. Effect of a multidisciplinary amyotrophic lateral sclerosis (ALS) clinic on ALS survival: a population based study, 1996–2000. *J Neurol Neurosurg Psychiatr* 2003; **74**: 1258–61.
16 Butz M, Wollinsky KH, Wiedemuth-Catrinescu U, Sperfeld A, Winter S, Mehrkens HH *et al.* Longitudinal effects of noninvasive positive-pressure ventilation in patients with amyotrophic lateral sclerosis. *Am J Phys Med Rehabil* 2003; **82**: 597–604.
17 Newsom-Davis IC, Lyall RA, Leigh PN, Moxham J, Goldstein LH. The effect of non-invasive positive pressure ventilation (NIPPV) on cognitive function in ALS: a prospective study. *J Neurol Neurosurg Psychiatry* 2001; **71**: 482–7.
18 Bourke SC, Gibson GJ. Non-invasive ventilation in ALS: current practice and future role. *Amyotroph Lateral Scler Other Motor Neuron Disord* 2004; **5**: 67–71.
19 Bourke SC, Tomlinson M, Williams TL, Bullock RE, Shaw PJ, Gibson GJ. Effects of non-invasive ventilation on survival and quality of like in patients with amyotrophic lateral sclerosis: a randomised controlled trial. *Lancet Neurol* 2006; **5**:140–47.